ABSTRACT

BUUR, JENNIFER LEEANN. Applications of Physiologically Based Pharmacokinetic Models in Veterinary Medicine. (Under the direction of Drs. Ronald E. Baynes and Jim E. Riviere.)

Classical approaches to pharmacokinetics, such as compartmental and non-compartmental analysis, provide the basis for most dosing regimens and meat and milk withholding intervals. These models are limited by their descriptive nature to dose, route of administration, and species. In addition, current pharmacokinetic modeling approaches are unable to predict possible adverse drug reactions due to drug interactions. As combination drug therapy is rapidly increasing, so too does the chance for an adverse drug reaction due to drug interactions. There is a need within veterinary medicine for more predictive and flexible pharmacokinetic modeling approaches that can also be used to explore the possibilities and consequences of adverse drug reactions.

Physiologically based pharmacokinetic (PBPK) models predict drug disposition based on mass balance. This mechanistic approach is predictive and flexible in terms of dose, route of administration, and species. Current uses of PBPK models include human health risk assessment, design of rational dosing regimens, and mechanistic studies of drug interactions. In veterinary medicine, there are only a few validated models.

Protection of the safety of the food supply is an important application of pharmacokinetics. By federal law, no animal products are allowed into the food chain until drug residue levels are below set tolerance limits. Sulfamethazine is a sulfonamide antibiotic that is commonly found above tolerance limits in swine. Sulfonamide drugs are associated with hypersensitivity reactions in humans and are carcinogenic in certain strains of rats. Thus violative residues could contribute to a significant public health hazard. To address this concern, a PBPK model was designed and validated for intravenous use of sulfamethazine in

swine. This model had tissue blocks for all edible tissues. Correlation coefficients for each tissue ranged from 0.86 to 0.99. The model accurately predicted withdrawal intervals after intravenous extralabel drug use. This model was expanded to include population variability and oral route of administration. The model was subjected to Monte Carlo analysis where parameter values were defined by log normal distributions. After validation, this probabilistic PBPK model approach was used to establish the meat withdrawal time for the upper limit of the 95% confidence interval for the 99th percentile of the population for the labeled oral dose. The model predicted a withdrawal time of 21 days.

Sulfamethazine has also been implicated in adverse drug reactions. It was postulated that the altered drug disposition in horses was due to protein binding interactions between sulfamethazine and flunixin meglumine. Flunixin meglumine has recently been approved for use in swine. Thus there is an increased likelihood that a drug interaction could be seen in swine. To explore this possibility, a PBPK model for sulfamethazine was designed that included linear plasma protein binding and competitive inhibition of plasma protein binding due to flunixin meglumine. The validated PBPK model accurately predicted both free and total sulfamethazine concentrations alone and in the presence of flunixin meglumine. The interaction predicted and identified *in vivo* was transient and would not contribute to a clinically relevant adverse drug reaction. However, this was the first time a validated PBPK model was used to predict drug interactions due to alterations in protein binding.

Based on the success of the PBPK models for sulfamethazine in swine, it can be concluded that the PBPK approach can be effectively applied to problems in veterinary medicine. Ultimately, this type of modeling will enhance the safety and efficacy of dosing regimens while further protecting our food supply. In addition, the investigation of drug interactions based on physiological mechanisms will continue to enhance our understanding of basic pharmacology.

APPLICATIONS OF PHYSIOLOGICALLY BASED PHARMACOKINETIC MODELS IN VETERINARY MEDICINE

by

JENNIFER LEEANN BUUR

A dissertation submitted to the Graduate Faculty of
North Carolina State University
In partial fulfillment of the
Requirements for the degree of
Doctor of Philosophy

COMPARATIVE BIOMEDICAL SCIENCES

Raleigh, NC
2007

Approved by:

Ronald Baynes, DVM, PhD

Jim Riviere, DVM PhD

Arthur Craigmill, PhD

Mark Papich, DVM, MS

Geof Smith, DVM, PhD

DEDICATION

"And I will try to find a higher purpose and meaning to life."

Richard Bach

Jonathan Livingston Seagull

To Erik N. Nielsen.

We both know what you have and haven't done to deserve this.

You truly are my golden one.

I love you.

BIOGRAPHY

Jennifer Leeann Buur was born and raised in the greater Los Angeles area of California. She completed her pre-veterinary course work at Washington State University in Pullman, Washington and received her Doctor of Veterinary Medicine in 1999 from the University of Wisconsin-Madison. After graduation, she joined private practice in Southern California were she gained clinical experience in small animal, exotic, zoo animal, wildlife rehabilitation, and shelter medicine. She left private practice in 2003 to pursue a dual residency and Doctor of Philosophy program in veterinary clinical pharmacology at North Carolina State University. She successfully completed her residency and in 2006 obtained status as a Diplomate of the American College of Veterinary Clinical Pharmacology. She is currently pursuing a Doctor of Philosophy in Comparative Biomedical Sciences under the direction of Drs. Ronald Baynes and Jim Riviere.

ACKNOWLEDGEMENTS

I am grateful for the support, encouragement, and training provided my committee members Drs. Ronald Baynes, Jim Riviere, Geof Smith, Arthur Craigmill, and Mark Papich. The technical support provided by Jim Yeatts, Beth Barlow, Patty Routh and Connie Engle was invaluable. I am also thankful for the guidance and humor of my colleagues Deon van der Merwe, Ronnette Gehring, Jessica Ryman-Rasmussan, and Scott Weldy. Last but not least, I must acknowledge the support, love, and reality checks given by my parents, Gregory and Starrann Buur. Without all of these people, I could not have accomplished what I have. Thank you.

TABLE OF CONTENTS

LIST OF TABLES viii

LIST OF FIGURES x

LIST OF ABBREVIATIONS xiii

1. INTRODUCTION 1

References 5

2. LITERATURE REVIEW 6

Pharmacokinetic Models 7

Quantifying Uncertainty in Pharmacokinetic Models 17

PBPK Applications 19

Model Compounds 26

Analytical Techniques 30

Summary 32

References 34

3. DEVELOPMENT OF A PHYSIOLOGICALLY BASED PHARMACOKINETIC MODEL FOR ESTIMATING SULFAMETHAZINE CONCENTRATIONS IN SWINE AND APPLICATION TO PREDICTION OF VIOLATIVE RESIDUES IN EDIBLE TISSUES 45

Abstract 46

Introduction 47

Materials and Methods 48

Results 54

Discussion 59

Acknowledgements 63

References 64

4. USE OF PROBABILISTIC MODELING WITHIN A PHYSIOLOGICALLY BASED PHARMACOKINETIC MODEL TO PREDICT SULFAMETHAZINE RESIDUE WITHDRAWAL TIMES IN EDIBLE TISSUES IN SWINE 67

Abstract 68

Introduction 69

Methods 72

Results 79

Discussion 82

Acknowledgments 86

References 87

5. PHARMACOKINETICS OF FLUNIXIN MEGLUMINE IN SWINE AFTER INTRAVENOUS DOSING 92

Introduction 93

Methods 93

Results 96

Discussion 97

Acknowledgements 99

References 100

6. A PHYSIOLOGICALLY BASED PHARMACOKINETIC MODEL OF PROTEIN BINDING INTERACTION BETWEEN SULFAMETHAZINE AND FLUNIXIN MEGLUMINE IN SWINE 103

Abstract 104

Introduction 105

Materials and Methods 106

Results 116

Discussion 118

Acknowledgments 124

References 125

7. CONCLUSIONS AND FUTURE DIRECTIONS 128
Conclusions 129
Future Directions 131
References 133

APPENDICES 134
PBPK Sulfamethazine Meat Withdrawal Time Model Code 135
PBPK Sulfamethazine Protein Binding Interaction Model Code 145

LIST OF TABLES

Table 2.1 Published pharmacokinetic values for Sulfamethazine in swine after intravenous and oral dosing 28

Table 3.1 Organ weights and blood flow distributions for market-weight swine determined from published studies 50

Table 3.2 Differential equations used to describe the rate of change of sulfamethazine in each tissue compartment 52

Table 3.3 Starting and final values and upper and lower limits for constants of a model used to determine concentrations after IV administration of Sulfamethazine to pigs 55

Table 3.4 Results for model validation accomplished by comparison of predicted concentrations to observed concentrations by use of an external data set 55

Table 4.1 Final values for insensitive parameters used in model simulations 74

Table 4.2 Final distributions for sensitive parameters used in the Monte Carlo analysis 75

Table 4.4 Tissue concentrations from IV injection of 35 mg/kg Sulfamethazine 79

Table 4.3 Plasma concentrations after IV injection of 35 mg/kg Sulfamethazine 79

Table 4.5 Withdrawal time predictions and 95% confidence intervals in days for the 99th percentile of the population for each edible tissue after 100 Monte Carlo runs of 1000 simulations 81

Table 5.1 Pharmacokinetic parameters for Flunixin Meglumine after 2.0 mg/kg IV dose in swine.....96

Table 5.2 Percent plasma protein binding at physiological concentrations of Flunixin Meglumine in swine.....97

Table 6.1 Final values for parameters used within the Sulfamethazine PBPK model and Sulfamethazine-Flunixin protein binding interaction model 113

Table 6.2 Differential equations used to describe the rate of change of Sulfamethazine in each tissue compartment.....114

Table 6.3 Final protein binding kinetic parameters for Sulfamethazine in fresh and frozen porcine plasma and Flunixin in fresh porcine plasma 118

LIST OF FIGURES

Figure 2.1 Schematic representation of a generic physiologically based pharmacokinetic model 10

Figure 2.2 Schematic representation of a complex tissue block 10

Figure 2.3 Theoretical schematic illustration of the consequences of protein binding alterations in an open system for a low ER drug (A) or high ER drug (B) during steady state conditions 26

Figure 3.1 Schematic representation of a physiologically based pharmacokinetic model for use in determining concentrations after IV injection of Sulfamethazine in swine 49

Figure 3.2 Results for the final fitted model simulation (solid line), compared with results for an external data set (circles), for plasma (A), liver (B), kidney (C), adipose (D), and muscle (E) tissue compartments 56

Figure 3.3 Standardized residual plots for fit of the results of the model for plasma (A), liver (B), kidney (C), adipose (D), and muscle (E) tissue compartments 57

Figure 3.4 Graphs of predicted and observed data for validation of the model for plasma (A), liver (B), kidney (C), adipose (D), and muscle (E) tissue compartments 58

Figure 3.5 Predicted depletion curves for tissue concentrations of drug in tissue compartments after IV administration of Sulfamethazine at a dosage of 50 mg/kg in swine 59

Figure 4.1 Schematic diagram of the PBPK model for Sulfamethazine in pigs.....72

Figure 4.2 Schematic diagram of the oral dosing route of administration.....73

Figure 4.3 Monte Carlo simulations for Sulfamethazine concentrations in edible tissues after intravenous administration.....80

Figure 4.4 Monte Carlo simulations for Sulfamethazine concentration in edible tissues after oral administration 80

Figure 4.5 Representative distribution of the time it takes for Sulfamethazine concentrations to fall below the tolerance of 0.1 ppm in kidney tissue from a Monte Carlo run of 1000 simulations 81

Figure 5.1 Chromatographs for swine plasma spiked with Flunixin Meglumine at a level of 0.1 µg/mL (A) and blank (B) 95

Figure 5.2 Mean plasma concentration +/- SD of Flunixin Meglumine after a 2.0 IV dose in swine.....97

Figure 6.1 Schematic diagram of the PBPK model for Sulfamethazine in swine 112

Figure 6.2 Protein binding saturation curve for Sulfamethazine in frozen (squares) and fresh (triangles) porcine plasma 117

Figure 6.3 Representative protein binding saturation curve for Flunixin in fresh porcine plasma 117

Figure 6.4 Results of validation of sulfamethazine PBPK model in swine for total drug 119

Figure 6.5 Comparison between observed (squares with dashed line) and predicted (solid line) values of total drug concentration for individual pigs using the Sulfamethazine-Flunixin protein binding interaction model 120

Figure 6.6 Comparison between observed (squares with dashed line) and predicted (solid line) values of total drug concentration for a representative pig at the time of interaction 118

Figure 6.7 Comparison between observed (squares) and predicted (solid line) values of free drug concentration for individual pigs using the Sulfamethazine-Flunixin protein binding interaction model.....121

Figure 6.8 Residual plot for fit of the results of the Sulfamethazine-Flunixin protein binding model for total Sulfamethazine concentration.....122

Figure 6.9 Residual plot for fit of the results of the Sulfamethazine-Flunixin protein binding model for free Sulfamethazine concentration 122

LIST OF ABBREVIATIONS

AMDUCA - Animal Medicinal Drug Use Clarification Act

FARAD - Food Animal Residue Avoidance Databank

FLU - Flunixin Meglumine

NSAID - Non-Steroidal Anti-Inflammatory

PBPK - Physiologically Based Pharmacokinetic

SMZ - Sulfamethazine

US-EPA - United States Environmental Protection Agency

US-FDA - United States Food and Drug Administration

USDA-FSIS - United States Department of Agriculture-Food Safety Inspection Service

1. INTRODUCTION

"All models are wrong, some models are useful." George E. P.. Box

Pharmacokinetic models provide the basis for rational drug use. This includes the design of dosing regimens that are both safe and effective. In veterinary medicine, the large numbers of species and ability to prescribe drugs in extralabel manners contribute to the complexity of rational drug use. Indeed, in food animal medicine, a veterinarian must also take into account the safety of the food supply by providing meat withdrawal intervals for every drug used in both label and extralabel manners ("Federal Food, Drug, and Cosmetic Act," 2004). In addition, veterinarians are also faced with the challenges of combination drug therapy. As more drugs have become available, combination drug therapy has become the standard of practice for treating many diseases. This has led to an increase in the probability of adverse drug reactions due to drug-drug interactions (Saltvedt et al., 2005). Thus there is a need in veterinary medicine for a pharmacokinetic modeling technique that is able to accommodate the large numbers of species, doses, and routes of administration, as well as to predict and evaluate the consequences of drug-drug interactions.

Pharmacokinetics, in its most general sense, is the study of how xenobiotics move through the body. It is studied using mathematical models that describe the course of drugs through the stages of absorption, distribution, metabolism and excretion. Classical compartmental modeling is theoretical and descriptive in nature. The compartments, rates, and other factors are not related to physiology or any other mechanistic model. Compartments are mathematically described by rate constants and make no attempt to provide information about underlying processes. These models comprise the bulk of what is published on veterinary pharmacokinetics and form the basis for drug dosing regimens and meat withdrawal times. Other modeling techniques, such as non-compartmental and mixed effect modeling (population based), are used to describe the disposition of drugs. They are also descriptive in nature and make no attempt to define underlying mechanisms (Riviere,

1999). Physiologically based pharmacokinetic (PBPK) models, on the other hand, are based on mass-balance equations defined by physiological mechanisms. They are predictive in nature and allow for the use of *in vitro* mechanistic data and population variability data to be applied to *in vivo* modeling techniques (Grass et al., 2002). Subsequently, there is an opportunity to increase specification and accuracy within a model. This allows more confident application of the models in such areas as dosing regimens, tissue residues, allometric scaling, disease state pharmacokinetic alterations, and drug-drug interactions.

Current standards of practice rely on formularies for dosing regimens as well as government approval for meat and milk withholdinf times. These recommendations are based on classical compartmental pharmacokinetic analysis that use healthy animals. Theoretically, PBPK modeling can make dosing and withholding time calculations after extralabel drug use more accurate and in accordance with the Animal Medicinal Drug Use Clarification Act (AMDUCA) ("Animal Medicinal Drug Use Clarification Act," 1994). These regimens could be modified to include individual animal parameters or population variability. Indeed, the stringent requirement of the time for the upper limit of the 95% confidence interval for the 99th percentile of the population to be below tolerance limit, as required by the United States Food and Drug Administration (US-FDA) for regulatory approval, can be derived by PBPK as well as the currently accepted Tolerance Limit Method (US-FDA-CVM, June 21, 2005). However, there is a paucity of related PBPK models in the literature and the uses and limitations of PBPK modeling have not been explored with regards to veterinary medicine.

The purpose of this body of work is to validate the use of PBPK models in veterinary medicine. PBPK models will be applied to the practical situations of meat withdrawal time prediction, for both extralabel drug use and regulatory requirements, and the theoretical situation of drug-drug interactions. To do this sulfamethazine (SMZ) and flunixin meglumine (FLU) are used as test compounds in a PBPK model of swine. These drugs represent the

common drug classes of sulfonamide antimicrobials and non-steroidal anti-inflammatory (NSAID) agents and are commonly used in swine medicine. Chapter 2 provides the scientific foundation for the studies presented by reviewing the literature on modeling techniques in both pharmacokinetics and population diversity, the theoretical basis behind plasma protein binding interactions, current methods in withdrawal time and withdrawal interval estimation, and the pharmacokinetic profiles of SMZ and FLU in swine. This is followed by specific studies showing the application of PBPK models to meat withdrawal interval estimation after extralabel drug use (Chapter 3) and in accordance with the US-FDA requirements for new drug approval (Chapter 4). The pharmacokinetic profile for FLU in swine is determined in Chapter 5 and then is applied to the prediction of plasma protein binding interactions between SMZ and FLU using a PBPK model in Chapter 6. The specific studies are followed by a summary of findings and generalized conclusions as well as areas of further study (Chapter 7).

References

Animal Medicinal Drug Use Clarification Act (1994). United States Food and Drug Administration. Title 21 Code of Federal Regulations, part 530.

Federal Food, Drug, and Cosmetic Act (2004). Title 21, Code of Federal Regulations, 21-CFR-500.80.

Grass, G. M. & Sinko, P. J. (2002) Physiologically-based pharmacokinetic simulation modelling. *Advanced drug delivery reviews*, **54**, 433-451.

Riviere, J. E. (1999). *Comparative Pharmacokinetics: Principles, Techniques, and Applications*. Blackwell Publishing, Inc., Ames, Iowa.

Saltvedt, I., Spigset, O., Ruths, S., Fayers, P., Kaasa, S. & Sletvold, O. (2005) Patterns of drug prescription in a geriatric evaluation and management unit as compared with the general medical wards: a randomized study. *Eur J Clin Pharmacol*, **61**, 921-928.

US-FDA-CVM (June 21, 2005). *Guidance for Industry #3: General principles for evaluation of the safety of compounds used in food producing animals.* Center for Veterinary Medicine. U.S. Food and Drug Administration, Washington, DC.

2. LITERATURE REVIEW

Pharmacokinetic Models

Classical Compartmental and Non-Compartmental Models

Classical pharmacokinetic modeling can be compartmental or non-compartmental in nature. Both methods generate a series of parameters that describe the course of the drug throughout a system including absorption, distribution, metabolism, and elimination. These phases are incorporated through the generation of rate constants that are based on passive diffusion across membranes. The rate of diffusion across a membrane is described by

$$Rate\ of\ Diffusion = \frac{D \bullet P \bullet A}{h} \bullet \Delta C \qquad [1]$$

where D is the diffusivity coefficient of the drug, P is the partition coefficient of the drug, A is the surface area of the membrane, h is the thickness of the membrane, and ΔC represents the concentration gradient. The diffusivity coefficient represents the inherent properties of the drug itself including hydrogen bonding, stereochemistry and solubility. The partition coefficient represents the relative lipophilicity of the drug. These parameters, combined with the thickness and surface area of the membrane, are all combined into a constant, Kp, that represents the permeability coefficient of the drug. Inserting Kp into **Equation 1**, you get

$$Rate\ of\ Diffusion = Kp \bullet \Delta C \qquad [2]$$

This equation is linear in nature. Thus the assumption of linear or first order kinetics is inherent in classical pharmacokinetic modeling (Riviere, 1999).

Compartmental kinetics uses a system of defined theoretical compartments to link together each of the above phases. Each compartment represents a portion of the biological system with similar rates of entry and exit. They are linked together using a series of microequations. The number of compartments can be estimated from evaluation of plasma concentration-time curves on a semilog axis, but have no relevance to physiology. A change in slope on the concentration-time curve represents a different compartment. The slopes can then be used in

combination with dose and plasma concentration values to calculate the kinetic parameters of half life ($T_{1/2}$), volume of distribution (Vd), and clearance (CL). Using these parameters, dosing regimens and withdrawal times can be calculated (Rowland et al., 1995).

Non-compartmental analysis, in contrast, makes no assumptions about how many compartments are within the system. Instead non-compartmental analysis uses stochastic methods to describe drug disposition. This is based on calculations including areas under the plasma concentration-time curve (AUC) as well as the first moment (concentration-time-time) curve (AUMC). These models allow for the calculation of a Mean Residence Time (MRT), or the average time a molecule of drug remains in the plasma. Using MRT as well as AUC and AUMC, you can calculate the pharmacokinetic parameters of $T_{1/2}$, Vd, and CL (Brown, 2001). Noncompartmental models assume first order elimination. Like compartmental analysis, non-compartmental approaches also make no claims as to physiological relevance.

Classical methods of pharmacokinetic analysis are not very labor intensive. Experimentally, they require knowledge of dose, route of administration, and plasma concentration levels for the drug over a period of time. They can be computed using a wide variety of easy to use software. They are also well established in industry, within peer review literature, and provide the framework for almost all dosing regimens presented in formularies. However, these models are not mechanistic in nature. That is, they are limited to the description of plasma concentration for that specific drug within that specific set of animals at that specific dose. By using doses calculated from these methods, a clinician is assuming that the patient will act in exactly the same way as the animals used in the kinetic study. Since most studies are carried out in a small number of healthy animals and patients represent a large number of diseased animals, the assumption can often be erroneous. However, most of the drugs used in veterinary medicine have a very high therapeutic index. Thus the validity of this assumption is not necessarily of major consequence.

Alternative Pharmacokinetic Models

Beyond classical pharmacokinetic modeling, there are a wide variety of alternative modeling approaches. Population or mixed effect modeling, non-linear modeling, and physiologically based pharmacokinetic approaches have all been applied to pharmacokinetics (Riviere, 1999).

Non-linear modeling is very similar to classical modeling techniques. The main difference is due to the assumption that not all rates are first order in nature. This allows for zero order processes such as metabolism, active transport, and protein binding to be included within the model (Riviere, 1999). Like classical models, this approach is descriptive and focuses on a individual within the population.

Population based pharmacokinetic modeling, on the other hand, uses a pharmacostatistical approach to characterize both a structural pharmacokinetic model (fixed effects) and a statistical model (random effects). This technique can be used to predict the disposition of a drug within a population not directly studied. Unlike classical modeling which heavily samples a small number of subjects, population modeling requires the incorporation of multiple subjects that are sporadically and sparsely sampled. Thus the focus of population modeling is the population rather than the individual (Martin-Jimenez Tomas, 2000).

Physiologically based pharmacokinetic (PBPK) models incorporate physiological and mechanistic descriptions into the mathematical representation of drug disposition. These models, like population based modeling, can be predictive in nature. They can also be easily changed to incorporate alterations in physiological state, age, dose, route of administration, and species (Krishnan et al., 2001).

A PBPK model is a series of tissue blocks linked together by a fluid plasma block. The tissue blocks represent tissues according to anatomical and physiological properties. Tissues can

be combined into fewer blocks or separated into more blocks depending on the need of the researcher. For example, the simplest model includes a single high flow tissue block, a single low flow tissue block, and a single excretory tissue block (**Figure 2.1**). The number and characteristics of the tissue blocks is dependent upon the sensitivity and specificity needed in the model itself. Each tissue block is subdivided into subcompartments that represent the vascular space of blood flow through the tissue, extracellular space, and finally the intracellular space. These subcompartments, like the blocks themselves, can be combined and simplified if needed (**Figure 2.2**).

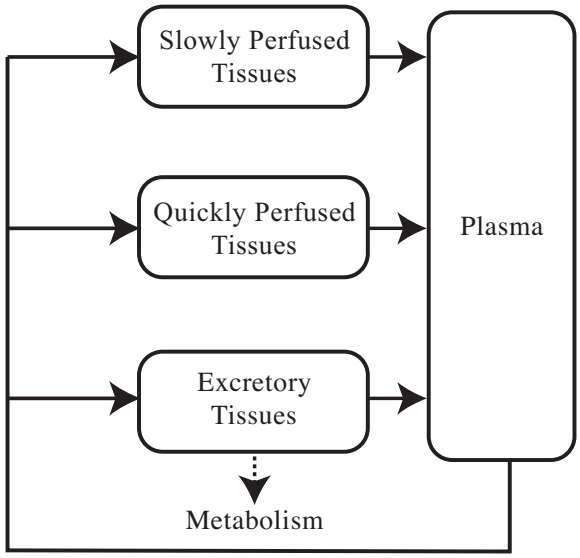

Figure 2.1 Schematic representation of a generic physiologically based pharmacokinetic model

Solid lines represent blood flow; dotted line represents elimination through metabolism or excretion.

Tissue blocks are then further categorized into either flow limited or membrane limited depending on the rate limiting characteristic of that specific tissue. Flow limited tissues are based on the assumptions of a well mixed model. That is, all partitioning of the drug from the blood into the tissue takes place instantaneously and in a homogenous manner. Thus the rate limiting step is the blood flow. This is normally the case for

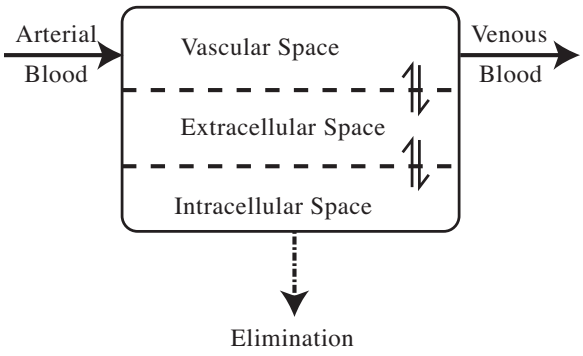

Figure 2.2 Schematic representation of a complex tissue block

Solid line arrows represent blood flow; dashed line arrow represents excretion; dual arrows represent mass transfer through subcompartments.

compounds that have a small molecular weight and are lipophilic. Organ systems that are relatively small in volume are also treated in this manner. Membrane limited tissues, on the other hand, are described when it is the diffusion across membranes that is the rate limiting step in partitioning. This occurs with higher molecular weight compounds that are polar in nature as well in large volume organs or in "protected" spaces such as the brain or testes (Ritschel et al., 1986).

Once the number of tissue blocks and their rate limiting features have been defined, the model is constructed by writing a series of mass balance differential equations. Mass balance is the mathematical concept that the total mass of a drug in a system is constant and can be accounted for. The differential equations describe the rate of change of concentration in the tissue block per unit time. For a flow limited tissue block, the simple form of this equation is

$$Vt \bullet \frac{dCt}{dt} = Qt \bullet (Ca - Cv) \qquad [3]$$

where Qt, Vt, and Ct are the blood flow, anatomic volume, and concentration of the drug in tissue t and Ca and Cv are the concentration of the drug in the arterial and venous circulations perfusing tissue t respectively. If you assume that Cv is in equilibrium with the vascular space, Cv can be further defined as

$$Cv = \frac{Ct}{Pt} \qquad [4]$$

where Pt is the tissue-to-blood partition coefficient for tissue t. Combining equations 3 and 4 yields:

$$Vt \bullet \frac{dCt}{dt} = Qt \bullet \left(Ca - \frac{Ct}{Pt} \right) \qquad [5]$$

The basic equation for a membrane limited tissue block, where the vascular space is assumed to be instantaneously in equilibrium with the extracellular space, is defined by the rate of change in the extracellular space per unit of time.

$$Ve \bullet \frac{dCe}{dt} = Qt \bullet (Ca - Ce) - Kt \bullet (Ce - Ci) \quad [6]$$

$$Vi \bullet \frac{dCi}{dt} = Kt \bullet \left(Ce - \frac{Ct}{Pt} \right) \quad [7]$$

where Ve and Ce are the anatomic volume and drug concentration of the extracellular space in tissue t; Vi and Ci are the volume of the intracellular space and the concentration of drug in the intracellular space respectively; Kt is the membrane permeability coefficient for tissue t.

Tissue blocks that metabolize or excrete the drug require further modification of **Equations 5 and 6**. The addition of a mass removal term, Rex, is then added to account for the loss of drug. Rex can be defined by any set of parameters ranging from a simple first order equation to detailed Michalis-Menten equations for multiple enzymes. The resulting equation for a flow limited tissue block is

$$Vt \bullet \frac{dCt}{dt} = Qt \bullet \left(Ca - \frac{Ct}{Pt} \right) - \text{Rex} \quad [8]$$

If Rex is a first order process, it could be described as

$$\text{Rex} = Kel \bullet Ct \quad [9]$$

where Kel is the first order elimination rate. Thus making the final equation

$$Vt \bullet \frac{dCt}{dt} = Qt \bullet \left(Ca - \frac{Ct}{Pt} \right) - Kel \bullet Ct \quad [10]$$

In much the same manner, the model can be further refined by adding terms to describe other processes including protein binding, tissue binding, active transport, biliary excretion, and enterohepatic metabolism.

The final step in writing the mathematical model is to write the equation that describe the plasma block. This block is again defined by mass balance where the inputs are the mass from each tissue block's venous return and the output is the arterial blood concentration. The rate of change in the plasma space per unit of time is then

$$Vp \bullet \frac{dCp}{dt} = \sum (Qt \bullet Cv) - (Qp \bullet Cp) \qquad [11]$$

where Vp, Qp, and Cp are the anatomic volume, the total blood flow, and the concentration of the drug in the plasma compartment respectively. Cv represents the venous concentration of the drug from tissue t that has blood flow Qt (Colburn, 1988; Gerlowski et al., 1983; Krishnan et al., 2001).

PBPK models include both physiological and physiochemical parameters. The physiological parameters include tissue volumes and blood flow rates. These are normally taken from the literature for the species of interest. The physiochemical parameters include partitioning coefficients for the drug as well as protein and tissue binding properties, Michalis-Menten metabolism constants, elimination rates, and absorption rates. These values can be found in the literature or, as is more often the case, be derived from *in vivo* and *in vitro* experiments (DeJongh et al., 1996; Reitz et al., 1988; Tsuji et al., 1983). In addition, *in silica* techniques that include quantitative structure-activity relationships (QSAR) can be used to estimate possible partition coefficient parameters (Beliveau et al., 2003; Fouchecourt et al., 2001; Yang et al., 1998). If parameters are unable to be derived or found in the literature, the parameter can be estimated using known data points. In this case, the model is fit to known data points until a "best fit" is achieved. There are several computational methods using maximum likelihood ratios that can produce these parameters. The resulting parameter values are used in subsequent simulations. Alternatively, parameters can be estimated by statistical distributions that represent possible population diversity (Price et al., 2003). It is important to note that there is a limit to the number of parameters that can be estimated by any single

curve fitting process. The purpose of curve fitting is to estimate a uniquely identifiable value for each parameter. Uniquely identifiable parameters are ones in which there is a single and unique solution for its value. Statistical limitations, including the degrees of freedom and number of data points available for each tissue block, limit the number of parameters that can be uniquely identified for any given curve fitting technique. Limitation of the curve fitting data set can result in either non-uniquely identifiable parameters (more than one, but still a finite number of values for the parameter) or unidentifiable parameters (infinite number of values) (Williams, 1990). Models that incorporate non-uniquely identifiable or unidentifiable parameters have little predictive value or biological relevance.

The accuracy of a PBPK model is directly related to the accuracy of the parameters used within the mass balance equations. If the parameters are not accurate or are not identifiable, the final model will not reflect true *in vivo* concentrations of the drug. Thus one major weakness of PBPK modeling is its dependence upon the source literature. However, PBPK models also allow for the inclusion of improved parameters as more information and mechanisms are elucidated.

Simulations are achieved by the simultaneous solving of the differential equations. Currently there are many software packages that are equipped to handle these types of computations. They can range from simple spreadsheet programs to more complex computer programming packages including Simusolv, ACSL, Cmatrix, MatLab and other fortran based programs (Ball et al., 1994; Johanson et al., 1988; Krishnan et al., 2001).

Validation of PBPK models occurs by comparing simulated values from the model with external data sets. Validation data sets are independent from data sets used for parameter estimation. Correlation plots, residual plots, and simulation graphs are evaluated to look at the overall goodness of fit of the model. There is no standardized way to apply statistics

in the evaluation of goodness of fit in PBPK modeling. However, the visual evaluation of these graphs do provide substantial information. The United States Environmental Protection Agency (US-EPA) recently published a guidance on the use of PBPK models in human health risk assessment that acknowledges the lack of stringent statistical evaluation for the validation of PBPK models. They suggest that visual inspection of simulation graphs is adequate in most instances (US-EPA, August, 2006).

Currently, the use of PBPK models is constrained mainly to toxicological applications including human health risk assessment (Bailer et al., 1997; Clewell H. J., 3rd et al., 1997; el-Masri et al., 1995; Gentry et al., 2002). This is mainly due to the time and data intensive nature of the models and the lack of acceptance of these models within industry and regulatory agencies responsible for drug approvals. The US-EPA allows for the inclusion of PBPK models within the risk assessment section for new pesticides (Anonymous, August, 2006). Beyond the myriad of examples of PBPK models describing disposition of individual toxicants, PBPK models have also been applied to the generation of reference doses and in the prediction of the disposition of chemical mixtures (Gentry et al., 2003; Haddad et al., 2001; Leavens et al., 1996). PBPK approaches allow for the inclusion of allometric scaling into the modeling of xenobiotic disposition (Clewell et al, 2004; Riviere et al, 1997). As is appropriate to human health risk assessment, the focus is on the scaling from rodents to humans (Young et al., 2001). However, these same techniques could be used to evaluate scaling between other types of mammals (ie. ruminants, horses) or non-mammals (i.e. reptiles, birds).

Beyond the applications in toxicology, PBPK is used in human medicine in the prediction of drug disposition for drugs with low therapeutic indices (i.e. cancer chemotherapeutics) as well as in patients with altered states of physiology such as pregnancy or pediatrics (Bjorkman, 2004; Kawai et al., 1994; Tsukamoto et al., 2001). However, the use of PBPK for specific

dose regimens, while touted as a strength of this modeling approach, has not been specifically published in the literature. In veterinary medicine, there is a paucity of PBPK models. Currently models have been validated for oxytetracycline in fish and sheep and sulfathiazole in swine (Brocklebank et al., 1997; Craigmill, 2003; Duddy et al., 1984). Like in human medicine, specific applications of these PBPK models have been mentioned but not published.

PBPK has also been applied to areas of theoretical research. PBPK models have been used to elucidate the underlying mechanisms and consequences of enzyme kinetic interactions, permeability alterations, absorption through the skin, and protein or tissue binding (Isaacs et al., 2004; Liu X. et al., 2005; Simmons, 1996; Teeguarden et al., 2005; van der Merwe et al., 2006). The PBPK approach has also been applied to drug development (Blesch et al., 2003; Charnick et al., 1995).

Summary

In summary, there are a wide variety of pharmacokinetic modeling approaches. These include classical techniques of compartment and non-compartmental analysis, non-linear, population, and PBPK modeling. Each modeling approach has its own set of strengths and weaknesses. PBPK models have some significant advantages over classical pharmacokinetic models. However, they are time and data intensive and are dependent upon the quality of data available for parameter estimation. Due to the variability between models and lack of a standardized statistical method for validation, PBPK models are also problematic to regulatory agencies. Advantages of the PBPK approach include the ability to incorporate multiple dosing routes of administration, dosages, species, as well as interindividual variability. PBPK models are predictive in nature and can be used to look at variability in populations and subpopulations. They can also continue to be refined as new data is derived and mechanisms are elucidated. Currently, they are mainly used in toxicology but could be applied to practical situations within veterinary medicine.

Quantifying Uncertainty in Pharmacokinetic Models

All models incorporate some amount of uncertainty. Uncertainty can come from random variability, lack of knowledge, or error (Frederick, 1993; Jang et al., 1999). There are a wide variety of ways that uncertainty can be incorporated into pharmacokinetic models. Within population based pharmacokinetic modeling, uncertainty is modeled within the statistical model and covariates are incorporated that reduce the calculated error (Martin-Jimenez Tomas, 2000). Within other types of models, uncertainty is often incorporated by defining parameters in terms of distributions rather than single point estimates. Simple Monte Carlo sampling techniques are used to incorporate distributions and randomness into parameter values. Markov Chain Monte Carlo analysis allows for the incorporation of population variability into parameter estimation (Wakefield, 1996). And finally, bootstrap resampling approaches are used to assess uncertainty and derive confidence intervals around simulations (Hunt et al., 1998). The end result of each of these techniques is a more transparent method of including stochastic methodology into the modeling system.

Simple Monte Carlo sampling is a stochastic approach that, unlike the point estimates used in deterministic approaches, uses a combination of random numbers and probability to determine the value of a parameter. In this simplistic form, it allows for the estimation of uncertainty and the evaluation of the consequences of that uncertainty within a given mathematical model. In the case of pharmacokinetics, this allows for the incorporation of population variability. The end result is that simulations represent not just a single, average member of the population, but the diversity of the population itself.

Simple Monte Carlo sampling is an iterative process. Values for each parameter are determined by a statistical distribution defined by the parameter's probability density function (pdf). For each simulation, a random value is generated for each parameter based on the pdf. These values are placed into the mathematical model, the model is run, and the simulation is stored.

These steps are repeated for N number of times (ranging from 500 to over 10,000 depending on the situation). The entire set of simulations are then analyzed and conclusions are drawn regarding the population. This process relies on several major assumptions. The first is that the pdf used to describe the parameters is true. The second is that parameters are distributed independently (Wittwer, 2004). Within a PBPK model, the independence assumption is often invalid. This results in overestimation of the consequences of variability (Thomas et al., 1996).

Simple Monte Carlo sampling techniques have been used in a variety of ways since they explore the consequences of uncertainty within a system. Simple Monte Carlo sampling has been incorporated into PBPK models and used in human health risk assessment (Clewell H. J., 3rd et al., 1996; Clewell H. J. et al., 1999; Gearhart et al., 1993; Sweeney L. M. et al., 2001). It is considered to be a useful tool in industry and is an accepted method of incorporating uncertainty into simulations required by US-EPA (US-EPA, March 1997). Its use in the estimation of meat withdrawal times has been theorized (Lathers, 2002). In veterinary medicine, the use of simple Monte Carlo sampling techniques centers around epidemiological studies in disease risk factors, prevention of disease, and prevalence of disease within the population (Hopp et al., 2003; Karsten et al., 2005).

Bootstrap approaches use a similar iterative process as what was described for simple Monte Carlo sampling. In bootstrap techniques, however, the data set used to derive parameter values is an actual data set of observed values and not a pdf. This allows for the generation of confidence intervals around simulations (Iwi et al., 1999; Parke et al., 1999).

Markov Chain Monte Carlo simulations are a type of Bayesian analysis that can be used for parameter estimation. In this scenario the same type of iterative process that is used in simple Monte Carlo sampling is performed. Parameter values are sampled from an *a priori* distribution. Each iteration is analyzed using a likelihood function that dictates how

probable a population is to produce a particular set of data. Parameter distributions are then updated based on each iteration and its likelihood ratio. Eventually, parameter distributions converge into a stable pdf that is now termed *a posteriori* distribution. In this way, the pdf of the population are included within the parameter estimation process (Jonsson et al., 2003, Krishnan K. et al., 2005). Markov chain Monte Carlo techniques are used in toxicology to assess risk due to environmental exposures and in veterinary medicine to identify risk factors associated with disease (Green et al., 2004; Jonsson et al., 2002).

No matter how uncertainty is incorporated into PBPK models, it provides an added dimension to the usefulness of PBPK as a tool. Indeed, it allows PBPK models to be used as a tool for both individual applications (ie. dosing regimens or estimated meat withdrawal time intervals after extralabel drug use) and population based applications (herd health management or public health).

PBPK Applications

Regulatory Applications

The ability to accurately incorporate population variability creates an opportunity for PBPK models to be used in regulatory applications that ensure food safety. Beyond the use of PBPK in US-EPA assessments, appropriate pharmacokinetic analysis is essential to protection of our meat supply. To ensure public health, the United States Food and Drug Administration (US-FDA) requires that all animal products that enter the food supply are free from harmful levels of drugs. To ensure this, for all approved drugs used in food animals, a meat withdrawal time (time between the last dose of drug given and when animal products can be placed in the human food chain) is derived that guarantees drug residues will fall below stated tolerance levels. This must hold true for the upper limit of the 95% confidence interval for the 99th percentile of the population ("Federal Food, Drug, and Cosmetic Act," 2004). The tolerance is the concentration of drug below which is considered safe for human consumption.

Currently, meat withdrawal times are calculated using the Tolerance Limit Method. This method calculates a regression line for the linear portion of the depletion curve of the drug of interest in the tissue of interest. Data taken from individual animals serially slaughtered is used to estimate the variance associated with this regression curve. Using the variance, a new line is plotted that represents the 99th percentile of the population. A 95% confidence interval is then calculated around the 2nd regression line. The meat withdrawal time is then derived by plotting the depletion curve for the upper limit of the 95% confidence interval and determining the time for that curve to be below the stated tolerance limit (US-FDA-CVM, June 21, 2005).

The Tolerance Limit Method assumes linearity, normality, homoscedasticity, and independent sampling. Critics cite violations of these assumptions as reasons for error and inconsistency within the method (Concordet et al., 1997a; Fisch, 2000). They present the argument that since the time points used to generate the original data rarely contain the final withdrawal time, that one must assume that depletion continues at the same rate. There are many instances of drugs that show multi-exponential decay patterns in which this assumption of linearity does not hold true. Furthermore, the linear depletion curve can be described by as few as 4 different time points. Thus not only can the inference space from the residue study not include the withdrawal time, but the regression line could be artificially influenced by data points taken from a different phase of depletion due to the relative paucity of time points included within the regression line. In addition, critics put forth that there is no basis for the assumption of a log normal distribution and that it would under predict withdrawal times. They also question the assumption of homoscedasticy and cite variability in analytical method and population variability as reasons why this may not hold true. Finally, critics raise questions regarding the independence of samples taken from the same animal, such as milk or biopsy (Concordet et al., 1997a; Fisch, 2000). Taken as a whole, these concerns have encouraged debate and discussion about the validity of the underlying statistics inherent within the Tolerance Limit Method.

The US-FDA has responded to these concerns (Martinez et al., 2000). They address the concern of linearity by simply stating that proper study design will ensure that the assumption of linearity is met and the withdrawal time will fall within the inference space. If all samples are truly independent, then, they contend, the assumptions of a log normal distribution and of homoscedasticity would be true. They also state that since variance is required to be calculated at every time point and then statistically evaluated for discrepancies, instances where the assumption is not valid would be detected. Finally, they agree that statistical independence of sampling would not be the case in situations such as multiple biopsies. Again, they defend the method by stating that these concerns are addressed by proper study design (Martinez et al., 2000).

The debate over proper statistical methods has led to a discussion regarding alternative approaches to the calculation of meat withdrawal times. These alternative methods include non-parametric and Bayesian methods. Briefly, non-parametric methods do not assume any underlying statistical distribution and thus do not allow for interpolation between or beyond the time points tested. Instead, it assumes that the probability of detecting a residue above the tolerance limit decreases over time. It also assumes, as do parametric methods, that all samples are independent and that samples are taken during the depletion portion of the concentration-time curve. Data, using this method, are tested using binomial procedures until an appropriate withdrawal time is found. An appropriate withdrwal time is considered to be when the tissue residue limits are below the Minimum Residue Limit (MRL) established by the government. This limits the final withdrawal time to be a time point when samples are taken. Also, the multiplicity of testing can result in an increase in Type I error (H_0 is rejected when it is true) which can only be reduced by increasing the number of samples taken. Bayesian methods have also been suggested for such situations where there are violations in both parametric and non-parametric assumptions. Using Markov Chain Monte Carlo methods, flexibility now is introduced into the model and its estimates while reducing the

dependence upon approximations. Similarly, simple Monte Carlo analysis has been used to evaluate the assumptions of various withdrawal time estimation methods (Concordet et al., 1997b; Fisch, 2000).

Beyond the determination of withdrawal times for labeled uses, veterinarians must also estimate withdrawal intervals when drugs are used in an extralabel manner. Risk assessment strategies, most notably the Animal Medicinal Drug Use Clarification Act (AMDUCA), have been put in place to help preserve the safety of the food supply and still allow for appropriate treatment of food producing animals (Gehring et al., 2006). Under AMDUCA, veterinarians are allowed to use drugs in an extralabel manner when there is a valid veterinary-client-patient relationship, the drug is being used for therapeutic purposes, no other drug is approved for use in that condition in that species, the drug is a US-FDA approved therapeutic that is not specifically prohibited from extralabel drug use, and no violative residues in food will result. However, extralabel use of feed additives is specifically prohibited except when used in minor species ("Animal Medicinal Drug Use Clarification Act," 1994). Withdrawal intervals, in this instance, must be based on scientific information and substantially extended to ensure food safety. Currently, the Food Animal Residue Avoidance Databank (FARAD) provides estimated withdrawal intervals to veterinarians by applying the principles of pharmacokinetics to situations of altered dose, route of administration, or species. FARAD uses a combination of methods to produce these withdrawal intervals including classical and population based pharmacokinetic analysis of published and proprietary data, the Extrapolated Withdrawal-Interval Estimator (EWE) Algorithm, foreign drug approval recommendations, and half-life multipliers (Gehring et al., 2004; Martin-Jimenez T. et al., 2002; Payne et al., 1999).

PBPK modeling could be used as a tool to satisfy regulatory agencies and comply with current law. Because PBPK models can incorporate uncertainty in ways that allow for the quantification of risk, it could potentially be used as an alternative to the Tolerance Limit

Method. Indeed, PBPK models are already used as tools within the US-EPA in other areas of human health risk assessment (US-EPA, August, 2006). In addition, PBPK models have been postulated to be useful tools in the prediction of meat withdrawal intervals in situations of extralabel drug use (Craigmill, 2003).

Drug-Drug Interactions

Beyond the practical application of PBPK modeling to regulatory concerns, PBPK approaches can be used to elucidate the underlying mechanisms and clinical consequences of drug-drug interactions. Combination drug therapy is quickly becoming the standard of practice in both human and veterinary medicine. As the number of drugs concurrently prescribed increases, so too does the chance for drug interactions (Saltvedt et al., 2005). Possible areas of interaction relate to altered metabolism (ie. enzyme kinetics), distribution (ie. protein binding), or efficacy (ie. pharmacodynamic).

Among the known routes for drug interactions, alteration of enzyme kinetics has been the most studied using a PBPK approach. Mechanisms of induction and inhibition have been successfully modeled using PBPK models due to the unique ability to incorporate *in vitro* data such as enzyme kinetics into the model itself (Kanamitsu et al., 2000; Reitz et al., 1988). Validated models have been published that not only predict alterations in drug disposition due to enzyme alterations, but also that explore the underlying mechanisms of the interactions themselves (Isaacs et al., 2004; Leavens et al., 1996; Simmons, 1996). Models that incorporate enzyme kinetics have been validated for fetal, neonatal, and adult exposures of single compounds as well as simple mixtures (Bjorkman, 2004; Haddad et al., 2001). These models have then been applied to human health risk assessment.

There are substantial quantities of PBPK models that incorporate protein binding and single or multiple pharmacodynamic effects (Leavens et al., 1996; Teeguarden et al., 2005;

Tsuji et al., 1983; Yassen et al., 2005). However, there have not been any published PBPK models that look at interactions within or between these characteristics. Indeed, aside from the modeling of enzyme interactions, there is a paucity of PBPK models for other areas of possible drug interactions.

Protein binding interaction is an area where the physiological nature of PBPK models would be useful to explore both mechanism and clinical impacts of possible drug interactions. Albumin is the most common binding protein found in plasma and thus the site for potential interactions. There is evidence that albumin is highly flexible and contains multiple sites for drug binding, both specific and non-specific in nature (Kragh-Hansen, 1988). However, there are significant species differences in binding characteristics of drugs to plasma albumin (Kosa et al., 1997). In humans, both antimicrobial agents and non-steroidal anti-inflammatory agents have been found to bind to albumin (Honore et al., 1984; Zeitlinger et al., 2004).

Within PBPK modeling, there are a large number of models that incorporate plasma protein binding to albumin. In fact, these models have been used to explore the effects of binding parameters on tissue distribution and alterations in efficacy and toxicity (Liu X. et al., 2005; Teeguarden et al., 2005). However, there are no published models showing potential interactions at the level of plasma protein binding.

Plasma protein binding is important in determining the safety and efficacy of chemotherapeutics. Both are determined by the concentration of free drug since only unbound drug is available for distribution into other sites or to produce a pharmacological or toxicological effect. The amount of free drug in a system is related to the maximum binding

capacity (Bmax) of the individual drug and the equilibrium dissociation constant (Kd), which is the concentration of drug at half of Bmax. For linear binding,

$$C_{free} = \frac{C_{tot} \bullet Kd}{B\max + Kd} \quad [12]$$

where C_{free} and C_{tot} are the concentrations of free and total drugs respectively (Toutain et al., 2002). Both Kd and Bmax can be altered in the presence of other substances (Ascenzi et al., 2006). Based on **Equation 12**, the result would be an alteration in the free drug concentration.

The clinical relevance of these interactions in an open system is a topic of confusion (Benet et al., 2002; Toutain et al., 2002). There are several mathematical proofs for why these interactions may not be clinically relevant. However, these theoretical models have not been validated by *in vivo* experiments. The most common proof is summarized as follows. Free fraction of a drug is defined as

$$fu = \frac{C_{free}}{C_{tot}} \quad [13]$$

where fu is the free fraction of the drug. For low extraction ratio drugs (ER<0.3),

$$CL_{tot} = fu \bullet CL_{\text{int}} \quad [14]$$

$$CL_{free} = CL_{\text{int}} \quad [15]$$

$$C = \frac{ER}{CL} \quad [16]$$

CL_{int}, $CL_{free,}$ and CL_{tot} are intrinsic, free, and total drug clearance respectively; C is concentration of drug at steady state; and ER is extraction ratio of the drug. CL_{tot} is dependent upon fu while CL_{int} is independent of fu. Thus CL_{tot} will increase and CL_{free} will stay the same when fu is increased. Since steady state concentrations are determined by CL (**Equation 16**), the result is a decrease in C_{tot} and a transient increase of C_{free} during times of competition. The resulting alteration in fu would fall back to the normal value after 4 half lives (**Figure**

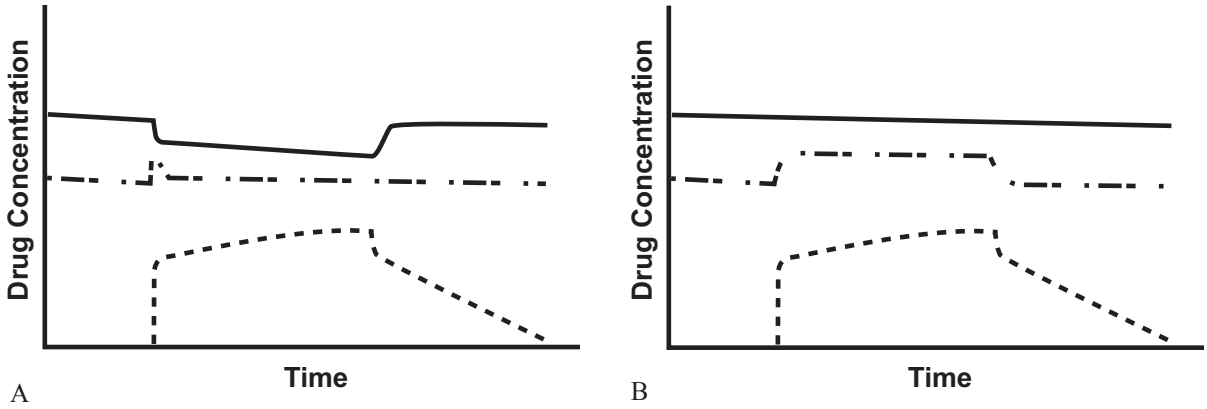

Figure 2.3 Theoretical schematic illustration of the consequences of protein binding alterations in an open system for a low ER drug (A) or high ER drug (B) during steady state conditions

Solid line represents total drug; dot-dashed line represents free drug; dotted line represents binding inhibitor

2.3). The corollary to this argument is that high ER drugs could have a sustained increase in fu since CL_{free} is now dependent upon fu while CL_{tot} would remain the same (**Figure 2.3**) (Rowland et al., 1995). However, there are very few high ER drugs used in veterinary and human medicine that are also highly protein bound. Clinically relevant drug interactions due to protein binding would be uncommon (Benet et al., 2002; Toutain et al., 2002).

While protein binding interactions may not be relevant to alterations in clinical effect, they can be relevant to therapeutic drug monitoring. Most techniques measure total drug concentration. As can be seen in **Figure 2.3**, the C_{tot} decreases in the presence of a competitive inhibitor. This could lead to erroneous increases in dose that could lead to toxicity or other adverse drug reactions (Benet et al., 2002).

Model Compounds

Sulfamethazine

Sulfamethazine (SMZ), also known as sulfadimidine, is a sulfonamide antimicrobial labeled for use in pigs as a feed additive to prevent and treat cervical abscesses, colibacillosis, swine

dysentery, and bacterial pneumonia, as well as for increasing feed efficiency in the presence of other disease such as atrophic rhinitis (Anonymous, 2006). Sulfamethazine is a zwitter ion (has both acidic and basic functional groups) with pKa's of 2.65 and 7.4. It has a molecular weight of 278.33 g/mol. Sulfamethazine's polar nature is reflected in the octanol:water partition coefficient ($K_{o/w}$) of 1.41 and a log ($K_{o/w}$) of 0.15 at pH 7 (Carda-Broch et al., 2004). The US-FDA and other international regulatory agencies have set a residue tolerance limit for sulfamethazine to be 0.1 ppm in all edible tissues of swine ("Federal Food, Drug, and Cosmetic Act," 1982)

The pharmacokinetics of SMZ have been extensively studied in multiple species including carp, cattle, chickens, goats, horses, humans, rats, sheep, snails, swine, and turtles (Nouws J.F.M. et al., 1986b; Paulson et al., 1983). In swine, SMZ is directly metabolized to N4-acetyl metabolite in the liver by the N-Acetyltransferase 2 (NAT-2) enzyme rather than the more common phase I pathway of hydroxylation found in most other species. The N4-acetyl metabolite is then cleared by the kidneys or is deacetylated back into the parent compound (Mengelers et al., 1997; Shimoda et al., 1997). Both genetic and gender differences in the NAT-2 enzyme have been documented in hamsters, humans, mice, rabbits, rats, and ruminants; resulting in the classification of fast and slow acetylators. However this variability has not been documented in swine (Hoogenboom et al., 1989; Mengelers et al., 1997). SMZ has a moderate extraction ratio of around 0.58 in the rabbit (du Souich et al., 1981).

Sulfamethazine in swine is most commonly described using a 2 compartmental model that is characterized by a short distribution phase followed by a longer elimination phase. On average, the elimination half life ($T_{1/2}$) in swine is 17 hours, total body clearance (CL_{body}) is 33 mL/kg/h and the volume of distribution (Vd) is 0.54 L/kg. Bioavailability (F) of oral preparations ranges from 48 to 89 % depending on formulation and the presence of feed (Kokue et al., 1988; Kuiper et al., 1988; Nouws J. F. et al., 1989; Nouws J. F. et al., 1986a;

Table 2.1 Published pharmacokinetic values for Sulfamethazine in swine after intravenous and oral dosing

Parameter	Abbreviation	Unit	Mean	Range	
				Lower	Upper
Elimination Half Life	$T_{1/2}$	h	16.8	9.8	28
Total Body Clearance	CL_t	mL/kg/h	33	21	54
Renal Clearance	CL_r	mL/kg/h	21	5	34
Volume of Distribution	Vd	L/kg	0.54	0.28	0.77
Bioavailability (oral dose)	F	%	74	48	89
Rate of Absorption	K_a	1/h	0.34	0.12	0.5
Protein Binding		%	69.5	64	72

Nouws J.F.M. et al., 1986b; Piva et al., 1997; Poucke et al., 1994; Romvary et al., 1976; Shimoda et al., 1997; Sweeney R. W. et al., 1993; Yuan et al., 1997). Sulfamethazine is moderately protein bound (ranging from 60 to 87 %) to albumin at the warfarin binding site (Munsey et al., 1996). A summary of the average pharmacokinetic parameters for SMZ in swine is presented in **Table 2.1**.

Flunixin Meglumine

Flunixin Meglumine (FLU) is a non-steroidal anti-inflammatory (NSAID) used in many species. It is currently labeled for intramuscular (IM) use in swine for the treatment of pyrexia associated with respiratory disease (Anonymous, 2006). The molecular weight of the salt is 491.46 g/mol. It is a weak acid with a pKa of 5.82 and a log ($K_{o/w}$) of 5.22 for the free flunixin acid (TerraQSAR-LOGP).

The pharmacokinetics of FLU have been studied in camels, cattle, chickens, equines (including donkeys, mules, and horses), felines, goats, llamas, rabbits, and sheep (Anderson et al., 1990; Baert et al., 2002; Cheng et al., 1998; Coakley et al., 1999; Elmas et al., 2006; Horii et al., 2004; Konigsson et al., 2003; Navarre et al., 2001; Oukessou, 1994). In swine

after IM dosing, FLU is characterized by a 2 compartment model. The mean elimination $T_{1/2}$ is between 3 to 4 hours; Vd is 2.003 L/kg; and CL_{body} is 390 mL/kg/h. Bioavailability of an IM dose is reported to be 87% ("Freedom of Information Summary," 2005). Flunixin is cleared via biliary excretion and there is evidence of enterohepatic recycling in cats, cattle, and goats (Anderson et al., 1990; Horii et al., 2004; Konigsson et al., 2003). It is over 99% protein bound in plasma in cats, cattle, and horses (Anderson et al., 1990; Coakley et al., 1999; Horii et al., 2004).

Clinical relevance

According to the United States Department of Agriculture-Food Safety Inspection Service (USDA-FSIS) Red Book, in 2000 SMZ was the number one violative residue found in swine and in 2003 was the only sulfonamide found in violation of tolerance limits (FSIS, 2001; FSIS, 2004). This presents a significant public health concern due to both a large percentage of human allergic reactions related to sulfonamide drugs and evidence that SMZ can contribute to the formation of thyroid tumors in rats (Poirier et al., 1999; Slatore et al., 2004; Wong et al., 2005). The current meat withdrawal time is 15 days.

In addition to the meat safety issues, sulfonamides have been associated with serious adverse drug reactions due to drug interactions. In particular, SMZ and Cyclosporin A were reported to have had a significant drug interaction (Jones et al., 1986). In veterinary medicine, there is a report of altered pharmacokinetics of SMZ when given in the presence of FLU in horses. The authors concluded that the alterations were based on protein binding interactions (el-Banna, 1999). The concurrent use of an antimicrobial agent and an NSAID is becoming the standard of practice in both human and veterinary medicine, making SMZ and FLU reasonable model drugs to use for both food safety and drug-drug interaction models.

Analytical Techniques

Chromatography

Chromatography is a common method for the quantification of drugs within biological systems. Thin layer chromatography (TLC), liquid chromatography (LC) including high pressure (HPLC) or ultra-high pressure (UPLC) chromatography, and gas chromatography (GC) are all methods that use the different physiochemical properties of drugs to provide adequate separation between the molecule of interest and biological interferences. The results can be used for both confirmation and quantification of drugs within a biological matrix (de Silva, 1985; Stolker et al., 2005). Each method has its own uses, advantages, and disadvantages.

Separations by TLC are achieved by differences in adsorption or partition properties of the plate and the molecules of interest. This technique is rapid, inexpensive, and allows for visual semi-quantification. Quantification can be achieved directly by fluorescence, fluorescence quenching, and densitometry; or indirectly by using TLC as a clean up technique prior to some other form of quantification such as HPLC (de Silva, 1985).

Gas chromatography methods offer high levels of sensitivity and specificity. They are suited for drugs that are heat stable and semi-volatile or volatile in nature. The mobile phase in GC analysis consists of an inert gas that serves as a medium to pass the gaseous drug through a column where differences in binding properties will allow for adequate separation. The wide variety of detectors that can be connected to GC systems allows for significant versatility (de Silva, 1985). The model drugs described above are neither semi-volatile or volatile in nature. Thus LC methods were developed for both plasma and tissue quantification.

Both HPLC and UPLC methods use liquids, rather than gas, as the mobile phase. They can be run in normal phase (organic solvent as the mobile phase) or reverse phase (inorganic

solvent as the mobile phase) conditions depending on the molecule of interest. Differences between HPLC and UPLC are derived from the pressures generated within the system. The higher pressures found in UPLC systems allow for quicker analysis and slightly altered separation properties. Like GC systems, LC systems can be combined with a wide variety of detectors making them versatile, sensitive, and specific. LC methods are suited to the analysis of thermally unstable compounds, non-volatile compounds or zwitterionic compounds. It is the method of choice for the quantification of SMZ in tissues (de Silva, 1985; Stolker et al., 2005).

Protein Binding Parameters

The protein binding parameters Kd (equilibrium dissociation constant) and Bmax (maximal binding) can be determined from analysis of *in vitro* saturation binding experiments. Saturation binding experiments require the quantification of specific binding of drug at various concentrations while levels of protein are held constant. Quantification of bound drug is most often done using radioligand approaches. However, unlabeled drug can be quantified *in vivo* using microdialysis, or *in vitro* using equilibrium dialysis, ultrafiltration, high-performance frontal analysis, and automated sequential trace enrichment of dialysate (Liu Z. et al., 1999).

Ultrafiltration methods are simple and quick to perform. Plasma samples containing both bound and free drug are placed in a cartridge that contains a semipermeable membrane. Free drug is forced through the membrane using the negative pressure created during centrifugation and collected as ultrafiltrate. Ultrafiltrate is subjected to chromatographic analysis and free drug concentration is quantified. There is often a very small volume of ultrafiltrate collected that can make quantification of highly bound drugs difficult due to limitations in detection within the analytical method. This method assumes that there is no adsorption of drug to the membrane, the drug-protein binding is at equilibrium, the binding

equilibrium does not change with altered concentrations of protein, and there is no leakage of bound proteins through the membrane. Unlike equilibrium dialysis, there are no issues with volume shifts and dilution of samples. And unlike high-performance frontal analysis it does not require large volumes of sample for analysis. These traits make it a very common procedure for therapeutic drug monitoring as well as in basic pharmacology research (Liu Z. et al., 1999; Wright et al., 1996).

Once obtained, specific binding data is used to estimate Kd and Bmax. Values are estimated using nonlinear regression techniques that fit a one site binding hyperbola equation (**Equation 17**) to the data using least likelihood ratios.

$$C_{bound} = \frac{B\max \bullet C_{tot}}{Kd + C_{tot}} \qquad [17]$$

C_{bound} is the concentration of specifically bound drug. Older methods including Scatchard, double reciprocal, or Rosenthal plots require the transformation of data to linearize the data. The transformation process distorts error and violates assumptions of linear regression by altering the relationship between the values on the X and Y axis. Since nonlinear techniques do not require the transformation of data, they provide more accurate parameter estimations. However, this type of analysis does assume that binding follows the law of mass action, the sample is at equilibrium, there is only one site for binding, there is no cooperativity, and only a small fraction of the drug is bound. The last assumption addresses alterations in binding affinities due to ligand depletion. Ligand depletion creates variability between concentrations. It is minimized by reducing the amount of protein or by increasing the amount of drug in the system (Motulsky, 1995).

Summary

There are several ways to mathematically model the disposition of drugs. These include compartmental, non-compartmental, population, and PBPK approaches. PBPK models

have the advantages of being mechanistic, predictive, flexible in terms of dose, route of administration and species, and can include *in vitro* mechanistic data. The accuracy of these models can be continually improved over time as more is learned regarding the underlying processes of drug disposition. In addition, PBPK models can incorporate uncertainty by the use of Bayesian techniques like simple Monte Carlo sampling that use a combination of statistical distributions and randomness to predict population parameters.

The versatility of PBPK models makes them uniquely suited to applications in food safety where they could serve as an alternative method to the Tolerance Limit Method currently used for establishing meat withdrawal times for labeled drugs and as a collaborative method for the estimation of meat withdrawal intervals for drugs used in an extralabel manner. Beyond the practical applications, PBPK models are also used to study the underlying mechanisms that determine drug disposition for single drug exposures as well as in times of concurrent drug administration. The techniques have been used in enzyme alterations and could be extended to situations involving protein binding interactions.

To look at the possible applications of PBPK models in veterinary medicine, SMZ and FLU were chosen as model drugs. Large number of violative tissue residue levels in swine have been attributed to SMZ. This represents a significant risk to human health. In addition, SMZ is reported to have significant drug interactions that are thought to be due to plasma protein interactions. The large body of literature detailing SMZ kinetics in swine provide the basis for PBPK model parameterization and validation. FLU has not been extensively studied in swine. However, it has recently become an approved product. This could lead to a potential increase in the number of cases where SMZ and FLU will be given concurrently. Reports of interactions between these drugs in other species make modeling possible interactions both clinically and theoretically relevant.

References

Anderson, K. L., Neff-Davis, C. A., Davis, L. E. & Bass, V. D. (1990) Pharmacokinetics of flunixin meglumine in lactating cattle after single and multiple intramuscular and intravenous administrations. *American Journal of Veterinary Research*, **51**, 1464-1467.

Animal Medicinal Drug Use Clarification Act (1994). United States Food and Drug Administration. Title 21 Code of Federal Regulations, part 530.

Anonymous (2006). *Compendium of Veterinary Products*, 9th Edition Eds S. Inglis. Adrian J. Bayley, Port Huron, Michigan.

Ascenzi, P., Bocedi, A., Notari, S., Fanali, G., Fesce, R. & Fasano, M. (2006) Allosteric modulation of drug binding to human serum albumin. *Mini Rev Med Chem*, **6**, 483-489.

Baert, K. & De Backer, P. (2002) Disposition of sodium salicylate, flunixin and meloxicam after intravenous administration in broiler chickens. *Journal of Veterinary Pharmacology and Therapeutics*, **25**, 449-453.

Bailer, A. J. & Dankovic, D. A. (1997) An introduction to the use of physiologically based pharmacokinetic models in risk assessment. *Statistical methods in medical research*, **6**, 341-358.

Ball, R. & Schwartz, S. L. (1994) CMATRIX: software for physiologically based pharmacokinetic modeling using a symbolic matrix representation system. *Comput Biol Med*, **24**, 269-276.

Beliveau, M., Tardif, R. & Krishnan, K. (2003) Quantitative structure-property relationships for physiologically based pharmacokinetic modeling of volatile organic chemicals in rats. *Toxicol Appl Pharmacol*, **189**, 221-232.

Benet, L. Z. & Hoener, B. A. (2002) Changes in plasma protein binding have little clinical relevance. *Clin Pharmacol Ther*, **71**, 115-121.

Bjorkman, S. (2004) Prediction of drug disposition in infants and children by means of physiologically based pharmacokinetic (PBPK) modelling: theophylline and midazolam as model drugs. *British Journal of Clinical Pharmacology*, **59**, 691-704.

Blesch, K. S., Gieschke, R., Tsukamoto, Y., Reigner, B. G., Burger, H. U. & Steimer, J. L. (2003) Clinical pharmacokinetic/pharmacodynamic and physiologically based pharmacokinetic modeling in new drug development: the capecitabine experience. *Invest New Drugs*, **21**, 195-223.

Brocklebank, J. R., Namdari, R. & Law, F. C. (1997) An oxytetracycline residue depletion study to assess the physiologically based pharmacokinetic (PBPK) model in farmed Atlantic salmon. *Can Vet J*, **38**, 645-646.

Brown, S. A. (2001). Pharmacokinetics: Disposition and Fate of Drugs in the Body. In *Veterinary Pharmacology and Therapeutics*, 8th Edition. Eds. H. R. Adams. Iowa State University Press, Ames, Iowa, 15-56.

Carda-Broch, S. & Berthod, A. (2004) Counter current chromatography for the measurement of the hydrophobicity of sulfonamide amphoteric compounds. *Chromatographia*, **59**, 79-87.

Charnick, S. B., Kawai, R., Nedelman, J. R., Lemaire, M., Niederberger, W. & Sato, H. (1995) Perspectives in pharmacokinetics. Physiologically based pharmacokinetic modeling as a tool for drug development. *J Pharmacokinet Biopharm*, **23**, 217-229.

Cheng, Z., Mckeller, Q. & Nolan, A. (1998) Pharmacokinetic studies of flunixin meglumine and phenylbutazone in plasma, exudate and transudate in sheep. *Journal of Veterinary Pharmacology and Therapeutics*, **21**, 315-321.

Clewell, H. J., 3rd & Andersen, M. E. (1996) Use of physiologically based pharmacokinetic modeling to investigate individual versus population risk. *Toxicology*, **111**, 315-329.

Clewell, H. J., 3rd, Gentry, P. R. & Gearhart, J. M. (1997) Investigation of the potential impact of benchmark dose and pharmacokinetic modeling in noncancer risk assessment. *J Toxicol Environ Health*, **52**, 475-515.

Clewell, H. J., Gearhart, J. M., Gentry, P. R., Covington, T. R., Vanlandingham, C. B., Crump, K. S. & Shipp, A. M. (1999) Evaluation of the uncertainty in an oral reference dose for methylmercury due to interindividual variability in pharmacokinetics. *Risk Anal*, **19**, 547-558.

Clewell H. J., Gentry, P. R., Covington, T. R., Sarangapani, R. & Teeguarden, J. G. (2004) Evaluation of the potential impact of age- and gender-specific pharmacokinetic differences on tissue dosimetry. *Toxicol Sci,* **79**, 381-393.

Coakley, M., Peck, K. E., Taylor, T. S., Matthews, N. S. & Mealey, K. L. (1999) Pharmacokinetics of flunixin meglumine in donkeys, mules, and horses. *American Journal of Veterinary Research*, **60**, 1441-1444.

Colburn, W. A. (1988) Physiologic pharmacokinetic modeling. *Journal of clinical pharmacology*, **28**, 673-677.

Concordet, D. & Toutain, P. L. (1997a) The withdrawal time estimation of veterinary drugs revisited. *J Vet Pharmacol Ther*, **20**, 380-386.

Concordet, D. & Toutain, P. L. (1997b) The withdrawal time estimation of veterinary drugs: a non-parametric approach. *J Vet Pharmacol Ther*, **20**, 374-379.

Craigmill, A. L. (2003) A physiologically based pharmacokinetic model for oxytetracycline residues in sheep. *J Vet Pharmacol Ther*, **26**, 55-63.

de Silva, J. A. (1985) Analytical strategies for therapeutic monitoring of drugs in biological fluids. *J Chromatogr*, **340**, 3-30.

DeJongh, J. & Blaauboer, B. J. (1996) Simulation of toluene kinetics in the rat by a physiologically based pharmacokinetic model with application of biotransformation parameters derived independently in vitro and in vivo. *Fundam Appl Toxicol*, **32**, 260-268.

du Souich, P. & Courteau, H. (1981) Induction of acetylating capacity with complete Freund's adjuvant and hydrocortisone in the rabbit. *Drug Metab Dispos*, **9**, 279-283.

Duddy, J., Hayden, T. L., Bourne, D. W., Fiske, W. D., Benedek, I. H., Stanley, D., Gonzalez, A. & Heierman, W. (1984) Physiological model for distribution of sulfathiazole in swine. *J Pharm Sci*, **73**, 1525-1528.

el-Banna, H. A. (1999) Pharmacokinetic interactions between flunixin and sulphadimidine in horses. *Dtsch Tierarztl Wochenschr*, **106**, 400-403.

Elmas, M., Yazar, E., Uney, K. & Karabacak, A. (2006) Pharmacokinetics of flunixin after intravenous administration in healthy and endotoxaemic rabbits. *Veterinary Research Communications*, **30**, 73-81.

el-Masri, H. A., Thomas, R. S., Benjamin, S. A. & Yang, R. S. (1995) Physiologically based pharmacokinetic/pharmacodynamic modeling of chemical mixtures and possible applications in risk assessment. *Toxicology*, **105**, 275-282.

Federal Food, Drug, and Cosmetic Act (1982). Title 21, Code of Federal Regulations, 21-CFR-556.670.

Federal Food, Drug, and Cosmetic Act (2004). Title 21, Code of Federal Regulations, 21-CFR-500.80.

Fisch, R. D. (2000) Withdrawal time estimation of veterinary drugs: extending the range of statistical methods. *J Vet Pharmacol Ther*, **23**, 159-162.

FSIS (2001). *2000 FSIS National Residue Program Data.* Food Safety Inspection Service. United States Department of Agriculture, Washington, DC.

FSIS (2004). *2003 FSIS National Residue Program Data*. Food Safety Inspection Service. United States Department of Agriculture, Washington, DC.

Fouchecourt, M. O., Beliveau, M. & Krishnan, K. (2001) Quantitative structure-pharmacokinetic relationship modelling. *Sci Total Environ*, **274**, 125-135.

Frederick, C. B. (1993) Limiting the uncertainty in risk assessment by the development of physiologically based pharmacokinetic and pharmacodynamic models. *Toxicol Lett*, **68**, 159-175.

Freedom of Information Summary (2005). Supplemental New Animal Drug Application, NADA 101-479.

Gearhart, J. M., Mahle, D. A., Greene, R. J., Seckel, C. S., Flemming, C. D., Fisher, J. W. & Clewell, H. J., 3rd (1993) Variability of physiologically based pharmacokinetic (PBPK) model parameters and their effects on PBPK model predictions in a risk assessment for perchloroethylene (PCE). *Toxicol Lett*, **68**, 131-144.

Gehring, R., Baynes, R. E., Craigmill, A. L. & Riviere, J. E. (2004) Feasibility of using half-life multipliers to estimate extended withdrawal intervals following the extralabel use of drugs in food-producing animals. *J Food Prot*, **67**, 555-560.

Gehring, R., Baynes, R. E. & Riviere, J. E. (2006) Application of risk assessment and management principles to the extralabel use of drugs in food-producing animals. *J Vet Pharmacol Ther*, **29**, 5-14.

Gentry, P. R., Covington, T. R., Andersen, M. E. & Clewell, H. J., 3rd (2002) Application of a physiologically based pharmacokinetic model for isopropanol in the derivation of a reference dose and reference concentration. *Regul Toxicol Pharmacol*, **36**, 51-68.

Gentry, P. R., Covington, T. R., Clewell, H. J., 3rd & Anderson, M. E. (2003) Application of a physiologically based pharmacokinetic model for reference dose and reference concentration estimation for acetone. *Journal of toxicology and environmental health. Part A*, **66**, 2209-2225.

Gerlowski, L. E. & Jain, R. K. (1983) Physiologically based pharmacokinetic modeling: principles and applications. *J Pharm Sci*, **72**, 1103-1127.

Green, M. J., Burton, P. R., Green, L. E., Schukken, Y. H., Bradley, A. J., Peeler, E. J. & Medley, G. F. (2004) The use of Markov chain Monte Carlo for analysis of correlated binary data: patterns of somatic cells in milk and the risk of clinical mastitis in dairy cows. *Prev Vet Med*, **64**, 157-174.

Haddad, S., Beliveau, M., Tardif, R. & Krishnan, K. (2001) A PBPK modeling-based approach to account for interactions in the health risk assessment of chemical mixtures. *Toxicol Sci*, **63**, 125-131.

Honore, B. & Brodersen, R. (1984) Albumin binding of anti-inflammatory drugs. Utility of a site-oriented versus a stoichiometric analysis. *Mol Pharmacol*, **25**, 137-150.

Hoogenboom, L. A., Pastoor, F. J., Clous, W. E., Hesse, S. E. & Kuiper, H. A. (1989) The use of porcine hepatocytes for biotransformation studies of veterinary drugs. *Xenobiotica*, **19**, 1207-1219.

Hopp, P., Webb, C. R. & Jarp, J. (2003) Monte Carlo simulation of surveillance strategies for scrapie in Norwegian sheep. *Prev Vet Med*, **61**, 103-125.

Horii, Y., Ikenaga, M., Shimoda, M. & Kokue, E. (2004) Pharmacokinetics of flunixin in the cat: enterohepatic circulation and active transport mechanism in the liver. *Journal of Veterinary Pharmacology and Therapeutics*, **27**, 65-69.

Hunt, C. A., Givens, G. H. & Guzy, S. (1998) Bootstrapping for pharmacokinetic models: visualization of predictive and parameter uncertainty. *Pharm Res*, **15**, 690-697.

Isaacs, K. K., Evans, M. V. & Harris, T. R. (2004) Visualization-based analysis for a mixed-inhibition binary PBPK model: determination of inhibition mechanism. *J Pharmacokinet Pharmacodyn*, **31**, 215-242.

Iwi, G., Millard, R. K., Palmer, A. M., Preece, A. W. & Saunders, M. (1999) Bootstrap resampling: a powerful method of assessing confidence intervals for doses from experimental data. *Phys Med Biol*, **44**, N55-62.

Jang, J. Y., Droz, P. O. & Chung, H. K. (1999) Uncertainties in physiologically based pharmacokinetic models caused by several input parameters. *Int Arch Occup Environ Health*, **72**, 247-254.

Johanson, G. & Naslund, P. H. (1988) Spreadsheet programming--a new approach in physiologically based modeling of solvent toxicokinetics. *Toxicol Lett*, **41**, 115-127.

Jones, D. K., Hakim, M., Wallwork, J., Higenbottam, T. W. & White, D. J. (1986) Serious interaction between cyclosporin A and sulphadimidine. *Br Med J (Clin Res Ed)*, **292**, 728-729.

Jonsson, F. & Johanson, G. (2002) Physiologically based modeling of the inhalation kinetics of styrene in humans using a bayesian population approach. *Toxicol Appl Pharmacol*, **179**, 35-49.

Jonsson, F. & Johanson, G. (2003) The Bayesian population approach to physiological toxicokinetic-toxicodynamic models--an example using the MCSim software. *Toxicol Lett*, **138**, 143-150.

Kanamitsu, S., Ito, K., Green, C. E., Tyson, C. A., Shimada, N. & Sugiyama, Y. (2000) Prediction of in vivo interaction between triazolam and erythromycin based on in vitro studies using human liver microsomes and recombinant human CYP3A4. *Pharm Res*, **17**, 419-426.

Karsten, S., Rave, G. & Krieter, J. (2005) Monte Carlo simulation of classical swine fever epidemics and control. II. Validation of the model. *Vet Microbiol*, **108**, 199-205.

Kawai, R., Lemaire, M., Steimer, J. L., Bruelisauer, A., Niederberger, W. & Rowland, M. (1994) Physiologically based pharmacokinetic study on a cyclosporin derivative, SDZ IMM 125. *J Pharmacokinet Biopharm*, **22**, 327-365.

Kokue, E., Shimoda, M., Sakurada, K. & Wada, J. (1988) Pharmacokinetics of oral sulfa drugs and gastric emptying in the pig. *J Pharmacobiodyn*, **11**, 549-554.

Konigsson, K., Torneke, K., Engeland, I. V., Odensvik, K. & Kindahl, H. (2003) Pharmacokinetics and pharmacodynamic effects of flunixin after intravenous, intramuscular and oral administration to dairy goats. *Acta Veterinaria Scandinavica*, **44**, 153-159.

Kosa, T., Maruyama, T. & Otagiri, M. (1997) Species differences of serum albumins: I. Drug binding sites. *Pharm Res*, **14**, 1607-1612.

Kragh-Hansen, U. (1988) Evidence for a large and flexible region of human serum albumin possessing high affinity binding sites for salicylate, warfarin, and other ligands. *Mol Pharmacol*, **34**, 160-171.

Krishnan, K. & Andersen, M. E. (2001). Physiologically Based Pharmacokinetic Modeling in Toxicology. In *Principles and Methods of Toxicology,* Eds. A. W. Hayes. Taylor & Francis, Philadelphia, 193-241.

Krishnan, K. & Johanson, G. (2005) Physiologically-based pharmacokinetic and toxicokinetic models in cancer risk assessment. *J Environ Sci Health C Environ Carcinog Ecotoxicol Rev,* **23**, 31-53.

Kuiper, H. A., Aerts, R. M. L., Haagsma, N. & Gogh, H. V. (1988) Case study of the depletion of sulfamethazine from plasma and tissues upon oral administration to piglets affected with atrophic rhinitis. *Journal of Agriculture and Food Chemistry*, **36**, 822-825.

Lathers, C. M. (2002) Risk assessment in regulatory policy making for human and veterinary public health. *J Clin Pharmacol*, **42**, 846-866.

Leavens, T. L. & Bond, J. A. (1996) Pharmacokinetic model describing the disposition of butadiene and styrene in mice. *Toxicology*, **113**, 310-313.

Liu, X., Smith, B. J., Chen, C., Callegari, E., Becker, S. L., Chen, X., Cianfrogna, J., Doran, A. C., Doran, S. D., Gibbs, J. P., Hosea, N., Liu, J., Nelson, F. R., Szewc, M. A. & Van Deusen, J. (2005) Use of a physiologically based pharmacokinetic model to study the time to reach brain equilibrium: an experimental analysis of the role of blood-brain barrier permeability, plasma protein binding, and brain tissue binding. *J Pharmacol Exp Ther*, **313**, 1254-1262.

Liu, Z., Li, F. & Huang, Y. (1999) Determination of unbound drug concentration and protein-drug binding fraction in plasma. *Biomed Chromatogr*, **13**, 262-266.

Martinez, M., Friedlander, L., Condon, R., Meneses, J., O'rangers, J., Weber, N. & Miller, M. (2000) Response to criticisms of the US FDA parametric approach for withdrawal time estimation: rebuttal and comparison to the non-parametric method proposed by Concordet and Toutain. *J Vet Pharmacol Ther*, **23**, 21-35.

Martin-Jimenez, T. (2000). *Population Pharmacokinetic Modeling of the Serum Disposition, Interspecies Extrapolation and Residue Depletion of Gentamicin and Oxytetracycline.* Dissertation under the direction of J. E. Riviere at North Carolina State University, Raleigh, Department of Anatomy, Physiological Sciences, and Radiology.

Martin-Jimenez, T., Baynes, R. E., Craigmill, A. & Riviere, J. E. (2002) Extrapolated withdrawal-interval estimator (EWE) algorithm: a quantitative approach to establishing extralabel withdrawal times. *Regul Toxicol Pharmacol*, **36**, 131-137.

Mengelers, M. J., Kleter, G. A., Hoogenboom, L. A., Kuiper, H. A. & Van Miert, A. S. (1997) The biotransformation of sulfadimethoxine, sulfadimidine, sulfamethoxazole, trimethoprim and aditoprim by primary cultures of pig hepatocytes. *J Vet Pharmacol Ther*, **20**, 24-32.

Motulsky, H. (1995). *The GraphPad Guide to Analyzing Radioligand Binding Data.* GraphPad Software, Inc., San Diego, CA.

Munsey, T., Grigg, R. E., Mcormack, A., Symonds, H. W. & Bowmer, C. J. (1996) Binding of sulphamethazine to pig plasma proteins and albumin. *J Vet Pharmacol Ther*, **19**, 135-141.

Navarre, C. B., Ravis, W. R., Nagilla, R., Deshmukh, D., Simpkins, A., Duran, S. H. & Pugh, D. G. (2001) Pharmacokinetics of flunixin meglumine in llamas following a single intravenous dose. *Journal of Veterinary Pharmacology and Therapeutics*, **24**, 361-364.

Nouws, J. F., Vree, T. B., Baakman, M., Driessens, F., Vellenga, L. & Mevius, D. J. (1986a) Pharmacokinetics, renal clearance, tissue distribution, and residue aspects of sulphadimidine and its N4-acetyl metabolite in pigs. *Vet Q*, **8**, 123-135.

Nouws, J. F. M., Vree, T. B., Breukink, H. J., Vanmiert, A. S. J. P. A. M. & Grondel, J. (1986b). Pharmacokinetics, hydroxylation and acetylation of sulphadimidine in mammals, birds, fish, reptiles and molluscs. *Comparative Veterinary Pharmacology, Toxicology, and Therapy:* Proceedings of the 3rd Congress of European Association for Veterinary Pharmacology and Toxicology, Lancaster, UK, 301-318.

Nouws, J. F., Mevius, D., Vree, T. B. & Degen, M. (1989) Pharmacokinetics and renal clearance of sulphadimidine, sulphamerazine and sulphadiazine and their N4-acetyl and hydroxy metabolites in pigs. *Vet Q*, **11**, 78-86.

Oukessou, M. (1994) Kinetic disposition of flunixin meglumine in the camel (Camelus dromedarius). *Veterinary Research*, **25**, 71-75.

Parke, J., Holford, N. H. & Charles, B. G. (1999) A procedure for generating bootstrap samples for the validation of nonlinear mixed-effects population models. *Comput Methods Programs Biomed*, **59**, 19-29.

Payne, M. A., Craigmill, A. L., Riviere, J. E., Baynes, R. E., Webb, A. I. & Sundlof, S. F. (1999) The Food Animal Residue Avoidance Databank (FARAD). Past, present and future. *Vet Clin North Am Food Anim Pract*, **15**, 75-88.

Piva, A., Anfossi, P., Meola, E., Pietri, A., Panciroli, A., Bertuzzi, T. & Formigoni, A. (1997) Effect of microcapsulation on absorption processes in the pig. *Livestock Production Sciences*, **51**, 53-61.

Poirier, L. A., Doerge, D. R., Gaylor, D. W., Miller, M. A., Lorentzen, R. J., Casciano, D. A., Kadlubar, F. F. & Schwetz, B. A. (1999) An FDA review of sulfamethazine toxicity. *Regul Toxicol Pharmacol*, **30**, 217-222.

Poucke, L. S. G. V. & Peteghem, C. H. V. (1994) Pharmacokinetics and tissue residues of sulfathiazole and sulfamethazine in pigs. *Journal of Food Protection*, **57**, 796-801.

Paulson, G., Struble, C. & Mitchell, A. (1983). Comparative metabolism of sulfamethazine [4-amino-N-(dimethyl-2-pyrimidinyl)benzenesulfonamide] in the rat, chicken, pig and sheep. *Pesticide Chemistry*: Proceedings from the 5th International Congress, 375-380.

Price, P. S., Conolly, R. B., Chaisson, C. F., Gross, E. A., Young, J. S., Mathis, E. T. & Tedder, D. R. (2003) Modeling interindividual variation in physiological factors used in PBPK models of humans. *Crit Rev Toxicol*, **33**, 469-503.

Reitz, R. H., Mendrala, A. L., Park, C. N., Andersen, M. E. & Guengerich, F. P. (1988) Incorporation of in vitro enzyme data into the physiologically-based pharmacokinetic (PB-PK) model for methylene chloride: implications for risk assessment. *Toxicol Lett*, **43**, 97-116.

Ritschel, W. A. & Banerjee, P. S. (1986) Physiological pharmacokinetic models: principles, applications, limitations and outlook. *Methods and findings in experimental and clinical pharmacology*, **8**, 603-614.

Riviere, J. E., Martin-Jimenez, T., Sundlof, S. F. & Craigmill, A. L. (1997) Interspecies allometric analysis of the comparative pharmacokinetics of 44 drugs across veterinary and laboratory animal species. *J Vet Pharmacol Ther*, **20**, 453-463.

Riviere, J. E. (1999). *Comparative Pharmacokinetics: Principles, Techniques, and Applications.* Blackwell Publishing, Inc., Ames, Iowa.

Romvary, A. & Horvay, M. S. (1976) Data on the pharmacokinetics of sulfonamid-trimethoprim Combinations in sucking pigs. *Zentralbl Veterinarmed A*, **23**, 781-792.

Rowland, M. & Tozer, T. N. (1995). *Clinical Pharmacokinetics: Concepts and Applications.* 3rd Edition. Lippincott Williams and Wilkins, Baltimore, MD.

Saltvedt, I., Spigset, O., Ruths, S., Fayers, P., Kaasa, S. & Sletvold, O. (2005) Patterns of drug prescription in a geriatric evaluation and management unit as compared with the general medical wards: a randomized study. *Eur J Clin Pharmacol*, **61**, 921-928.

Shimoda, M., Okamoto, K., Sikazwe, G., Fujii, C. & Son, D. S. (1997) Deacetylation as a determinant of sulphonamide pharmacokinetics in pigs. *Vet Q*, **19**, 186-191.

Simmons, J. E. (1996) Application of physiologically based pharmacokinetic modelling to combination toxicology. *Food Chem Toxicol*, **34**, 1067-1073.

Slatore, C. G. & Tilles, S. A. (2004) Sulfonamide hypersensitivity. *Immunol Allergy Clin North Am*, **24**, 477-490, vii.

Stolker, A. A. & Brinkman, U. A. (2005) Analytical strategies for residue analysis of veterinary drugs and growth-promoting agents in food-producing animals--a review. *J Chromatogr A*, **1067**, 15-53.

Sweeney, L. M., Tyler, T. R., Kirman, C. R., Corley, R. A., Reitz, R. H., Paustenbach, D. J., Holson, J. F., Whorton, M. D., Thompson, K. M. & Gargas, M. L. (2001) Proposed occupational exposure limits for select ethylene glycol ethers using PBPK models and Monte Carlo simulations. *Toxicological sciences*, **62**, 124-139.

Sweeney, R. W., Bardalaye, P. C., Smith, C. M., Soma, L. R. & Uboh, C. E. (1993) Pharmacokinetic model for predicting sulfamethazine disposition in pigs. *Am J Vet Res*, **54**, 750-754.

Teeguarden, J. G., Waechter, J. M., Jr., Clewell, H. J., 3rd, Covington, T. R. & Barton, H. A. (2005) Evaluation of oral and intravenous route pharmacokinetics, plasma protein binding, and uterine tissue dose metrics of bisphenol A: a physiologically based pharmacokinetic approach. *Toxicol Sci*, **85**, 823-838.

TerraQSAR-LOGP computed octanol/water partition coefficients (CLOGPs): Anti-inflammatory Compounds. Terrabase Inc. www.terrabase-inc.com/anti-inflamms, Accessed January 31, 2007.

Thomas, R. S., Lytle, W. E., Keefe, T. J., Constan, A. A. & Yang, R. S. (1996) Incorporating Monte Carlo simulation into physiologically based pharmacokinetic models using advanced continuous simulation language (ACSL): a computational method. *Fundamental and applied toxicology*, **31**, 19-28.

Toutain, P. L. & Bousquet-Melou, A. (2002) Free drug fraction vs free drug concentration: a matter of frequent confusion. *J Vet Pharmacol Ther*, **25**, 460-463.

Tsuji, A., Yoshikawa, T., Nishide, K., Minami, H., Kimura, M., Nakashima, E., Terasaki, T., Miyamoto, E., Nightingale, C. H. & Yamana, T. (1983) Physiologically based pharmacokinetic model for beta-lactam antibiotics I: Tissue distribution and elimination in rats. *J Pharm Sci*, **72**, 1239-1252.

Tsukamoto, Y., Kato, Y., Ura, M., Horii, I., Ishikawa, T., Ishitsuka, H. & Sugiyama, Y. (2001) Investigation of 5-FU disposition after oral administration of capecitabine, a triple-prodrug of 5-FU, using a physiologically based pharmacokinetic model in a human cancer xenograft model: comparison of the simulated 5-FU exposures in the tumour tissue between human and xenograft model. *Biopharm Drug Dispos*, **22**, 1-14.

US-EPA (August, 2006). *Approaches for the Application of Physiologically Based Pharmacokinetic (PBPK) Models and Supporting Data in Risk Assessment.* Office of Research and Development. National Center for Environmental Assessment. U.S. Environmental Protection Agency, Washington, DC.

US-EPA (March 1997). *Guiding Principles for Monte Carlo Analysis.* Risk Assessment Forum. U.S. Environmental Protection Agency, Washington, DC.

US-FDA-CVM (June 21, 2005). *Guidance for Industry #3: General principles for evaluation of the safety of compounds used in food producing animals.* Center for Veterinary Medicine. U.S. Food and Drug Administration, Washington, DC.

van der Merwe, D., Brooks, J. D., Gehring, R., Baynes, R. E., Monteiro-Riviere, N. A. & Riviere, J. E. (2006) A physiologically based pharmacokinetic model of organophosphate dermal absorption. *Toxicol Sci*, **89**, 188-204.

Wakefield, J. (1996) Bayesian individualization via sampling-based methods. *J Pharmacokinet Biopharm*, **24**, 103-131.

Williams, P. L. (1990) Structural identifiability of pharmacokinetic models--compartments and experimental design. *J Vet Pharmacol Ther*, **13**, 121-131.

Wittwer, J. W. (2004). Monte Carlo Simulation Basics. Vertex42.com vertex42.com/excelarticles/mc/montecarlosimulation, Accessed January 25, 2007.

Wong, G. A. & Shear, N. H. (2005) Adverse drug interactions and reactions in dermatology: current issues of clinical relevance. *Dermatol Clin*, **23**, 335-342.

Wright, J. D., Boudinot, F. D. & Ujhelyi, M. R. (1996) Measurement and analysis of unbound drug concentrations. *Clin Pharmacokinet*, **30**, 445-462.

Yang, R. S., Thomas, R. S., Gustafson, D. L., Campain, J., Benjamin, S. A., Verhaar, H. J. & Mumtaz, M. M. (1998) Approaches to developing alternative and predictive toxicology based on PBPK/PD and QSAR modeling. *Environ Health Perspect*, **106 Suppl 6**, 1385-1393.

Yassen, A., Olofsen, E., Dahan, A. & Danhof, M. (2005) Pharmacokinetic-pharmacodynamic modeling of the antinociceptive effect of buprenorphine and fentanyl in rats: role of receptor equilibration kinetics. *J Pharmacol Exp Ther*, **313**, 1136-1149.

Young, J. F., Wosilait, W. D. & Luecke, R. H. (2001) Analysis of methylmercury disposition in humans utilizing a PBPK model and animal pharmacokinetic data. *J Toxicol Environ Health A*, **63**, 19-52.

Yuan, Z. H., Miao, X. Q. & Yin, Y. H. (1997) Pharmacokinetics of ampicillin and sulfadimidine in pigs infected experimentally with Streptococcus suum. *J Vet Pharmacol Ther*, **20**, 318-322.

Zeitlinger, M. A., Sauermann, R., Traunmuller, F., Georgopoulos, A., Muller, M. & Joukhadar, C. (2004) Impact of plasma protein binding on antimicrobial activity using time-killing curves. *J Antimicrob Chemother*, **54**, 876-880.

3. DEVELOPMENT OF A PHYSIOLOGICALLY BASED PHARMACOKINETIC MODEL FOR ESTIMATING SULFAMETHAZINE CONCENTRATIONS IN SWINE AND APPLICATION TO PREDICTION OF VIOLATIVE RESIDUES IN EDIBLE TISSUES

Jennifer L. Buur, Ronald E. Baynes, Arthur L. Craigmill, and Jim E. Riviere

2005

Published in the *American Journal of Veterinary Research*, 66(10), 1686-1693

Abstract

Objective

To develop a flow-limited, physiologically based pharmacokinetic model for use in estimating concentrations of sulfamethazine after IV administration to swine.

Sample Population—Four published studies provided physiological values for organ weights, blood flows, clearance, and tissue-to-blood partition coefficients. Three published studies provided data on plasma and other tissue compartments for model validation.

Procedure

For the parent compound, the model included compartments for blood, adipose, muscle, liver, and kidney tissue compartments with an extra compartment representing the remaining carcass. Compartments for the N-acetyl metabolite included liver and the remaining body. The model was created and optimized by use of computer software. Sensitivity analysis was completed to evaluate the importance of each constant on the whole model. The model was validated and used to estimate a withhold interval after an IV injection at a dose of 50 mg/kg. The withhold interval was compared to the interval estimated by the Food Animal Residue Avoidance Databank (FARAD).

Results

Specific tissue correlations for plasma, adipose, muscle, kidney, and liver tissue compartments were 0.93, 0.86, 0.99, 0.94, and 0.98, respectively. The model typically over predicted concentrations at early time points but had excellent accuracy at later time points. The withhold interval estimated by use of the model was 120 hours, compared with 100 hours estimated by FARAD.

Conclusions and Clinical Relevance

Use of this model enabled us to accurately predict sulfamethazine pharmacokinetics in swine and has applications for food safety and prediction of drug residues in edible tissues.

Introduction

Sulfamethazine is an antimicrobial commonly used as a feed additive in swine production. It is currently labeled for use in the prevention and treatment of cervical abscesses, colibacillosis, swine dysentery, and bacterial pneumonia as well as for increased feed efficiency in swine with other diseases, such as atrophic rhinitis (Entriken, 2001). The United States Food and Drug Administration (US-FDA) and other international regulatory agencies have set a residue tolerance limit for sulfamethazine at 0.1 μg/g in all edible swine tissues ("Federal Food, Drug, and Cosmetic Act," 1982). However in 2000, sulfamethazine represented the drug found most often as a cause of violative residues in swine (FSIS, 2001).

Under provisions of the Animal Medicinal Drug Use Clarification Act (AMDUCA), veterinarians in the United States are allowed to use drugs in an extralabel manner only when there is a valid veterinarian-client-patient relationship, the drug is used for therapeutic use, no other product is approved for use in that species, the drug is an US-FDA approved human or animal drug, no violative residues in food will result, and the drug is not specifically prohibited. In addition, drugs used in this manner cannot be feed additives unless they are used in a minor species ("Animal Medicinal Drug Use Clarification Act," 1994). To insure that no violative residues are found in food, an appropriate extended withdrawal period must be specified by the attending veterinarian. The Food Animal Residue Avoidance Databank (FARAD) helps veterinarians provide these extended withdrawal times by applying principles of pharmacokinetics to scenarios for alternate routes and doses. Currently, this is accomplished through intensive literature searches, use of classical pharmacokinetic models, and use of techniques for modeling population pharmacokinetics (Martin-Jimenez et al., 2002). Often there is insufficient information regarding adsorption, distribution, metabolism, and excretion of a drug to allow for a scientifically accurate estimate of drug residues in tissues at specific time points after administration. When there is a lack of data on depletion of drug concentrations in tissues, the recommended withdrawal times provided by FARAD

are based instead on depletion curves of plasma concentrations, which are the only data available to scale systemic drug exposure between label and extralabel dosing. In these cases, data would be unavailable to directly correlate drug depletion to tolerance concentrations allowed in tissues (Damian et al., 1997; Gehring et al., 2004).

Physiologically based pharmacokinetic (PBPK) models are used to describe and predict the kinetics of xenobiotics on the basis of physiological mechanisms by linking physiologic tissue blocks together via a communal plasma compartment. These models have been used in human medicine to predict therapeutic doses for chemotherapeutics, drug development, and in toxicologic studies for development of reference concentrations and doses (Charnick et al., 1995; Clewell et al., 1997; Gentry et al., 2003; Grass et al., 2002). They have also been used in conjunction with pharmacodynamic studies to investigate mechanisms of action in novel or toxic compounds for which classical testing is insufficient (Kawai et al., 1994). In veterinary medicine, PBPK models have been described for sulfathiazole administration to swine and oxytetracycline administration to sheep and fish (Brocklebank et al., 1997; Craigmill, 2003; Duddy et al., 1984).

The objectives of the study reported here were to develop and validate a PBPK model and to estimate sulfamethazine concentrations after IV administration in swine. We also applied the model to the prediction of extended withholding intervals for use under AMDUCA.

Materials and Methods

Development of a PBPK model

A flow-limited PBPK model was developed for predictive purposes. For predicting sulfamethazine concentrations, it consisted of tissue compartments for edible tissues (blood, muscle, adipose, liver, and kidney) and a single compartment representing the remainder of the carcass. Additional compartments for the N-acetyl metabolite were created and included

compartments for the liver and blood specifically and a generalized compartment representing the remainder of the body. No concentration-vs-time data were available for the carcass compartment or for tissue concentrations of the N-acetyl metabolite. Thus, a model with 9 compartments was developed (**Figure 3.1**).

Physiological constants of organ volume, tissue blood volume and blood flow for market-weight pigs were obtained from published reports (**Table 3.1**) (Kawai et al., 1994; Lundeen et al., 1983; Pond, 2001; Tranquilli et al., 1982). The density of plasma was assumed to be 1 g/mL. Physiochemical constants of tissue-to-blood partition coefficients were calculated from published values (Haasnoot et al., 1996; Mitchell et al., 1986; Nouws et al., 1986; Sweeney et al., 1993). Hepatic blood flow was modeled as the combination of hepatic arterial and portal circulations. Other biological constants included in the model are also found in **Table 3.1**.

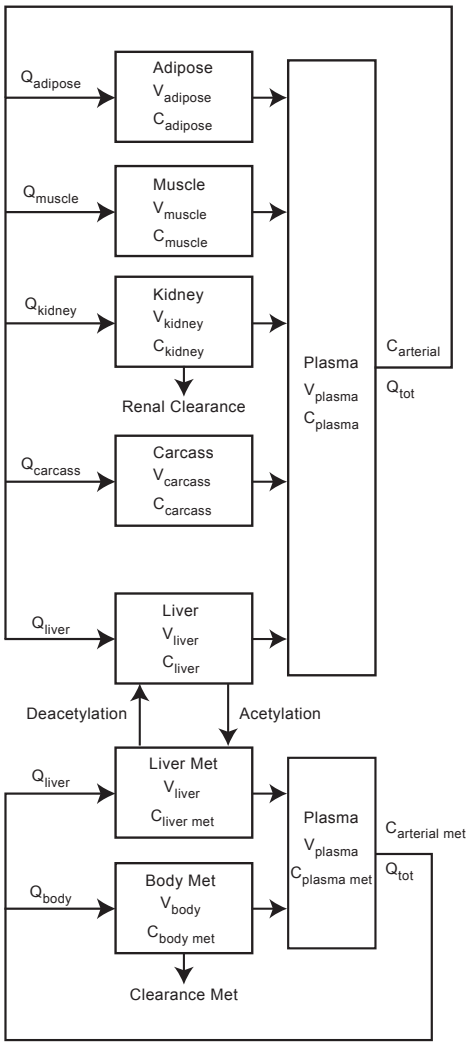

Figure 3.1 Schematic representation of a physiologically based pharmacokinetic model for use in determining concentrations after IV injection of Sulfamethazine in swine

Notice the tissue volume ($V_{adipose}$, V_{muscle}, V_{kidney}, V_{plasma}, $V_{carcass}$, V_{liver}, and V_{body}, respectively) and tissue concentration ($C_{adipose}$, C_{muscle}, C_{kidney}, C_{plasma}, $C_{arterial}$, $C_{carcass}$, C_{liver}, $C_{plasma\ met}$, $C_{liver\ met}$, and $C_{body\ met}$ respectively) within each tissue compartment and tissue blood flow ($Q_{adipose}$, Q_{muscle}, Q_{kidney}, $Q_{carcass}$, Q_{liver}, and Q_{body}, respectively) for each compartment. Q_{tot} = Cardiac output; Liver met = Liver metabolite; Body met = Body metabolite; Clearance met = Clearance metabolite.

Table 3.1 Organ weights and blood flow distributions for market-weight swine determined from published studies

Organ	Blood flow[a] (percentage of cardiac output)*	Organ weight[b] (percentage of body weight)	Vascular space[c] (percentage of organ weight)
Adipose	0.08	0.340	0.040
Kidneys	0.10	0.004	0.105
Liver	0.24†	0.020	0.115
Muscle	0.25	0.400	0.026
Carcass‡	0.33	0.176	ND
Blood	1.00	0.060	ND

*Mean cardiac output determined in 3 studies was 12 L/kg/h and PCV was 33%. †Value incorporates hepatic arterial and portal circulations. ‡Values calculated as 1 minus the sum of values for the other organs. ND = Not determined. Source a: Tranquilli, 1982; Lundeen, 1983. b: Pond, 2001. c: Kawai, 1994

Values for renal and hepatic clearance were based on kinetic data published elsewhere (Nouws et al., 1989; Sweeney et al., 1993; Yuan et al., 1997). The main pathway of metabolism in pigs is direct acetylation of sulfamethazine to the N4-acetyl metabolite. Michalis-Menten kinetics were not incorporated into this model because it has been reported that clinically relevant doses do not saturate the hepatic acetyltransferase enzyme and thus zero-order kinetics are not needed (Mengelers et al., 1997). Therefore, hepatic clearance was modeled by use of a linear-excretion constant. Enterohepatic recycling of the parent compound was considered insubstantial and not included in the model. Because the deacetylation of the N-acetyl metabolite can increase plasma concentrations of the parent compound, we incorporated this aspect into the model (Shimoda et al., 1997). Compartments for the N-acetyl metabolite were linked to the model for the parent compound through the liver because these reactions mainly take place in hepatocytes. Renal clearance is mainly through filtration. Because there is no evidence of active secretion, renal clearance was modeled by use of a first-order excretion constant. Starting values for hepatic and renal clearance were the mean of the published values.

Protein binding was incorporated into the model by the inclusion of a mass-balance equation within the blood compartment. The fraction of unbound drug was calculated and then applied to the total mass of drug within the plasma compartment. Binding of drug within tissues was not incorporated into the model.

A homogenization term was created that combined tissue concentration with tissue blood concentration. This represented the process used in quantitative analysis of tissue samples whereby the total drug within the sample is directly related to the proportion of tissue blood and tissue within the sample. The amount of drug within the vascular space was then calculated. The concentration of the total homogenized sample concentration was expressed by use of the following equation:

$$Ch_t = (Vbc_t \bullet Ctb) + [(1 - Vbc_t) \bullet C_t] \qquad [1]$$

where Ch_t is the concentration of sulfamethazine in the homogenized sample, Vbc_t is the volume of the vascular space for a given tissue (reported as a percentage of organ weight), Ctb is the concentration of sulfamethazine in the tissue blood, and C_t is the concentration of sulfamethazine in the tissue.

Model simulations were solved by use of a commercially available computer program (ACSLxtreme, version 1.4, Aegis Technologies Group Inc, Huntsville, Ala) that was equipped with a graphic modulator for model development and an optimizer for sensitivity, determination of constants, and prediction analysis. Differential equations were used to describe the rate of change in mass in each compartment (**Table 3.2**).

Sensitivity analysis and optimization of constants

Data used for optimization of the N-acetyl metabolite distribution were obtained from 2 studies (Nouws et al., 1989; Nouws et al., 1986). Data used for sensitivity and optimization of sulfamethazine were obtained from a single study (Nouws et al., 1989). Optimization of

Table 3.2 Differential equations used to describe the rate of change of sulfamethazine in each tissue compartment

Tissue Compartment	Equation
Muscle	$\frac{dC_{muscle}}{dt} \bullet V_{muscle} = \left(C_{arterial} - \frac{C_{muscle}}{P_{muscle}} \right) \bullet Q_{muscle}$
Adipose	$\frac{dC_{adipose}}{dt} \bullet V_{adipose} = \left(C_{arterial} - \frac{C_{adipose}}{P_{adipose}} \right) \bullet Q_{adipose}$
Carcass	$\frac{dC_{carcass}}{dt} \bullet V_{carcass} = \left(C_{arterial} - \frac{C_{carcass}}{P_{carcass}} \right) \bullet Q_{carcass}$
Kidney	$\frac{dC_{kidney}}{dt} \bullet V_{kidney} = \left(C_{arterial} - \frac{C_{kidney}}{P_{kidney}} \right) \bullet Q_{kidney} - \left(C_{arterial} \bullet Cl_{renal} \right)$
Liver	$\frac{dC_{liver}}{dt} \bullet V_{liver} = \left(C_{arterial} - \frac{C_{liver}}{P_{liver}} \right) \bullet Q_{liver} - \left(C_{arterial} \bullet Cl_{aceytlation} \right) + \left(C_{livermetabolite} \bullet Cl_{deacetylation} \right)$
Plasma	$\frac{dC_{plasma}}{dt} \bullet V_{plasma} = \left(\frac{C_{kidney}}{P_{kidney}} \bullet Q_{kidney} \right) + \left(\frac{C_{muscle}}{P_{muscle}} \bullet Q_{muscle} \right) + \left(\frac{C_{adipose}}{P_{adipose}} \bullet Q_{adipose} \right) + \left(\frac{C_{liver}}{P_{liver}} \bullet Q_{liver} \right) + \left(\frac{C_{carcass}}{P_{carcass}} \bullet Q_{carcass} \right) + IVDose - \left(C_{plasma} \bullet Q_{tot} \right)$

dC_{muscle}, $dC_{adipose}$, $dC_{carcass}$, $dC_{kidney,}$ dC_{liver}, and dC_{plasma} = Change in concentration of sulfamethazine in each tissue compartment, respectively. dt = Change in time. $C_{arterial}$, C_{muscle}, $C_{adipose}$, $C_{carcass}$, $C_{kidney,}$ C_{liver}, and C_{plasma} = Concentration of sulfamethazine in each tissue compartment, respectively. P_{muscle}, $P_{adipose}$, $P_{carcass}$, $P_{kidney,}$ and P_{liver} = Tissue-to-blood partition coefficient for each tissue compartment, respectively. Q_{muscle}, $Q_{adipose}$, $Q_{carcass}$, $Q_{kidney,}$ and Q_{liver} = Blood flow to each tissue compartment, respectively. V_{muscle}, $V_{adipose}$, $V_{carcass}$, $V_{kidney,}$ V_{liver}, and V_{plasma} = Tissue volume for each compartment, respectively. Cl_{renal}, $Cl_{acetylation}$, and $Cl_{deacetylation}$ = Clearance for each method (renal, acetylation, and deacetylation, respectively). $C_{liver\ metabolite}$ = Concentration of N-acetyl metabolite. IV dose = Total amount of drug injected. Q_{tot} = Cardiac output.

constants was limited to mean (n = 12) plasma concentration data. Sensitivity analysis was performed for several constants, including hepatic clearance, renal clearance, protein binding, tissue-to-blood partition coefficients (muscle, adipose, liver, and kidneys), and blood flow (muscle, adipose, liver, and kidneys). Final determination and optimization of constants was accomplished for blood flows to compartments (liver, kidneys, muscle, and adipose),

hepatic clearance, renal clearance, protein binding, and partition coefficients (muscle, liver, kidneys, and adipose) for sulfamethazine. Determination and optimization of constants was accomplished for N-acetyl protein binding, N-acetyl deacetylation rate, renal clearance, and partition coefficients (liver and body). Model constants were adjusted to best fit the curve by use of a maximum-likelihood estimation algorithm. Limits were set to insure biologically plausible values.

Model validation

The model was validated by comparison with an external data set created from published studies and estimates included in the FARAD database. Studies were excluded from comparison on the basis of assay methods and physiological status of the pigs. Excluded studies incorporated colorimetric analysis of drug concentrations, general anesthesia, and experimentally infected pigs. The resulting data set encompassed 3 studies performed separately by 3 research groups (Nouws et al., 1986; Sweeney et al., 1993; Yuan et al., 1997). Pigs ranged in weight from 18 to 32 kg. Dosages ranged from 20 to 50 mg/kg. Sulfamethazine concentrations were reported for plasma, muscle, kidney, liver, and adipose tissues. Data points represented the means of values reported in studies and were obtained by use of a data extraction program (UN-SCAN-IT, version 6.0, Silk Scientific Inc, Orem, Utah). Mean values in our study were calculated from 6, 7, and 3 samples/ data point for the each of the 3 studies, respectively (Nouws et al., 1986; Sweeney et al., 1993; Yuan et al., 1997).

Predicted values for tissue concentrations were reported as a combination of tissue and tissue blood samples that would mimic the homogenization process used in analysis of tissue samples. Simulated predicted values were compared with values for observed data points, and regression lines were plotted. Linear regression correlation values were calculated. Residual plots were also created and evaluated for spread and distribution. All simulations were adjusted on the basis of dosage.

Application of model to determine interval to prevent violative residues in tissues

The optimized model was then used to determine a reasonable tissue-withhold interval after IV administration of sulfamethazine at a dosage of 50 mg/kg. This was compared with the value currently provided by FARAD to practitioners. Currently, FARAD estimates a withhold interval by use of 10 times the plasma half-life of sulfamethazine, an approach that is appropriate for many drug classes.

Results

Because sulfamethazine is a small polar molecule with small tissue-to-blood partition coefficients, a diffusion-limited model was also created (data not shown) to determine whether blood flow or permeability would be rate-limiting. The diffusion-limited model did not significantly increase the predictive power of the model; therefore, the simpler flow-limited model was accepted.

Sensitivity analysis revealed that hepatic clearance, renal clearance, and protein binding of sulfamethazine were the most important constants included in the model. Because of the lack of available tissue data, it is quite possible that the partition coefficients did not reveal their true sensitivity and importance within this model. Results of the optimization for blood flows, renal clearance, hepatic clearance, protein binding, and tissue-to-blood partition coefficients for sulfamethazine and its N-acetyl metabolite were determined (**Table 3.3**).

When compared with means of external data sets, the model had correlations for plasma, kidney, liver, muscle, and adipose tissues of 0.93, 0.94, 0.99, 0.99, and 0.86, respectively. Results for validation of the model were determined (**Table 3.4**). Residual analysis revealed a pattern of over prediction of values at early time points in all tissues with the exception of muscle, in which the model under predicted values at all time points. However, good

Table 3.3 Starting and final values and upper and lower limits for constants of a model used to determine concentrations after IV administration of Sulfamethazine to pigs.

Constant	Lower limit	Starting value	Upper limit	Final value
Hepatic clearance (mL/[min X kg])	0.05	0.078	3	0.62
Renal clearance (mL/[min X kg])	0.01	0.59	4	0.03
Protein binding (%)	0.5	0.64	1	0.57
Tissue-to-blood partition coefficient				
Adipose	0.01	0.1	5	0.336
Kidney	0.01	0.38	5	1.68
Liver	0.01	0.4	5	0.378
Muscle	0.01	0.17	5	0.08
Blood flow (% cardiac output)				
Liver	0.01	0.24	0.5	0.38
Kidney	0.01	0.1	0.5	0.1188
Muscle	0.01	0.25	0.5	0.25
Adipose	0.01	0.08	0.5	0.08
Acetyl metabolite protein binding (%)	0.5	65	1	0.57
Acetyl metabolite liver tissue-to-blood partition coefficient	0.01	0.23	5	0.079
Acetyl metabolite body tissue-to-blood partition coefficient	0.01	1	5	1.297
Rate of deacetylation (/h)	0.01	0.357	5	3.66
Acetyl metabolite clearance (mL/[min X kg])	0.01	0.5	5	2.558

Table 3.4 Results for model validation accomplished by comparison of predicted concentrations to observed concentrations by use of an external data set

Tissue	Slope (m)	Intercept (b)	R^2
Plasma	0.7358	5.498	0.9286
Kidney	0.2469	4.8166	0.9422
Liver	0.4082	2.1849	0.9792
Muscle	1.4278	1.0028	0.9945
Adipose	0.3338	1.3145	0.8554

Slope (m) and. Intercept (b) for the regression line y = mx + b
R^2 = Correlation coefficient

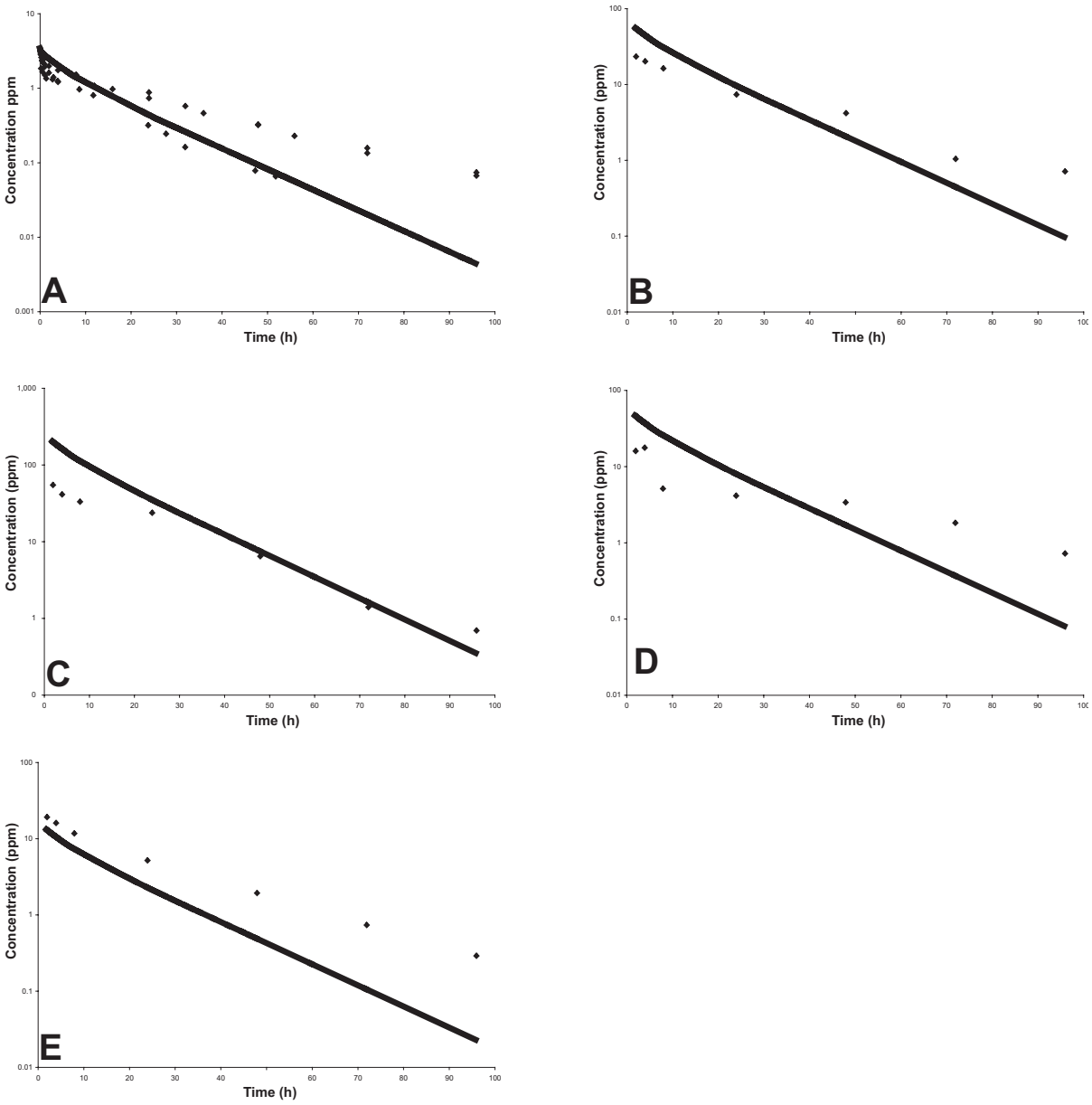

Figure 3.2 Results for the final fitted model simulation (solid line), compared with results for an external data set (circles), for plasma (A), liver (B), kidney (C), adipose (D), and muscle (E) tissue compartments

accuracy was found at the terminal time points. Results of the resulting simulations are plotted (**Figure 3.2**). Results of the residual analysis and validation procedure were also plotted (**Figures 3.3 and 3.4**).

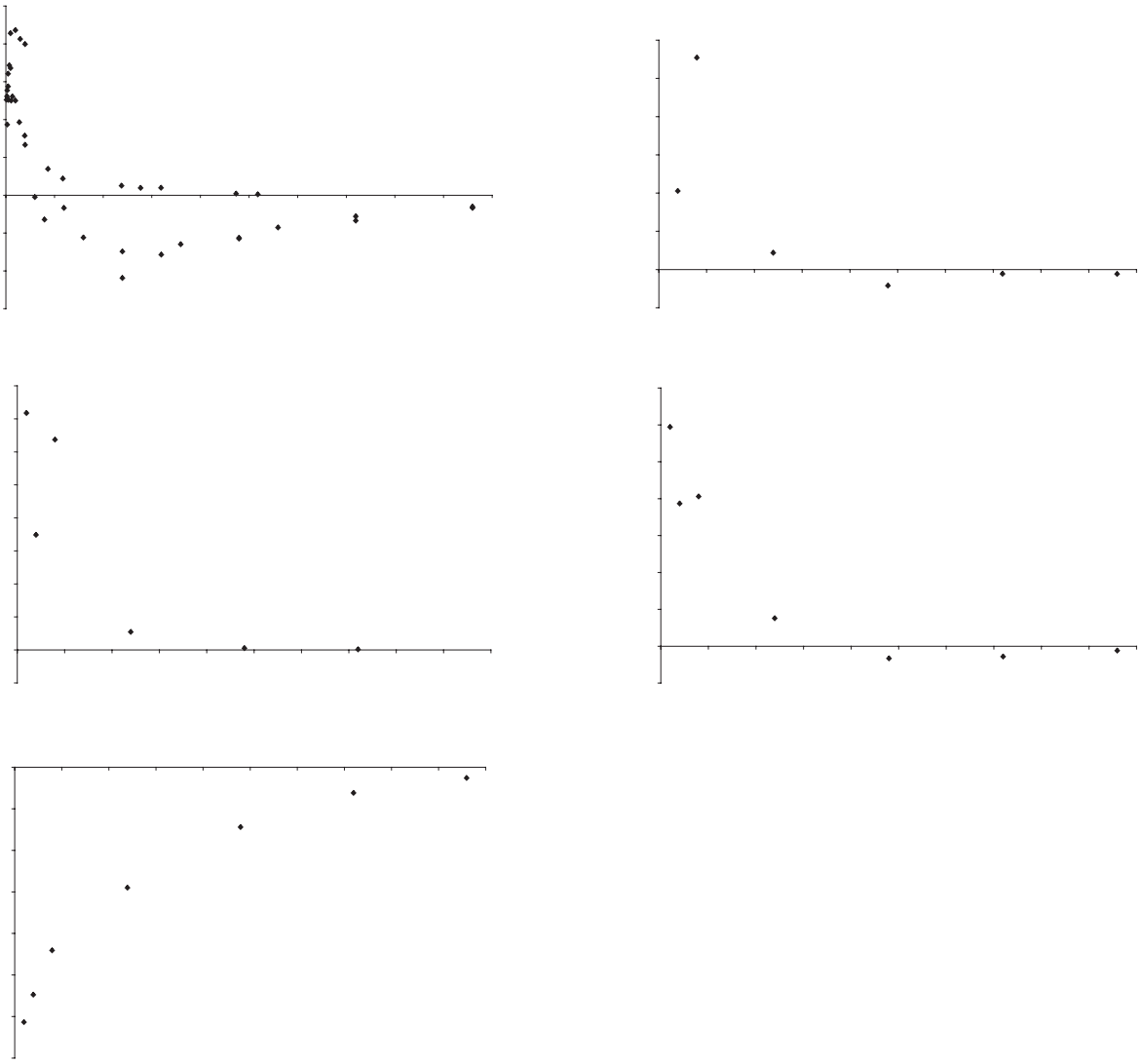

Figure 3.3 Standardized residual plots for fit of the results of the model for plasma (A), liver (B), kidney (C), adipose (D), and muscle (E) tissue compartments

Depletion curves of edible tissues after IV administration of sulfamethazine at a dosage of 50 mg/kg, in relation to the tolerance value of 0.1 μg/g, were plotted (**Figure 3.5**). These depletion curves represented the 50th percentile of the population, not the upper limit of the 95% confidence interval of the 99th percentile of the population needed to satisfy regulatory agencies such as the US-FDA–Center for Veterinary Medicine. The model predicted that all tissue concentrations

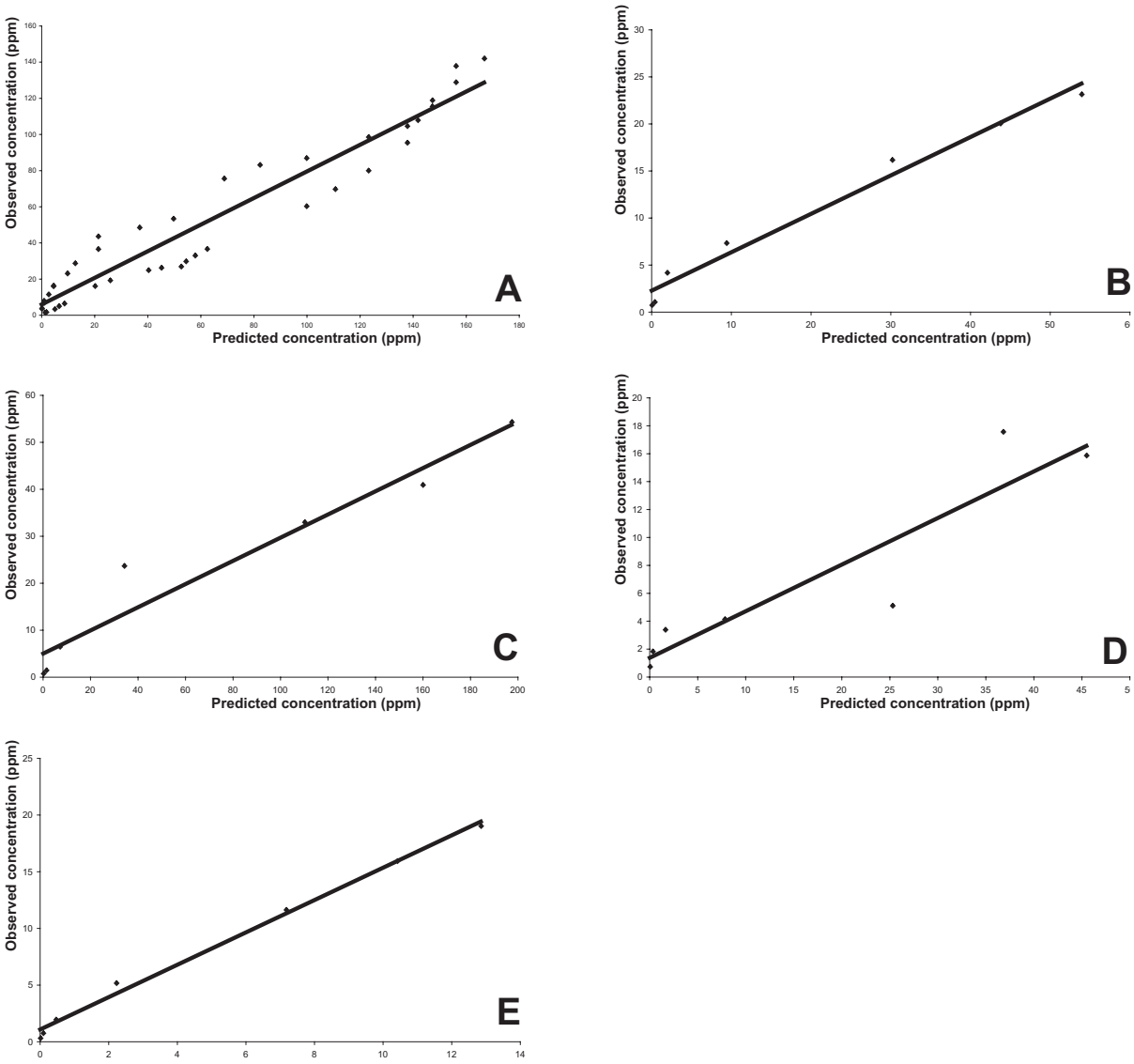

Figure 3.4 Graphs of predicted and observed data for validation of the model for plasma (A), liver (B), kidney (C), adipose (D), and muscle (E) tissue compartments

The solid line represents the line of best fit. Observed data was obtained from published studies. Notice that the scale of the x-axis differs among graphs in the figure.

would be below the tolerance value of 0.1 µg/g by 120 hours after injection and that plasma concentrations would be below the tolerance value by 109 hours after injection. The kidneys had the longest duration for sulfamethazine concentrations above the tolerance value. Because this would constitute an extralabel use of sulfamethazine, there currently is no withdrawal time listed

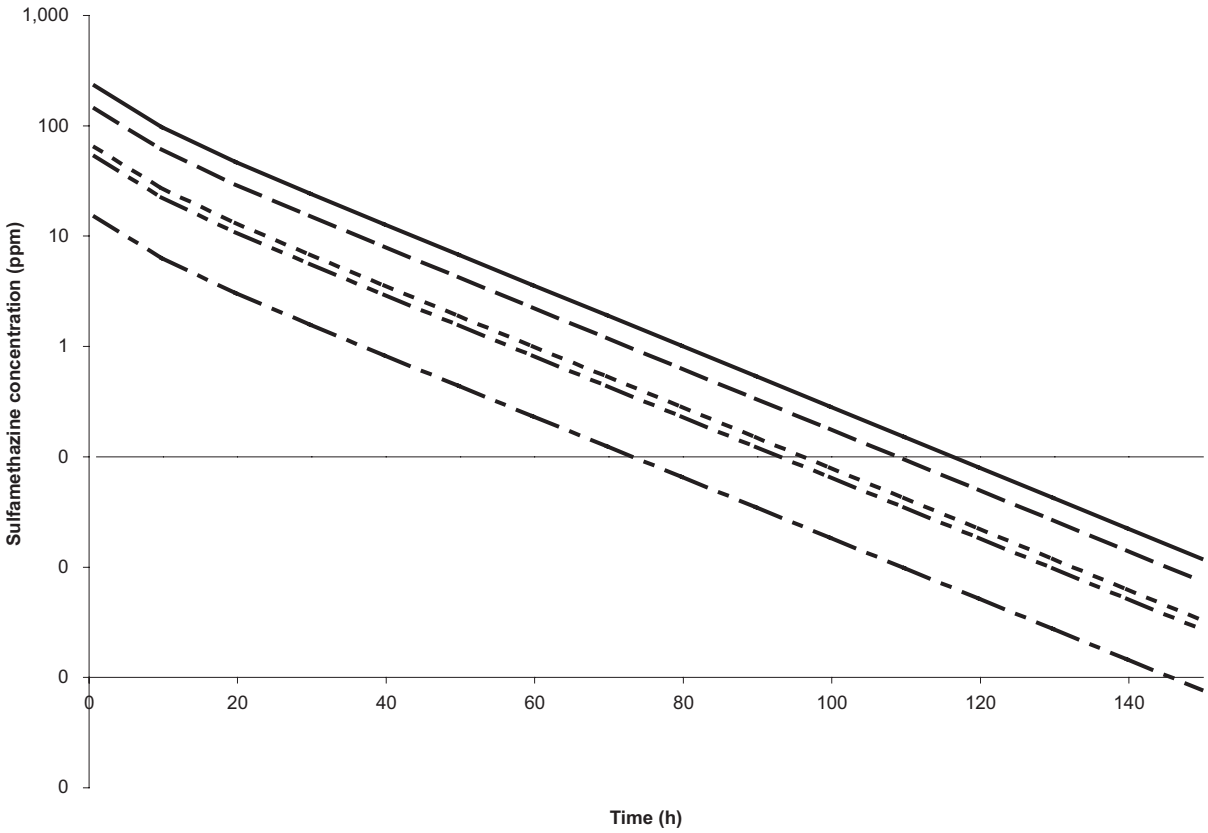

Figure 3.5 Predicted depletion curves for tissue concentrations of drug in tissue compartments after IV administration of Sulfamethazine at a dosage of 50 mg/kg in swine

adipose (thin dotted and dashed line), kidney (thick solid line), liver (thick dashed line), muscle (thick dotted and dashed line), and plasma (thin dashed line) The horizontal line represents the tolerance limit of 0.1 μg/g

on the US-FDA-approved product. The current FARAD recommendation is 100 hours and is determined on the basis of a value that is 10 times the plasma half-life.

Discussion

We developed and validated a model for plasma and tissue pharmacokinetics of sulfamethazine after IV administration to swine. To increase the accuracy and robustness of the model, several techniques were used.

Addition of the N-acetyl metabolite and its deacetylation back to the parent compound was incorporated in the model, which was found to increase the accuracy of concentrations at later time points. The importance of this metabolic pathway differs among sulfonamides. In 1 study, investigators documented that this is an important metabolic pathway for sulfamonomethoxine and sulfamethazine but that the deacetylation pathway has less importance for sulfadiazine (Shimoda et al., 1997). Another model of sulfathiazol did not include the deacetylation metabolic pathway (Duddy et al., 1984). However, it is unknown whether the pharmacokinetics of sulfathiazol are influenced by the deacetylation pathway.

A homogenization term was used to calculate the concentration of sulfamethazine in specific tissues that accounted for the techniques used experimentally to determine those specific tissue concentrations. Techniques used to calculate tissue concentrations require the homogenization of tissue blood along with cellular tissue. Due to the relatively larger mass of drug found in blood relative to the cellular tissues themselves, artificially increased tissue concentrations may result for drugs with small partition coefficients (Khor et al., 1991). Inclusion of the homogenization term increased correlation values and the resulting fit of data (data not shown), especially at terminal end points at which more drug is in the plasma compartment than in the cellular tissue matrix.

Protein binding was an important aspect of drug distribution in this model. Generally, when a drug is not considered to be highly protein bound (binding > 90%), this aspect is neglected to simplify the model (Munsey et al., 1996). In another study, investigators also stated that changing the free fraction of a drug does not result in a change of the free concentration of drug when the drug is at a steady state (Toutain et al., 2002). However, the model described here does not consider the drug at a steady state. It was seen in the results for our model that moderate protein binding of 57% can have an influence on the kinetics of sulfamethazine which may prolong tissue concentrations and increase the likelihood for violative residues in

tissues (data not shown). This phenomenon deserves further study and these findings deserve further study and confirmation.

The sensitivity analysis and optimization of constants were based on plasma concentrations, rather than tissue concentrations. This was attributable to a lack of available tissue data. Because we did not optimize constants for each specific tissue compartment, sensitivity of the model to partitioning coefficients was not observed. Instead, the analysis focused on constants (ie, protein binding and clearance) that would greatly change plasma concentration. It could be expected that with more tissue data, the partitioning coefficients could be further refined without much change to the overall plasma concentrations. This in turn could help with accuracy within the tissue compartments.

All tissue correlations were excellent. Only adipose tissue had a correlation coefficient <0.9. The accuracy of this model could be improved by use of individual data points rather than means as a comparison. This was not done because the individual data points were not reported in any of the studies used for optimization or validation. Unfortunately, standard deviation values were also not reported in those studies. Thus, individual variability was essentially ignored in the observed-to-predicted comparisons. Also, pigs used in the studies were not of market weight, for which the model was designed. This would change relative body mass and blood flow distributions. However, sensitivity and optimization of blood flows did not reveal any substantial inaccuracies in these measurements. Age changes could also alter the relative clearance of sulfamethazine. The acetylation-deacetylation metabolic pathway could be changed by induction of enzymes or increases in intrinsic enzymatic activity. Changes in renal clearance could develop over time because of changes in glomerular filtration rate. With the high sensitivity of the model to changes in clearance, age-related changes in clearance could impact the accuracy of the model.

Further refinement of partitioning coefficients could also improve accuracy. However, that would require a more robust data set for tissue concentrations that is not available in the published studies. We chose to not include the only set of tissue data in the optimization process so that the validation would reflect a purely external data set. Even with these limitations, this model could be used to accurately predict plasma and tissue concentrations over several doses.

The withhold time predicted by use of the model is greater than what would be currently recommended by FARAD because the model takes into account specific tolerance concentrations and tissue concentrations rather than extrapolating to 99.98% excretion by use of 10 times the plasma half-life. Because the kidneys actually retain sulfamethazine longer than does plasma, predicting a withhold time on the basis of plasma concentrations would under predict the true distribution of sulfamethazine within a pig. Studies such as this are required to determine those drugs for which simple rules of thumb or other half-life multipliers are applicable (Gehring et al., 2004).

In the study reported here, we developed a PBPK model for sulfamethazine after IV injection in pigs. We used this model to accurately predict an appropriate extended withdrawal interval to prevent violative residues in edible tissues. In contrast to compartmental pharmacokinetic models for sulfamethazine, the model reported here can be used to provide predictions for a range of doses and yields mechanistic information relating to drug distribution to tissues and pharmacokinetics. Use of this model emphasized the relationship between drug distribution in tissues and protein binding as well as the acetylation-deacetylation metabolic pathway. This model also provided information about pharmacokinetics for specific tissues that are often not included in compartmental or population pharmacokinetic models. This model can be further refined to include long-term oral administration and more specific protein-binding kinetics. As more population information becomes known, statistical inferences can be made

by use of Monte Carlo analysis or bootstrapping techniques that would parallel the power inherent in population pharmacokinetic models yet still provide physiochemical mechanistic information. The model can then be used to study additional physiological mechanisms and drug distributions, which may explain the reason that we still have instances of violative residues in edible tissues.

Acknowledgements

Supported in part by the Food Animal Residue Avoidance Databank (FARAD) and the USDA-CSREES 2002-45051-01362.

References

Animal Medicinal Drug Use Clarification Act (1994). United States Food and Drug Administration. Title 21 Code of Federal Regulations, part 530.

Brocklebank, J. R., Namdari, R. & Law, F. C. (1997) An oxytetracycline residue depletion study to assess the physiologically based pharmacokinetic (PBPK) model in farmed Atlantic salmon. *Can Vet J*, **38**, 645-646.

Charnick, S. B., Kawai, R., Nedelman, J. R., Lemaire, M., Niederberger, W. & Sato, H. (1995) Perspectives in pharmacokinetics. Physiologically based pharmacokinetic modeling as a tool for drug development. *J Pharmacokinet Biopharm*, **23**, 217-229.

Clewell, H. J., 3rd, Gentry, P. R. & Gearhart, J. M. (1997) Investigation of the potential impact of benchmark dose and pharmacokinetic modeling in noncancer risk assessment. *J Toxicol Environ Health*, **52**, 475-515.

Craigmill, A. L. (2003) A physiologically based pharmacokinetic model for oxytetracycline residues in sheep. *J Vet Pharmacol Ther*, **26**, 55-63.

Damian, P., Craigmill, A. & Riviere, J. (1997) Breaking new ground. *Journal of the American Veterinary Medical Association*, **210**, 633-634.

Duddy, J., Hayden, T. L., Bourne, D. W., Fiske, W. D., Benedek, I. H., Stanley, D., Gonzalez, A. & Heierman, W. (1984) Physiological model for distribution of sulfathiazole in swine. *J Pharm Sci*, **73**, 1525-1528.

Entriken, T. L. (2001). Product Monographs. In *Veterinary Pharmaceutical and Biologics, 12th Edition*. Eds. M. Valcarcel. Veterinary Healthcare Communications, Lenexa, Kansas, 2114-2115.

Federal Food, Drug, and Cosmetic Act (1982). Title 21, Code of Federal Regulations, 21-CFR-556.670.

FSIS (2001). *2000 FSIS National Residue Program Data.* Food Safety Inspection Service. United States Department of Agriculture, Washington, DC.

Gehring, R., Baynes, R. E., Craigmill, A. L. & Riviere, J. E. (2004) Feasibility of using half-life multipliers to estimate extended withdrawal intervals following the extralabel use of drugs in food-producing animals. *J Food Prot*, **67**, 555-560.

Gentry, P. R., Covington, T. R., Clewell, H. J., 3rd & Anderson, M. E. (2003) Application of a physiologically based pharmacokinetic model for reference dose and reference concentration estimation for acetone. *Journal of toxicology and environmental health. Part A*, **66**, 2209-2225.

Grass, G. M. & Sinko, P. J. (2002) Physiologically-based pharmacokinetic simulation modelling. *Advanced drug delivery reviews*, **54**, 433-451.

Haasnoot, W., Korsrud, G. O., Cazemier, G., Maneval, F., Keukens, H. & Nouws, J. (1996) Application of an enzyme immunoassay for the determination of sulphamethazine (sulphadimidine) residues in swine urine and plasma and their use as predictors of the level in edible tissue. *Food Addit Contam*, **13**, 811-821.

Kawai, R., Lemaire, M., Steimer, J. L., Bruelisauer, A., Niederberger, W. & Rowland, M. (1994) Physiologically based pharmacokinetic study on a cyclosporin derivative, SDZ IMM 125. *J Pharmacokinet Biopharm*, **22**, 327-365.

Khor, S. P., Bozigian, H. & Mayersohn, M. (1991) Potential error in the measurement of tissue to blood distribution coefficients in physiological pharmacokinetic modeling. Residual tissue blood. II. Distribution of phencyclidine in the rat. *Drug Metab Dispos*, **19**, 486-490.

Lundeen, G., Manohar, M. & Parks, C. (1983) Systemic distribution of blood flow in swine while awake and during 1.0 and 1.5 MAC isoflurane anesthesia with or without 50% nitrous oxide. *Anesth Analg*, **62**, 499-512.

Martin-Jimenez, T., Baynes, R. E., Craigmill, A. & Riviere, J. E. (2002) Extrapolated withdrawal-interval estimator (EWE) algorithm: a quantitative approach to establishing extralabel withdrawal times. *Regul Toxicol Pharmacol*, **36**, 131-137.

Mengelers, M. J., Kleter, G. A., Hoogenboom, L. A., Kuiper, H. A. & Van Miert, A. S. (1997) The biotransformation of sulfadimethoxine, sulfadimidine, sulfamethoxazole, trimethoprim and aditoprim by primary cultures of pig hepatocytes. *J Vet Pharmacol Ther*, **20**, 24-32.

Mitchell, A. D. & Paulson, G. D. (1986) Depletion kinetics of 14C-sulfamethazine [4-amino-N-(4, 6-dimethyl-2-pyrimidinyl)benzene[U-14C]sulfonamide] metabolism in swine. *Drug Metab Dispos*, **14**, 161-165.

Munsey, T., Grigg, R. E., McCormack, A., Symonds, H. W. & Bowmer, C. J. (1996) Binding of sulphamethazine to pig plasma proteins and albumin. *J Vet Pharmacol Ther*, **19**, 135-141.

Nouws, J. F., Mevius, D., Vree, T. B. & Degen, M. (1989) Pharmacokinetics and renal clearance of sulphadimidine, sulphamerazine and sulphadiazine and their N4-acetyl and hydroxy metabolites in pigs. *Vet Q*, **11**, 78-86.

Nouws, J. F., Vree, T. B., Baakman, M., Driessens, F., Vellenga, L. & Mevius, D. J. (1986) Pharmacokinetics, renal clearance, tissue distribution, and residue aspects of sulphadimidine and its N4-acetyl metabolite in pigs. *Vet Q*, **8**, 123-135.

Pond, W. G. (2001). *Biology of the Domestic Pig.* Cornell University Press, Ithaca.

Shimoda, M., Okamoto, K., Sikazwe, G., Fujii, C. & Son, D. S. (1997) Deacetylation as a determinant of sulphonamide pharmacokinetics in pigs. *Vet Q*, **19**, 186-191.

Sweeney, R. W., Bardalaye, P. C., Smith, C. M., Soma, L. R. & Uboh, C. E. (1993) Pharmacokinetic model for predicting sulfamethazine disposition in pigs. *Am J Vet Res*, **54**, 750-754.

Toutain, P. L. & Bousquet-Melou, A. (2002) Free drug fraction vs free drug concentration: a matter of frequent confusion. *J Vet Pharmacol Ther*, **25**, 460-463.

Tranquilli, W. J., Parks, C. M., Thurmon, J. C., Benson, G. J., Koritz, G. D., Manohar, M. & Theodorakis, M. C. (1982) Organ blood flow and distribution of cardiac output in nonanesthetized swine. *Am J Vet Res*, **43**, 895-897.

Yuan, Z. H., Miao, X. Q. & Yin, Y. H. (1997) Pharmacokinetics of ampicillin and sulfadimidine in pigs infected experimentally with Streptococcus suum. *J Vet Pharmacol Ther*, **20**, 318-322.

4. USE OF PROBABILISTIC MODELING WITHIN A PHYSIOLOGICALLY BASED PHARMACOKINETIC MODEL TO PREDICT SULFAMETHAZINE RESIDUE WITHDRAWAL TIMES IN EDIBLE TISSUES IN SWINE

Jennifer Buur, Ronald Baynes, Geof Smith, and Jim Riviere

2006

Published in *Antimicrobial Agents and Chemotherapy*, 50(7), 2344-2351

Abstract

The presence of antimicrobial agents in edible tissues of food producing animals remains a major public health concern. Probabilistic modeling techniques incorporated into a physiologically based pharmacokinetic (PBPK) model were used to predict residues of sulfamethazine in edible tissues in swine. A PBPK model for sulfamethazine in swine was adapted to include an oral dosing route. Distributions for sensitive parameters were determined and used in a Monte Carlo analysis to predict tissue residue times. Validation of the distributions was done by comparison of a Monte Carlo analysis to an external data set determined from the literature and an *in vivo* pilot study. The model was used to predict the upper limit of the 95% confidence interval of the 99th percentile of the population as recommended by the United States Food and Drug Administration (US-FDA). The external data set was used to calculate the withdrawal time using the tolerance limit algorithm designed by the US-FDA. Both methods were compared to the labeled withdrawal time for the same dose. The Monte Carlo method predicted a withdrawal time of 21 days based on kidney residues. The tolerance limit method applied to the time limited data set predicted a withdrawal time of 12 days. The existing US-FDA label withdrawal time is 15 days. PBPK models can incorporate probabilistic modeling techniques that make them useful in prediction of tissue residue times. These models can be used to calculate parameters required by the US-FDA and explore those conditions where the established withdrawal time may not be sufficient.

Introduction

Sulfamethazine is a sulfonamide antibiotic used in the swine industry as a feed or water additive. It is labeled for treatment of bacterial pneumonia, cervical abscesses, and bacterial swine enteritis, as well as in the prevention of these diseases during times of stress, maintenance of weight gains in the presence of atrophic rhinitis, growth promotion, and increased feed efficiency ("Vetgram Online Database," 2005). Research has shown that high concentrations of this drug may cause thyroid tumors in specific strains of rats (Poirier et al., 1999). Also, there is a wide range of human allergic reactions related to sulfonamide drugs in general (Slatore et al., 2004; Wong et al., 2005). Thus there is a large public health concern relating to possible adverse health effects of consuming sulfamethazine residues found in the edible tissues of swine that warrants development of predictive pharmacokinetic models.

Meat withdrawal periods are required by the US-FDA to ensure the safety of the meat supply and address this public health concern. A meat withdrawal period is the time between when a chemotherapeutic is administered to a food animal and when that animal is sent to slaughter. They are designed to guarantee that drug residues in edible tissues will be below tolerance limits before animals are sent to slaughter. Currently, withdrawal times are determined using the "Tolerance Limit Method." This method predicts a withdrawal time by calculating a regression line for the linear portion of the depletion curve. Individual animal data is then used to calculate the perceived population variance of the line and thus to predict the upper limit of the 95% confidence interval for the 99^{th} percentile of the population for the rate of elimination. The withdrawal time is calculated using the newly calculated regression line (US-FDA-CVM, June 21, 2005). The current tolerance level for sulfamethazine in swine was established in 1968 at 0.1 ppm (μg/mL for plasma and μg/mg for tissues) for all edible tissues ("Federal Food, Drug, and Cosmetic Act," 1982). According to the 2003 Food Safety Inspection Service (FSIS) red book, sulfamethazine was the only sulfonamide found in violation of tolerance levels in swine (FSIS, 2004), again stressing the public health significance of this compound.

Physiologically based pharmacokinetic models (PBPK) are predictive models that use mass balance equations to link tissue compartments via a plasma compartment. Unlike other pharmacokinetic modeling techniques, they are based on physiological mechanisms and can be used over a large range of doses and routes of administration (Riviere, 1999). Briefly, PBPK models consist of a number of tissue blocks linked together via blood flow through a communal plasma block. Each tissue block is mathematically modeled with mass balance equations and such parameters as tissue volume (rather than the traditional volume of distribution), blood:tissue partition coefficients, and percent tissue blood flow (Grass et al., 2002). Bioavailability is incorporated into PBPK models by mechanistically describing oral absorption rates and first pass metabolism inherent within the portal circulation. For the purposes of this manuscript, the term parameter refers to the physiological aspects incorporated into the mathematical model.

PBPK models have been used in toxicology to predict internal dose metrics which are applied to human health risk assessment (Bailer et al., 1997; el-Masri et al., 1995; Gentry et al., 2003). The United States Environmental Protection Agency (US-EPA) has recently published a draft guidance available for public review on the incorporation of PBPK models in risk assessment (US-EPA, August, 2006). In human medicine, PBPK models are used to calculate individual dosing regimens in situations where drugs with low therapeutic indices are needed, such as chemotherapeutics, or when there are severe alterations in patient physiology, such as infancy or pregnancy (Bjorkman, 2004; Kawai et al., 1994; Tsukamoto et al., 2001). PBPK models are also used in drug development studies (Blesch et al., 2003). Currently there are only a handful of PBPK models published for veterinary medicine (Brocklebank et al., 1997; Buur et al., 2005; Craigmill, 2003; Duddy et al., 1984).

Our previous work predicted meat withdrawal times after extralabel use of sulfamethazine intravenously in swine for the mean of the population (Buur et al., 2005). However,

sulfamethazine is rarely used as an intravenous preparation. Also, the model, while useful for the prediction of a meat withdrawal time for extralabel drug use under the guidelines of the Animal Medicinal Drug Use Clarification Act, does not take into account population variability ("Animal Medicinal Drug Use Clarification Act," 1994). Therefore, it cannot be used in industry to satisfy the stringent US-FDA regulatory requirements.

Monte Carlo is a probabilistic modeling technique that uses distributions rather than single points to define parameters. Random values from the set distributions are generated and then incorporated into the model for each simulation run. The number of simulations is defined by the user and can range from a single simulation to thousands of simulations. This allows for an output of multiple simulations whose scope represents the possible differences within a target population. Several studies in the literature show how this type of distribution sampling can be incorporated into PBPK modeling and have been applied to human health risk assessment (Cox, 1996; Jonsson et al., 2002; Sweeney L. M. et al., 2001; Thomas et al., 1996). It has also been postulated that the use of Monte Carlo techniques would be advantageous in the estimation of meat withdrawal times (Fisch, 2000). In veterinary medicine, the use of Monte Carlo techniques is mostly found in epidemiology where it is used to determine the risk factors for disease, model prevalence within a population, and investigate different strategies in disease prevention and control (Green et al., 2004; Hopp et al., 2003; Karsten et al., 2005). To our knowledge, there are no published studies applying Monte Carlo techniques to issues of meat safety.

The purpose of this study was to incorporate Monte Carlo techniques into a PBPK model and use that model to compute a meat withdrawal time according to the current US-FDA standards. Sulfamethazine was used as the representative drug in the representative species of swine.

Methods

Model Development

The PBPK model (**Figure 4.1**) used in this research was adapted from a previously published model of sulfamethazine in swine (Buur et al., 2005). Briefly, the model contains 5 tissue blocks (adipose, kidney, liver, muscle, and carcass) as well as a plasma compartment for sulfamethazine. It is linked through the liver to a 2 tissue compartment (liver and body) model for the N4-acetyl metabolite. Elimination was modeled through renal clearance as well as hepatic clearance for both the parent compound and its metabolite and was assumed to be first order. The original model also included an intravenous route of administration. Tissue concentrations were defined as a homogenate of drug found within the tissue as well as drug found within the tissue blood. Concentrations represent total drug. Concentrations were modeled using standard flow limited mass balance equations. We refer the reader to Buur et al for detailed information regarding the basic model (Buur et al., 2005).

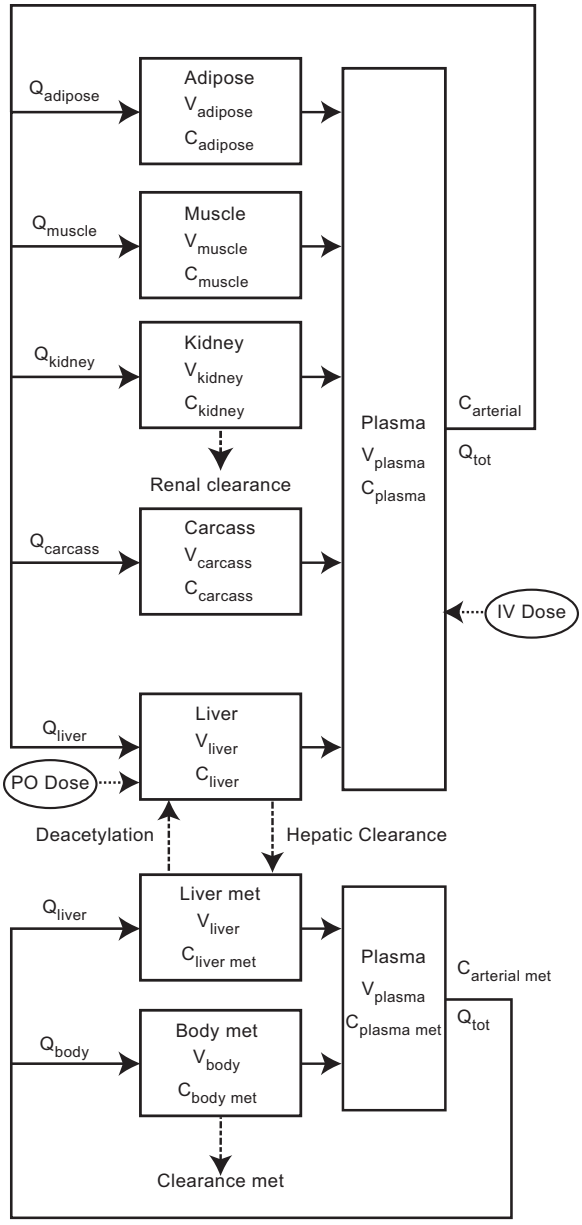

Figure 4.1 Schematic diagram of the PBPK model for Sulfamethazine in pigs

V, tissue volume; C, tissue concentration; Q, tissue blood flow; Qtot cardiac output.

An oral dosing module consisting of a 2 tissue compartment model that included stomach and intestine (**Figure 4.2**) has now been incorporated into the model. It was assumed that all the drug was immediately available in the stomach. Distribution into the intestine was controlled by the rate of gastric emptying (K_{st}). Once in the intestine, drug absorption was governed by the rate of absorption (K_a) using the following equation:

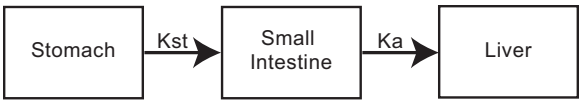

Figure 4.2 Schematic diagram of the oral dosing route of administration

Kst: Rate of gastric emptying; Ka: Rate of absorption

$$\frac{dCi}{dt} = Kst \bullet Cs - Ka \bullet Ci \qquad [1]$$

where Cs (g/L) and Ci (g/L) are the concentration of the drug in the stomach and intestine respectively; Kst is the rate of gastric emptying; Ka is the rate of absorption. Drug absorption was assumed to go directly into the liver from the portal circulation. Both the rate of gastric emptying and the rate of absorption were assumed to be linear processes.

Parameter Distributions

All parameters were subjected to sensitivity analysis to determine which had the largest effect on drug distribution (data not shown) after oral dosing. Sensitive parameters were defined to be those parameters that had a significant effect on sulfamethazine plasma pharmacokinetics relative to the other parameters. Insensitive parameters were defined by point estimates and were not subjected to Monte Carlo analysis. Insensitive parameters and their values are presented in **Table 4.1**. Readers are referred to Buur et al for details regarding how these parameters were established (Buur et al., 2005). Only parameters judged to be sensitive were subject to Monte Carlo analysis. Sensitive parameters included rate of absorption (Ka), rate of gastric emptying (Kst), hepatic clearance of sulfamethazine, plasma protein binding of sulfamethazine, and plasma protein binding of N4-acetyl metabolite (**Table 4.2**). Distributions for these sensitive parameters were taken from the literature (Guerin

et al., 2001; Kokue et al., 1988; Kuiper H.A. et al., 1985; Kuiper Harry A. et al., 1988; Nouws J. F. et al., 1989; Nouws J. F. et al., 1986a; Nouws J.F.M. et al., 1986b; Piva et al., 1997; Sweeney R. W. et al., 1993; Yuan et al., 1997). Boundaries for the distributions were determined by taking the largest reported standard deviation and then adding that to the maximum or subtracting that from the minimum value reported in the literature. Distributions were assumed to be log normal. Means and standard deviations for the resulting distributions were determined using an online freeware applet (www.stat.vt.edu/~sundar/java/applets/). Briefly, the probability density function was adjusted to visually represent the published means and ranges. The applet then reported the mean and standard deviation for a log normal distribution having that shape. Final distributions as well as nontransformed ranges are presented in **Table 4.2**.

Table 4.1 Final values for insensitive parameters used in model simulations

Partition Coefficient (plasma:tissue)	**Value[a]**
Adipose P	0.336
Kidney P	1.68
Liver P	0.378
Muscle P	0.08
Acetyl metabolite Liver P	0.079
Acetyl metabolite Body P	1.297
Blood Flow (% of total cardiac output)	
Liver blood flow	0.38
Kidney blood flow	0.1188
Muscle blood flow	0.25
Adipose blood flow	0.08
Metabolism of N4-acetyl metabolite	
Rate of deacetylation (1/h)	3.66
Acetyl metabolite Clearance (mL/min kg)	2.558

[a]Specifics on how these values were obtained can be found in Buur et al 2005

In Vivo Study

All procedures were approved by the North Carolina State University Institutional Animal Care and Use Committee. Five female Yorkshire cross pigs weighing between 82 and 105 kg were purchased from North Carolina State University Research Unit #2 and underwent

Table 4.2 Final distributions for sensitive parameters used in the Monte Carlo analysis

Parameter	Units	Distribution	Mean	Log Mean	Variance	Lower Bound[e]	Upper Bound[e]	Reference
Ka[a]	per hour	lognormal	0.1	-1	0.88	0.0682	3.01	1, 2, 3
Kst[b]	per hour	lognormal	0.1	-1	0.4	0.0183	1.05	1, 4
CL hepatic[c]	mL/min/kg	lognormal	0.39	-0.4	0.32	0.05	1.5	3, 5, 6, 7
P binding SMZ[d]	%	lognormal	0.42	-0.38	0.1	0.37	0.99	5, 6, 8, 9, 10
P binding met[d]	%	lognormal	0.35	-0.45	0.11	0.34	0.92	5, 6, 8, 9, 10

[a]Ka is rate of absorption. [b]Kst is rate of gastric emptying. [c]Cl hepatic is hepatic clearance. [d]P binding is protein binding of either sulfamethazine (SMZ) or N4-acetyl metabolite (met). [e]Boundaries reflect the range of nontransformed values seen throughout the lognormal distribution. References: 1, Kokue 1988; 2, Piva 1997; 3, Sweeney 1993; 4, Guerin 2001; 5, Nouws 1989; 6, Nouws 1986a; 7, Yuan 1997, 8, Kuiper 1985; 9, Kuiper 1988; 10, Nouws 1986b

jugular catheterization 3 days prior to the study. A single IV dose of 35 mg/kg sodium sulfamethazine was administered in the auricular vein and plasma samples were taken at times 0, 0.5, 1, 2, 6, 8, 12, 24, 31, 48, 54, 72, and 96 hours. Due to catheter malfunctions, not all plasma samples were available for every animal. Animals were euthanized at 4, 28, 51, 76, and 99 hours and muscle, adipose, liver, and kidney tissues were harvested for analysis. Blood samples were centrifuged and plasma harvested within 1 hour of sample collection. All tissue and plasma samples were frozen at –80 ºC until analyzed. Analysis occurred within 1 week of sampling. Tissues and plasma samples were analysis using the HPLC methods described below.

HPLC Methods

Sample preparation: Sample preparation for each tissue were based upon the method published by Furusawa (Furusawa, 2003). Briefly, for muscle, liver, adipose, and kidney tissues, 1 g of tissue was accurately weighed and added to 2 mL of 10% perchloric acid. Each sample was homogenized using a Brinkman Polytron Homogenizer (Razdale, Ontario, Canada) for 45 seconds and then centrifuged at 1200 rpm for 10 minutes at 24 ºC. Adipose tissue was centrifuged at 15 ºC. The supernatant from the muscle tissue was filtered through a 45 µm disk filter and injected into the HPLC system. Supernatant from liver and kidney

tissue as well as the aqueous phase from adipose tissue was processed further using solid phase extraction. An Oasis MCX 3cc 60 mg sorbent weight (Waters, Milford, MA, USA) cartridge was conditioned with 1 mL of methanol and 1 mL of water. The sample was added and the cartridge was then washed with 1 mL 0.1 N HCl and 1 mL methanol. Cartridges were dried under vacuum for 30 seconds. Samples were eluted with 1 mL ammonium hydroxide:acetonitrile (5:95 v/v) and the cartridges were again dried under vacuum. Elution volumes were evaporated to dryness in a Zymark Turbo Vap LV (Hopkington, MA) for 15 minutes at 50 ºC and 15 mmHg psi reagent grade Nitrogen gas. Residue was reconstituted in 0.5 mL ammonium acetate buffer (pH 4.5, 0.1 M), vortexed and then injected in the HPLC system. One milliliter of plasma was acidified by addition of 20 µL o-phosphoric acid and then subjected to the solid phase extraction process detailed above.

For all methods, the CV for both interday and intraday validations were below 15% and recoveries were between 90 and 105%. Standard curves were linear from 0.1 to 2.5 µg/mL. Any samples above the limits of the standard curve were diluted until results fell within the curve limits. Quality control samples were run on the day of analysis and recoveries were greater than 90%.

System: The HPLC system consisted of a Waters 600 Controller with Waters 717 Plus autosampler and Waters 996 Photodiode Array Detector (Milford, MA, USA). An Agilent Zorbax SB-C8 column (4.6 x 150 mm, 5µm) (Wilmington, DE) was used. All injection volumes were 10 µL and flow rates were 1 mL/minute. Autosampler and column temperatures were maintained at 25 ºC and 30 ºC respectively. Optimum detector wavelength was 267 nm. Mobile phase conditions for tissue samples and plasma samples were acetonitrile:ammonium acetate buffer (pH 4.5, 0.1 M) (19:81 v/v) and acetonitrile: ammonium acetate buffer (pH 4.5, 0.1 M) (17:83 v/v), respectively. All reagents used were HPLC reagent grade.

Monte Carlo Analysis

Monte Carlo analysis was performed using the Monte Carlo wizard included in the ACSLxtreme 2.01 software (Aegis Technology Group, Huntsville, AL, USA). Each Monte Carlo run included 100 simulations for validation and 1000 simulations for meat withdrawal time prediction. Every Monte Carlo analysis, no matter the number of simulations, was performed identically in a step wise manner. For each simulation, a number was randomly generated for each sensitive parameter according to the distributions defined in **Table 4.2**. Those numbers were incorporated into the mathematical model and used to generate both tissue and plasma concentration-time curves. This was repeated for the specified number of simulations.

For validation of the distributions, a single Monte Carlo analysis of 100 simulations was compared to an external data set created from the literature and from an *in vivo* pilot study. Published *in vivo* pharmacokinetic studies were excluded from the data set based on physiological status of the swine as well as assay methodology. Colorimetric analysis of drug concentrations, general anesthesia, and experimentally infected pigs were all excluded from the data set. The external data set for IV route included data from 4 published *in vivo* data sets and the *in vivo* pilot study data. Five published data sets for single oral dosing and 4 published *in vivo* data sets for multiple oral dosing were included in the external data set for the oral route. All concentration data points were normalized by dose or the ratio of accumulation factors as needed and weighted equally. Each data point from the published studies represents the mean value (UN-SCAN-IT, version 6.0, Silk Scientific Inc., Orem, Utah USA) for sulfamethazine concentration reported in the literature. Data points were also converted to µg/L or µg/g for comparison of plasma and tissue concentrations respectively. Means ranged in number of animals from 2 to 23 pigs. Overall, there were a total of 9 studies, 4 of which included tissue data, and the *in vivo* pilot study described above (Mitchell et al., 1986a; Mitchell et al., 1986b; Nouws J. F. et al., 1989; Nouws J. F. et al.,

1986a; Paulson G. et al., 1980; Paulson G. D. et al., 1987; Piva et al., 1997; Sweeney R. W. et al., 1993; Yuan et al., 1997). Doses ranged from 2.36 mg/kg to 50 mg/kg. Because the carcass block represents all portions of the pig not included in the other tissue blocks and thus cannot be quantitated, it was not included in the validation or application procedures. The validation run for IV route was simulated at 1 mg/kg. For the oral route, the dose was 10 mg/kg once daily for seven days. The parameter distributions were considered acceptable if upon comparison with the external data set, most data points were within the scope of the simulations.

Prediction of Withdrawal Time

Monte Carlo method: For each edible tissue, a series of 100 Monte Carlo runs (of 1000 simulations each) were made using the US-FDA labeled dose of 237.6 mg/kg orally on day 1 followed by 118.8 mg/kg orally on days 2, 3 and 4. For each run, a withdrawal time was calculated for the 99th percentile of the population. The withdrawal time for the 99th percentile of the population for each run was calculated to be the time when 99% of all simulations were below the tolerance level. A 95th percent confidence interval was then calculated for each set of 100 withdrawal times. The longest withdrawal time calculated using the upper limit of the 95th percent confidence interval was taken to be the estimated withdrawal time.

Tolerance limit method: In addition, the data set compiled for use in validation was used to calculate the withdrawal time based on the tolerance limit algorithm recommended by the US-FDA. Readers are referred to the US-FDA Guidance #3 for specific information regarding the exact method (US-FDA-CVM, June 21, 2005). Briefly, this method calculates an equation for the linear portion of the depletion curve of each tissue for the 99th percentile of the population using data points gathered during an *in vivo* study. The variance is calculated and assumed to be equal along all points of the elimination curve and is used

to calculate the 95% confidence interval. The tissue with the longest withdrawal time is selected to be the basis for the withdrawal time. Both withdrawal times calculated (Monte Carlo method and tolerance limit method) were compared to the existing US-FDA label withdrawal time of 15 days for sulfamethazine.

Results

In Vivo Study

Data from the in vivo study closely resembled means reported in the literature. **Tables 4.3 and 4.4** present specific plasma and tissue concentrations found from this pilot study. The plasma data showed slight variations at times 1 and 24 hours that deviated from the expected continual decline of an IV dose.

Table 4.3 Plasma concentrations after IV injection of 35 mg/kg Sulfamethazine

Time (h)	Mean (μg/mL)	SD (μg/mL)	n
0.5	181.3	14.9	4
1	121.5	31.9	4
2	149.2	9.4	4
6	125.1	24.4	5
8	100.4	20.2	4
12	64.1	20.6	3
24	74.1	8.6	4
31	56.1	21.4	3
48	29.6	2.7	3
54	18.3	8.8	2
72	9.1	7.3	2
96	7.1	n/a [a]	1

[a] n/a - not applicable.

Monte Carlo Analysis

Representative Monte Carlo runs for each tissue are presented in **Figure 4.3** (IV route) and **Figure 4.4** (oral route). Please note that the simulations are reported in μg/L or μg/g for plasma and tissue concentrations respectively. As evidenced by the large amount of data points covered by the simulations, excellent coverage was achieved for all tissues for the IV route of administration. The model tended to over predict early time points for all tissues but muscle, but covered all points

Table 4.4 Tissue concentrations from IV injection of 35 mg/kg Sulfamethazine

Time	Tissue Concentration (μg/mg) n=1			
(h)	Kidney	Liver	Adipose	Muscle
4.2	35.5	34.0	14.9	27.6
27.6	17.4	17.7	4.1	13.2
50.8	5.8	6.6	2.1	4.0
75.7	1.5	2.0	0.6	1.6
98.3	1.0	1.9	0.3	0.7

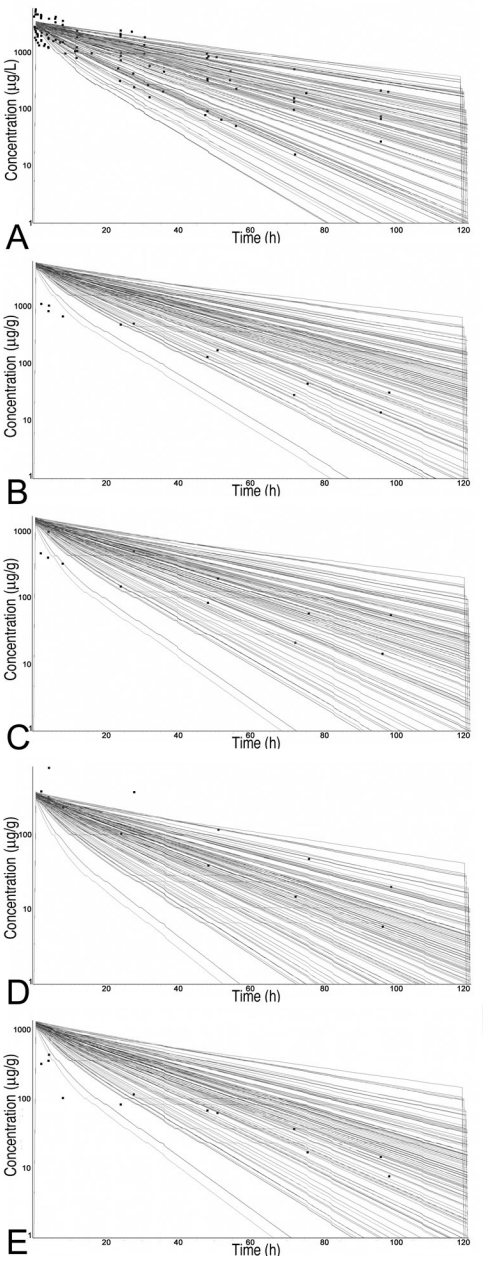

Figure 4.3 Monte Carlo simulations for Sulfamethazine concentrations in edible tissues after intravenous administration

Squares represent data points from the external data set (means from published studies and individual pig data from in vivo pilot study) and are normalized to a dose of 1 mg/kg. Tissue represented include A: plasma; B: kidney; C: liver; D: muscle; and E: fat

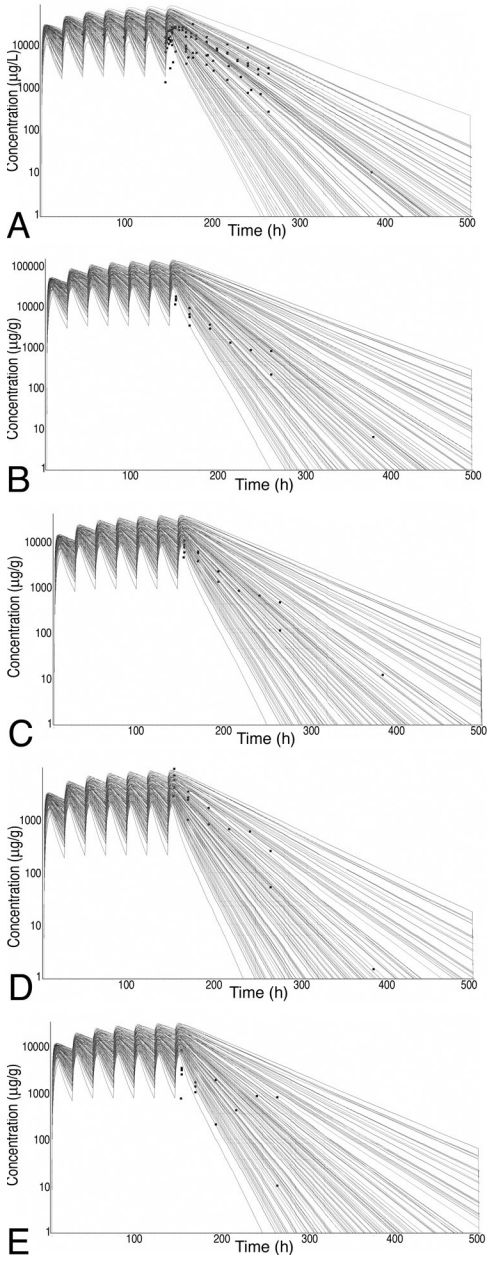

Figure 4.4 Monte Carlo simulations for Sulfamethazine concentration in edible tissues after oral administration

Doses were normalized to a standard dose of 10 mg/kg once daily for 7 days. Squares represent data points from the external data set (means from published studies). Tissue represented include A: plasma; B: kidney; C: liver; D: muscle; and E: fat

Table 4.5 Withdrawal time predictions and 95% confidence intervals in days for the 99th percentile of the population for each edible tissue after 100 Monte Carlo runs of 1000 simulations

Tissue	Mean (days)	Lower Bound 95% Confidence Interval (days)	Upper Bound 95% Confidence Interval (days)
Plasma	19.76	19.64	19.88
Kidney	20.84	20.72	20.97
Liver	17.97	17.86	18.07
Adipose	17.49	17.39	17.60
Muscle	14.69	14.60	14.79

during the elimination phase. Some early time points were under predicted for muscle. For oral route of administration, the only points not covered by the spread were early time points occurring during the absorption phase. Again, terminal time points had excellent coverage by the simulation spread. Terminal points are the most relevant to withdrawal time determination.

Prediction of Withdrawal Time

Monte Carlo method: A representative distribution of withdrawal times from a Monte Carlo run for the label dose in kidney tissue is presented in **Figure 4.5**. Similar distributions were seen for all other tissues. **Table 4.5** shows the results of the multiple Monte Carlo runs for each tissue and their corresponding confidence intervals. It can be seen that kidney tissue had the longest withdrawal time. We predict a

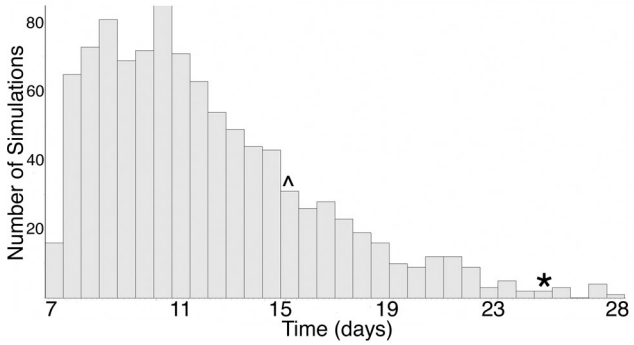

Figure 4.5 Representative distribution of the time it takes for Sulfamethazine concentrations to fall below the tolerance of 0.1 ppm in kidney tissue from a Monte Carlo run of 1000 simulations

* represents the 99th percentile of the distribution;
^ represents the current withdrawal time of 15 days.

withdrawal time of 21 days based on this analysis. This is 6 days longer than the current label withdrawal time of 15 days.

Tolerance limit method: The tolerance limit method predicts a withdrawal time of 12 days. This is 3 days less than the label withdrawal time of 15 days.

Discussion

We have successfully incorporated probabilistic modeling into a PBPK model and applied it to the prediction of meat withdrawal times. We were able to predict the upper limit of a 95% confidence interval for the 99th percentile of the population. Thus, the applied method allows for simulations to be conducted that meet the recommendations for establishment of meat withdrawal times established by the US-FDA ("Federal Food, Drug, and Cosmetic Act," 2004).

The validity of this model is directly dependent upon the distributions used to define key parameters. It was noted during the creation of these distributions that several probability density functions could be used that would describe the same mean and range that was found in the published literature. The different distributions did produce different population spreads (data not shown). Ranges of values for the parameter distributions were taken to be the broadest in terms of both variability in the population and uncertainty in the distributions reported. This would increase the overall spread of the Monte Carlo output and allow for a more conservative estimation for withdrawal time. The distributions could also overestimate population variance since we were unable to correct for the variance inherent within the literature studies. The wider distributions contribute to a more conservative estimation for a meat withdrawal time and should be considered when applying the model to practical situations. However, from a public health standpoint, it is better to err by creating a more conservative meat withdrawal time than risk the consequences of possible tissue residues.

Furthermore, the model can be easily updated as more data is generated regarding the true distributions of the parameters.

Log normal distributions were assumed for parameters based upon their acceptance within regulatory agencies such as the US-FDA and US-EPA with regards to population estimation. Again, further research into the exact distributions for both parameters and populations would continue to increase the accuracy of this model. It should be noted that a strength of this type of probabilistic modeling is the transparency of which the assumptions and results are reported. The 99th percentile of the population was established without assuming any specific distribution.

The accuracy of the model was determined by its ability to predict similar concentrations as those found in the external data set. Each point of the external data set represented a mean concentration from the pigs (n ranged from 3 to 6) used in the published studies. In order to get a more robust estimate of individual pig variations, a small *in vivo* pilot study was performed. While this study only produced a single data point for each tissue at each slaughter time, the results of the pilot study coincided well with previously published results for all tissues and allowed us to accept the means with a greater degree of confidence. In fact, the minor idiosyncrasies seen in the pilot study were graphically indistinguishable from other studies when plotted together (**Figure 4.3**). This again helped to establish robustness within the external data set. The external data set also incorporated a wide range of dosing regimens. Dose independence, due to the mechanistic nature of PBPK models, is a strength of PBPK models. This allows for validation against a wide range of doses and application to a dose not found within the external data set. The model tended to over predict early time points. This may reflect a difference between absorption *in vivo* and how absorption was calculated in the model. However, time points in the elimination portion of the curves were well covered by the Monte Carlo analysis. Since we are applying the model to the prediction

of meat withdrawal times, the accuracy of predicting later time points is more important. Further refining of the model could be made to increase the accuracy of early time point predictions.

Another source of variability within the population could be due to breed differences in metabolism and protein binding. To our knowledge, there are no reports of this in swine for sulfamethazine or for any other drug. Breed differences are most likely incorporated into the parameter distributions that were taken from the literature since these studies were carried out on various breeds and cross-breeds of swine. Variability within pigs can also be increased if the drug was given in feed to a pen of animals. Differences in social hierarchy and interpig personalities will mean a difference in overall drug intake and thus in the administered dose. All studies used for validation that were orally dosed, were done in such a manner (ie. gavage) as to be able to accurately determine the true dose given to each pig. Variability in the pharmacokinetics of the N4-acetyl metabolite could also effect the population pharmacokinetics of sulfamethazine. The metabolite was included in the model due to the unique deacetylation pathway that increases the concentration of the parent compound at later time points. In fact, the plasma protein binding of this metabolite was determined to be a sensitive parameter and was included in the Monte Carlo analysis. Ultimately, there are an infinite number of sources of variability between pigs in terms of drug disposition. Sensitivity analyses help to narrow the scope by identifying those parameters which impact on pharmacokinetic predictions. Therefore the Monte Carlo analysis did not include parameter distributions where parameters were determined to be insensitive.

The oral withdrawal time predicted by the Monte Carlo method is 6 days longer than the labeled withdrawal time. Sulfamethazine had an original withdrawal time of 5 days that was established in 1968. In 1980, the current withdrawal time of 15 days was established using an algorithm based on the sensitivity of the analytical tests available at that time (“Federal

Food, Drug, and Cosmetic Act," 1982). While this was the standard practice at that time, sensitivity and specificity of analytical techniques has substantially increased over the last 25 years. Thus the labeled withdrawal time may not cover the population according to the current rigorous standards now required by the US-FDA. Our model shows that the withdrawal time for approximately 20% of the population is often greater than the 15 days currently used. This could account for the significant amount of tissue residue violations found with this drug (FSIS, 2004). Beyond the differences between the methods used, other reasons for the differences in withdrawal time could be related to the distributions used. As was discussed above, multiple distributions can provide for the same shape and range of the curve. Also, we are comparing the means of several studies rather than individuals. You would expect an even greater spread between data points if more individuals were included. Individual pig data could contribute to an even longer withdrawal time if even larger variability was shown. The addition of the *in vivo* study for IV route did create a more robust external data set and allowed us to evaluate the model in terms of individual variability. Thus the model provided excellent coverage of individuals as well as means.

The tolerance limit method predicted a withdrawal time 3 days less than the label withdrawal time. This is most likely because the data set did not include points beyond 5 days post treatment, a limitation not present in a PBPK model. A major assumption in the Tolerance Limit Method is that there are enough time points on the depletion portion of the concentration-time curve to accurately assess the terminal slope. Given the kinetics of sulfamethazine in swine, the data set most likely does not have enough data to accurately determine that terminal slope. Thus the tolerance limit method is descriptive in nature and dependent upon the sample used. The PBPK model, on the other hand, is not dependent upon the data set for exact determination of terminal slopes. Thus its predictive nature, rather than the descriptive nature of the tolerance limit method, provides a strength for the prediction of withdrawal times.

In conclusion, we were able to incorporate probabilistic modeling into a PBPK model using Monte Carlo sampling and then successfully use the model to predict the tissue kinetics of sulfamethazine in swine. As a result of this, we believe that the current withdrawal time of 15 days may be inadequate to cover the upper limit of the 95% confidence interval for the 99th percentile of the swine population and should be reevaluated in light of sulfamethazine residue public health concerns.

Acknowledgments

Funding for this project was supported in part by the Food Animal Residue Avoidance Databank (FARAD) and USDA-Cooperative State Research, Education and Extension Service grant No. 2002-45051-01362.

References

Animal Medicinal Drug Use Clarification Act (1994). United States Food and Drug Administration. Title 21 Code of Federal Regulations, part 530.

Bailer, A. J. & Dankovic, D. A. (1997) An introduction to the use of physiologically based pharmacokinetic models in risk assessment. *Statistical methods in medical research*, **6**, 341-358.

Bjorkman, S. (2004) Prediction of drug disposition in infants and children by means of physiologically based pharmacokinetic (PBPK) modelling: theophylline and midazolam as model drugs. *British Journal of Clinical Pharmacology*, **59**, 691-704.

Blesch, K. S., Gieschke, R., Tsukamoto, Y., Reigner, B. G., Burger, H. U. & Steimer, J. L. (2003) Clinical pharmacokinetic/pharmacodynamic and physiologically based pharmacokinetic modeling in new drug development: the capecitabine experience. *Invest New Drugs*, **21**, 195-223.

Brocklebank, J. R., Namdari, R. & Law, F. C. (1997) An oxytetracycline residue depletion study to assess the physiologically based pharmacokinetic (PBPK) model in farmed Atlantic salmon. *Can Vet J*, **38**, 645-646.

Buur, J. L., Baynes, R. E., Craigmill, A. L. & Riviere, J. E. (2005) Development of a physiologic-based pharmacokinetic model for estimating sulfamethazine concentrations in swine and application to prediction of violative residues in edible tissues. *American Journal of Veterinary Research*, **66**, 1686-1693.

Cox, L. A., Jr. (1996) Reassessing benzene risks using internal doses and Monte-Carlo uncertainty analysis. *Environ Health Perspect*, **104 Suppl 6**, 1413-1429.

Craigmill, A. L. (2003) A physiologically based pharmacokinetic model for oxytetracycline residues in sheep. *J Vet Pharmacol Ther*, **26**, 55-63.

Duddy, J., Hayden, T. L., Bourne, D. W., Fiske, W. D., Benedek, I. H., Stanley, D., Gonzalez, A. & Heierman, W. (1984) Physiological model for distribution of sulfathiazole in swine. *J Pharm Sci*, **73**, 1525-1528.

el-Masri, H. A., Thomas, R. S., Benjamin, S. A. & Yang, R. S. (1995) Physiologically based pharmacokinetic/pharmacodynamic modeling of chemical mixtures and possible applications in risk assessment. *Toxicology*, **105**, 275-282.

Federal Food, Drug, and Cosmetic Act (1982). Title 21, Code of Federal Regulations, 21-CFR-556.670.

Federal Food, Drug, and Cosmetic Act (2004). Title 21, Code of Federal Regulations, 21-CFR-500.80.

Fisch, R. D. (2000) Withdrawal time estimation of veterinary drugs: extending the range of statistical methods. *J Vet Pharmacol Ther*, **23**, 159-162.

FSIS (2004). *2003 FSIS National Residue Program Data.* Food Safety Inspection Service. United States Department of Agriculture, Washington, DC.

Furusawa, N. (2003) A clean and rapid liquid chromatographic technique for sulfamethazine monitoring in pork tissues without using organic solvents. *J Chromatogr Sci*, **41**, 377-380.

Gentry, P. R., Covington, T. R., Clewell, H. J., 3rd & Anderson, M. E. (2003) Application of a physiologically based pharmacokinetic model for reference dose and reference concentration estimation for acetone. *Journal of toxicology and environmental health. Part A*, **66**, 2209-2225.

Grass, G. M. & Sinko, P. J. (2002) Physiologically-based pharmacokinetic simulation modelling. *Advanced drug delivery reviews*, **54**, 433-451.

Green, M. J., Burton, P. R., Green, L. E., Schukken, Y. H., Bradley, A. J., Peeler, E. J. & Medley, G. F. (2004) The use of Markov chain Monte Carlo for analysis of correlated binary data: patterns of somatic cells in milk and the risk of clinical mastitis in dairy cows. *Prev Vet Med*, **64**, 157-174.

Guerin, S., Ramonet, Y., Lecloarec, J., Meunier-Salaun, M. C., Bourguet, P. & Malbert, C. H. (2001) Changes in intragastric meal distribution are better predictors of gastric emptying rate in conscious pigs than are meal viscosity or dietary fibre concentration. *Br J Nutr*, **85**, 343-350.

Hopp, P., Webb, C. R. & Jarp, J. (2003) Monte Carlo simulation of surveillance strategies for scrapie in Norwegian sheep. *Prev Vet Med*, **61**, 103-125.

Jonsson, F. & Johanson, G. (2002) Physiologically based modeling of the inhalation kinetics of styrene in humans using a bayesian population approach. *Toxicol Appl Pharmacol*, **179**, 35-49.

Karsten, S., Rave, G. & Krieter, J. (2005) Monte Carlo simulation of classical swine fever epidemics and control. II. Validation of the model. *Vet Microbiol*, **108**, 199-205.

Kawai, R., Lemaire, M., Steimer, J. L., Bruelisauer, A., Niederberger, W. & Rowland, M. (1994) Physiologically based pharmacokinetic study on a cyclosporin derivative, SDZ IMM 125. *J Pharmacokinet Biopharm*, **22**, 327-365.

Kokue, E., Shimoda, M., Sakurada, K. & Wada, J. (1988) Pharmacokinetics of oral sulfa drugs and gastric emptying in the pig. *J Pharmacobiodyn*, **11**, 549-554.

Kuiper, H. A., Aerts, R. M. L., Haagsma, N. & Gogh, H. V. (1985). Pharmacokinetic behaviour of sulfamethazine in piglets upon oral administration through feed. *Comparative Veterinary Pharmacology, Toxicology, and Therapy:* Proceedings of the 3rd Congress of European Association for Veterinary Pharmacology and Toxicology, Ghent, Belgium, 54.

Kuiper, H. A., Aerts, R. M. L., Haagsma, N. & Gogh, H. V. (1988) Case study of the depletion of sulfamethazine from plasma and tissues upon oral administration to piglets affected with atrophic rhinitis. *Journal of Agriculture and Food Chemistry*, **36**, 822-825.

Mitchell, A. D. & Paulson, G. D. (1986a) Depletion kinetics of 14C-sulfamethazine [4-amino-N-(4, 6-dimethyl-2-pyrimidinyl)benzene[U-14C]sulfonamide] metabolism in swine. *Drug Metab Dispos*, **14**, 161-165.

Mitchell, A. D., Paulson, G. D. & Zaylskie, R. G. (1986b) Steady state kinetics of 14C-sulfamethazine [4-amino-N-(4,6-dimethyl-2-pyrimidinyl)benzene[U-14C]sulfonamide] metabolism in swine. *Drug Metab Dispos*, **14**, 155-160.

Nouws, J. F., Vree, T. B., Baakman, M., Driessens, F., Vellenga, L. & Mevius, D. J. (1986a) Pharmacokinetics, renal clearance, tissue distribution, and residue aspects of sulphadimidine and its N4-acetyl metabolite in pigs. *Vet Q*, **8**, 123-135.

Nouws, J. F. M., Vree, T. B., Breukink, H. J., Vanmiert, A. S. J. P. A. M. & Grondel, J. (1986b). Pharmacokinetics, hydroxylation and acetylation of sulphadimidine in mammals, birds, fish, reptiles and molluscs. *Comparative Veterinary Pharmacology, Toxicology, and Therapy:* Proceedings of the 3rd Congress of European Association for Veterinary Pharmacology and Toxicology, Lancaster, UK, 301-318.

Nouws, J. F., Mevius, D., Vree, T. B. & Degen, M. (1989) Pharmacokinetics and renal clearance of sulphadimidine, sulphamerazine and sulphadiazine and their N4-acetyl and hydroxy metabolites in pigs. *Vet Q*, **11**, 78-86.

Paulson, G. & Struble, G. (1980) I. A unique deaminated metabolite of sulfamethazine [4-amino-N-(4,6-dimethyl-2-pyrimidinyl) benzenesulfonamide] in swine. *Life Sci*, **27**, 1811-1817.

Paulson, G. D. & Feil, V. J. (1987) Evidence for diazotization of 14C-sulfamethazine [4-amino-N-(4,6-dimethyl-2-pyrimidinyl)benzene[U-14C]sulfonamide] in swine. The effect of nitrite. *Drug Metab Dispos*, **15**, 841-845.

Piva, A., Anfossi, P., Meola, E., Pietri, A., Panciroli, A., Bertuzzi, T. & Formigoni, A. (1997) Effect of microcapsulation on absorption processes in the pig. *Livestock Production Sciences*, **51**, 53-61.

Poirier, L. A., Doerge, D. R., Gaylor, D. W., Miller, M. A., Lorentzen, R. J., Casciano, D. A., Kadlubar, F. F. & Schwetz, B. A. (1999) An FDA review of sulfamethazine toxicity. *Regul Toxicol Pharmacol*, **30**, 217-222.

Riviere, J. E. (1999). *Comparative Pharmacokinetics: Principles, Techniques, and Applications.* Blackwell Publishing, Inc., Ames, Iowa.

Slatore, C. G. & Tilles, S. A. (2004) Sulfonamide hypersensitivity. *Immunol Allergy Clin North Am*, **24**, 477-490, vii.

Sweeney, L. M., Tyler, T. R., Kirman, C. R., Corley, R. A., Reitz, R. H., Paustenbach, D. J., Holson, J. F., Whorton, M. D., Thompson, K. M. & Gargas, M. L. (2001) Proposed occupational exposure limits for select ethylene glycol ethers using PBPK models and Monte Carlo simulations. *Toxicological sciences*, **62**, 124-139.

Sweeney, R. W., Bardalaye, P. C., Smith, C. M., Soma, L. R. & Uboh, C. E. (1993) Pharmacokinetic model for predicting sulfamethazine disposition in pigs. *Am J Vet Res*, **54**, 750-754.

Thomas, R. S., Lytle, W. E., Keefe, T. J., Constan, A. A. & Yang, R. S. (1996) Incorporating Monte Carlo simulation into physiologically based pharmacokinetic models using advanced continuous simulation language (ACSL): a computational method. *Fundamental and applied toxicology*, **31**, 19-28.

Tsukamoto, Y., Kato, Y., Ura, M., Horii, I., Ishikawa, T., Ishitsuka, H. & Sugiyama, Y. (2001) Investigation of 5-FU disposition after oral administration of capecitabine, a triple-prodrug of 5-FU, using a physiologically based pharmacokinetic model in a human cancer xenograft model: comparison of the simulated 5-FU exposures in the tumour tissue between human and xenograft model. *Biopharm Drug Dispos*, **22**, 1-14.

US-EPA (August, 2006). *Approaches for the Application of Physiologically Based Pharmacokinetic (PBPK) Models and Supporting Data in Risk Assessment.* Office of Research and Development. National Center for Environmental Assessment. U.S. Environmental Protection Agency, Washington, DC.

US-FDA-CVM (June 21, 2005). *Guidance for Industry #3: General principles for evaluation of the safety of compounds used in food producing animals*. Center for Veterinary Medicine. U.S. Food and Drug Administration, Washington, DC.

Vetgram Online Database. (2005). Food Animal Residue Avoidance Databank www.farad.org/vetgram/VetGramSearch, Accessed September 2005.

Wong, G. A. & Shear, N. H. (2005) Adverse drug interactions and reactions in dermatology: current issues of clinical relevance. *Dermatol Clin*, **23**, 335-342.

Yuan, Z. H., Miao, X. Q. & Yin, Y. H. (1997) Pharmacokinetics of ampicillin and sulfadimidine in pigs infected experimentally with Streptococcus suum. *J Vet Pharmacol Ther*, **20**, 318-322.

5. PHARMACOKINETICS OF FLUNIXIN MEGLUMINE IN SWINE AFTER INTRAVENOUS DOSING

Jennifer Buur, Ronald Baynes, Geof Smith, and Jim Riviere

2006

Published in the *Journal of Veterinary Pharmacology and Therapeutics*, 29, 437-440

Introduction

Flunixin meglumine is a non-steroidal anti-inflammatory drug (NSAID) used in many species. It is licensed for use in the United States for beef cattle, dairy cattle, and horses, and is indicated for the regulation of inflammation in endotoxemia and the control of pyrexia associated with respiratory disease. It is also approved for use for the treatment of respiratory disease in swine in Germany. Recently, flunixin was approved for use in swine after intramuscular injection in the United States (Anonymous, 2006). However, intravenous (IV) use remains a common route of extralabel drug use. There is a need for pharmacokinetic parameters to be available to calculate appropriate meat withholding times that are required by the Animal Medicinal Drug Use Clarification Act ("Animal Medicinal Drug Use Clarification Act," 1994). Pharmacokinetic parameters have been established for flunixin in a variety of species including cattle, goat, sheep, llama, camel, donkey, horse, chicken, rabbit, cat and dog (Anderson et al., 1990; Baert et al., 2002; Cheng et al., 1998; Coakley et al., 1999; Elmas et al., 2006; Horii et al., 2004; Konigsson et al., 2003; Navarre et al., 2001; Odensvik et al., 1995; Ogino et al., 2005; Oukessou, 1994; Rantala et al., 2002). However, to our knowledge, there has not been a published pharmacokinetic study of flunixin meglumine in swine. The purpose of this study was to explore the pharmacokinetic parameters of flunixin meglumine in swine after IV dosing.

Methods

Five healthy landrace-yorkshire cross pigs weighing between 18.6 and 26.5 kg received a 2.0 mg/kg IV dose of flunixin meglumine via a dedicated lumen of a double lumen jugular catheter. The day before the study, pigs were placed under anesthesia using ketamine, tiletamine, and xylazine and double lumen jugular catheters were placed using a blind guide wire technique. Placement of catheters was confirmed by successful blood draws. Blood draws of 10 mL were performed at 0, 0.25, 0.5, 1, 2, 4, 8, 12, 24, 31, and 48 hours after injection using the alternate lumen of the double lumen catheter. Blood was drawn into

heparinized tubes, spun immediately and plasma was collected. Plasma was frozen at –80 ºC until processed. All samples were analyzed within 1 week of the study. Pigs were confirmed to be healthy by physical exam prior to use in the study. All protocols were approved by the North Carolina State University Institutional Animal Care and Use Committee.

Total flunixin concentration was quantified using ultra high pressure liquid chromatography (UPLC) with mass spectrometric (MS) detection. Plasma samples of 0.5 mL were acidified with 20 µL O-phosphoric acid and added to an Waters Oasis MCX cartridge (6 mL, 150 mg sorbent weight) after the cartridge was conditioned with 3 mL of methanol followed by 3 mL of water. The loaded cartridge was washed with 3 mL of 0.1 N hydrochloric acid followed by 3 mL of methanol:0.1 N hydrochloric acid solution (90:10 v/v) and dried under vacuum for 30 seconds. Flunixin was eluted with 3 mL methanol:ammonium hydroxide (95:5 v/v), evaporated to dryness, reconstituted in 250 µL of mobile phase, and filtered through a 0.22 µm nylon syringe filter. Injection volume was 10 µL. Concentrations were derived by comparing peak areas of the samples to those of an external standard curve made from spiked plasma samples put through the same clean up process.

The Acquity UPLC-MS (Waters) consisted of a BEH C18 column (1.7 µm, 2.1 x 50 mm) and filter disk. The mobile phase was acetonitrile:1% acetic acid in water (50:50 v/v). The EMD 1000 was a single quadrupole mass spectrometer run in ESI+ mode. The ion used for quantification was 297. Column temperature was 30 ºC and sample temperature was 24 ºC. Run times were 1.5 minutes. **Figure 5.1** shows representative chromatographs for both blank plasma and plasma spiked at a level of 0.1 µg/mL. The limit of detection was 0.01 µg/mL and the limit of quantification was 0.02 µg/mL. Relative standard deviations for both interday and intraday were less than 15 % at all concentrations. Recoveries for all concentrations were within 15% of true concentration. The linear range was between 0.01 and 10 µg/mL.

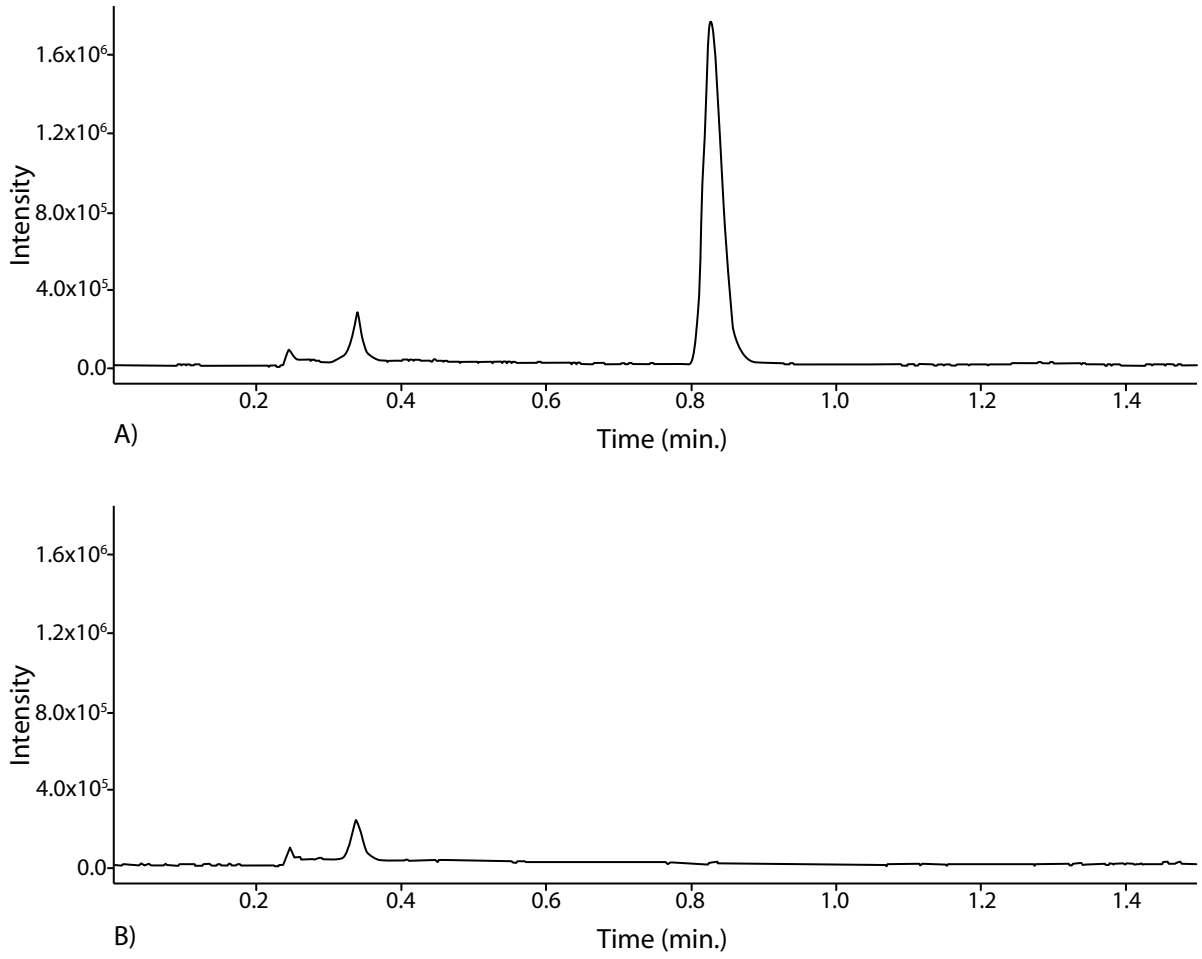

Figure 5.1 Chromatographs for swine plasma spiked with Flunixin Meglumine at a level of 0.1 µg/mL (A) and blank (B)

To determine the percent of protein binding, ultracentrifugation was performed for physiologically relevant concentrations. Briefly, frozen porcine plasma (pooled from 3 pigs) was spiked with flunixin to final concentrations of 0, 0.3, 1, 3, and 10 µg/mL. Plasma was allowed to equilibrate in a 37 ºC water bath for 60 minutes. After equilibration, 1 mL of spiked plasma was transferred into a Millipore Centrifree YM-30 ultrafiltration cartridge (30,000 molecular weight cut off) and spun at 3000 rpm for 30 minutes. The ultrafiltrate was filtered using a 0.22 µm syringe filter and 10 µL were injected onto the UPLC-MS for quantification. Ultracentrifugation was performed in triplicate. Total drug concentration was

confirmed using the technique listed above. Concentration of bound drug was calculated from the difference between total and free drug concentrations. Percent bound was defined as

$$\text{Percent Bound} = \frac{Cb}{Ct} \bullet 100 \qquad [1]$$

where Cb is concentration bound and Ct is total concentration.

Pharmacokinetic analysis was performed using WinNonlin Professional, Version 5.0.1 (Pharsight) software. Compartmental analysis was evaluated based on coefficient of determination and Akaike's Information Criteria (AIC) for the best fit model. Samples were weighted using $1/Y^2$ and area under the plasma concentration-time curve (AUC) was computed using the trapezoidal method with the last triangle extrapolated to infinity.

Results

Flunixin was best described using a 2 compartment open model. **Figure 5.2** shows the predicted plasma concentration vs. time profile vs. the observed plasma concentrations for flunixin in swine after IV administration. All plasma concentrations were below limit of quantification by 48 hours and 2 pigs were below limit of quantification by 31 hours. A secondary peak was observed for 2 pigs. The elimination half life and total body clearance were 7.76 h and 297 mL/h/kg respectively. The volume of distribution at steady state

Table 5.1 Pharmacokinetic parameters for Flunixin Meglumine after 2.0 mg/kg IV dose in swine

Parameter	Units	Mean	SD
$t_{1/2\beta}$	h	7.99	1.4
$t_{1/2\beta}$	h	7.76*	
AUC	hr•μg/mL	7.74	3.1
CL	mL/h/kg	297.92	93.9
MRT	h	6.02	1.6
V_{ss}	mL/kg	1826.72	722.6
V_{area}	mL/kg	3425.24	1488.7
$t_{1/2\alpha}$	h	0.33	0.06
$t_{1/2\alpha}$	h	0.32*	
α	1/h	2.14	0.4
β	1/h	0.09	0.02

* harmonic mean. $t_{1/2}$, half life for distribution (α) or elimination (β) phase; AUC, area under the plasma concentration-time curve; CL, total body clearance; MRT, mean residence time; V_{ss}, volume of distribution at steady state; V_{area}, volume of distribution based on AUC

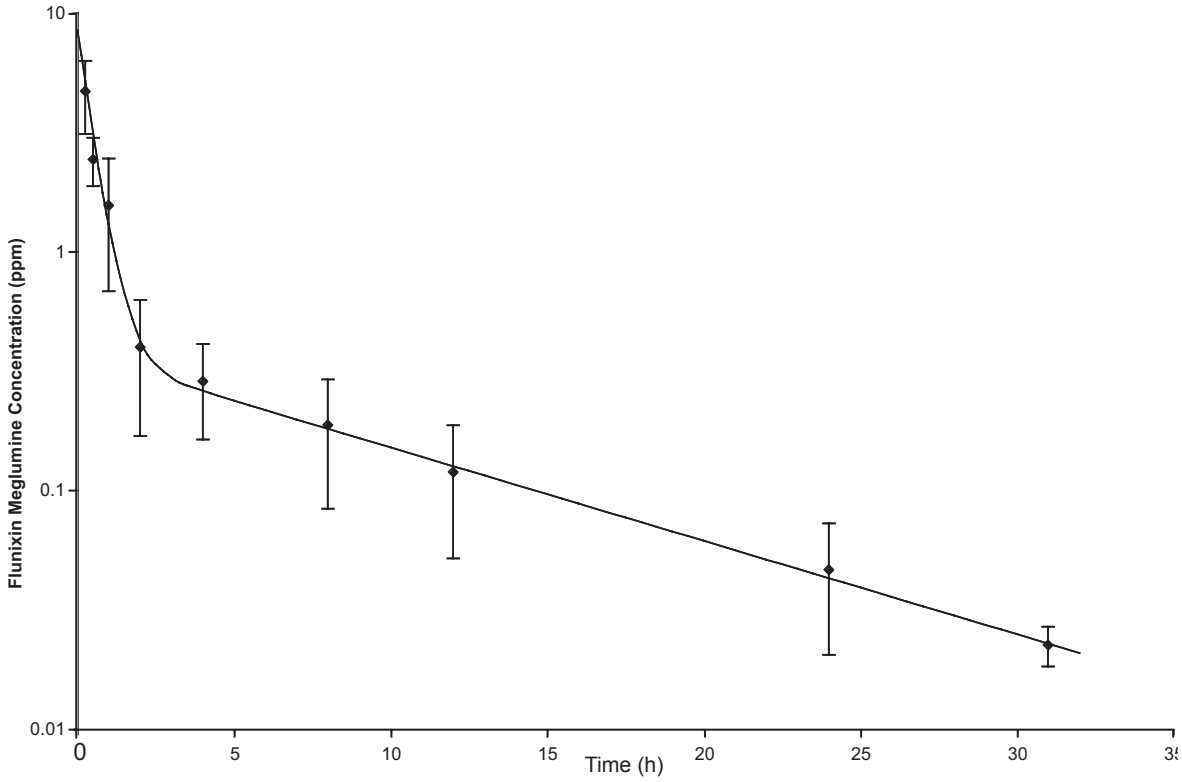

Figure 5.2 Mean plasma concentration +/- SD of Flunixin Meglumine after a 2.0 IV dose in swine

(Vdss) was 1826 mL/kg. **Table 5.1** presents the pharmacokinetic parameters after IV dosing. Flunixin was greater than 98% protein bound at all physiologically relevant concentrations (**Table 5.2**).

Discussion

Variability at inflection time points was enhanced due to the variable presence of a secondary peak. The peak most likely correlates to enterohepatic recycling of flunixin. The secondary

Table 5.2 Percent plasma protein binding at physiological concentrations of Flunixin Meglumine in swine

Total Concentration	Percent Protein Bound	
µg/mL	Mean	SD
0.3	99.13	0.002
1	99.25	0.004
3	98.95	0.001
10	98.71	0.002

peak was seen in 2 out of the 5 pigs. Enterohepatic recycling has been reported for flunixin in other species including cattle, cats and goats (Horii et al., 2004; Konigsson et al., 2003; Odensvik et al., 1995).

The total body clearance of 0.30 L/kg/h reported here is larger than what has been reported in other species that ranged from 0.03 L/kg/h in horses to 0.15 L/kg/h in cattle (Anderson et al., 1990; Pellegrini-Masini et al., 2004). However this value correlates well with the clearance (0.39 L/kg/h) reported on the label of the approved product. The half life for flunixin in these pigs (7.76 h) after IV dosing is longer than that reported for the swine product (4 h) but is within the range of half lives reported in other species that ranged from 1.16 h in dogs to 8.12 h in cattle (Anonymous, 2006; Ogino et al., 2005). This could also be explained by the large Vdss observed in our study. A variable range in terminal half life has been reported in cattle and is believed to be due to variable enterohepatic circulation (Anonymous, 2006). This could also be the case for swine. The 98% percent protein binding of flunixin in pigs parallels values for percent plasma protein binding found in other species.

The most surprising aspect of this study was the large Vdss. Because flunixin is highly protein bound, one would predict a much smaller Vdss. Flunixin has a wide range of Vdss, ranging from 30 (llama) to 782 (cattle) mL/kg in other species (Anonymous, 2006; Navarre et al., 2001). While over twice the value reported for any other species, the Vdss of 1826 mL/kg found in these pigs correlates well with the reported Vdss from the labeled product (2003 mL/kg). Large Vdss have been reported in other NSAIDS used in human and veterinary medicine including Celecoxib (4.5 and 2.3 L/kg for humans and dogs respectively), Etoricoxib (1.7 L/kg in humans), and Firocoxib (2.5 and 2.9 L/kg in cats and dogs respectively) (Agrawal et al., 2003; Davies et al., 2000; McCann et al., 2004; McCann et al., 2005; Paulson et al., 2001). Like flunixin, Celecoxib and Etoricoxib are also highly protein bound in humans (Agrawal et al., 2004; Davies et al., 2000). Protein

binding for firocoxib was not reported for any species. The lager Vdss has been attributed to higher lipophilicity. A larger Vdss may also be explained by altered and high affinity tissue binding properties (Riviere, 1999). Thus tissue residue studies need to be explored as residue violations may occur if withholding intervals are based completely on plasma drug concentrations.

In conclusion, plasma pharmacokinetics of flunixin meglumine after IV dosing in swine is characterized by a 2 compartment model, large Vdss, and high protein binding. Further studies including tissue depletion studies are needed to accurately predict an appropriate meat withholding period for extralabel drug use.

Acknowledgements

Funding for this project was supported in part by the Food Animal Residue Avoidance Databank (FARAD) and USDA-Cooperative State Research, Education and Extension Service grant No. 2002-45051-01362.

References

Agrawal, N. G., Matthews, C. Z., Mazenko, R. S., Kline, W. F., Woolf, E. J., Porras, A. G., Geer, L. A., Wong, P. H., Cho, M., Cote, J., Marbury, T. C., Moncrief, J. W., Alcorn, H., Jr., Swan, S., Sack, M. R., Robson, R. A., Petty, K. J., Schwartz, J. I. & Gottesdiener, K. M. (2004) Pharmacokinetics of etoricoxib in patients with renal impairment. *J Clin Pharmacol*, **44**, 48-58.

Agrawal, N. G., Porras, A. G., Matthews, C. Z., Rose, M. J., Woolf, E. J., Musser, B. J., Dynder, A. L., Mazina, K. E., Lasseter, K. C., Hunt, T. L., Schwartz, J. I., Mccrea, J. B. & Gottesdiener, K. M. (2003) Single- and multiple-dose pharmacokinetics of etoricoxib, a selective inhibitor of cyclooxygenase-2, in man. *Journal of Clinical Pharmacology*, **43**, 268-276.

Anderson, K. L., Neff-Davis, C. A., Davis, L. E. & Bass, V. D. (1990) Pharmacokinetics of flunixin meglumine in lactating cattle after single and multiple intramuscular and intravenous administrations. *American Journal of Veterinary Research*, **51**, 1464-1467.

Animal Medicinal Drug Use Clarification Act (1994). United States Food and Drug Administration. Title 21 Code of Federal Regulations, part 530.

Anonymous (2006). *Compendium of Veterinary Products,* 9th Edition Eds S. Inglis. Adrian J. Bayley, Port Huron, Michigan.

Baert, K. & De Backer, P. (2002) Disposition of sodium salicylate, flunixin and meloxicam after intravenous administration in broiler chickens. *Journal of Veterinary Pharmacology and Therapeutics*, **25**, 449-453.

Cheng, Z., Mckeller, Q. & Nolan, A. (1998) Pharmacokinetic studies of flunixin meglumine and phenylbutazone in plasma, exudate and transudate in sheep. *Journal of Veterinary Pharmacology and Therapeutics*, **21**, 315-321.

Coakley, M., Peck, K. E., Taylor, T. S., Matthews, N. S. & Mealey, K. L. (1999) Pharmacokinetics of flunixin meglumine in donkeys, mules, and horses. *American Journal of Veterinary Research*, **60**, 1441-1444.

Davies, N. M., McLachlan, A. J., Day, R. O. & Williams, K. M. (2000) Clinical pharmacokinetics and pharmacodynamics of celecoxib: a selective cyclo-oxygenase-2 inhibitor. *Clinical pharmacokinetics*, **38**, 225-242.

Elmas, M., Yazar, E., Uney, K. & Karabacak, A. (2006) Pharmacokinetics of flunixin after intravenous administration in healthy and endotoxaemic rabbits. *Veterinary Research Communications*, **30**, 73-81.

Horii, Y., Ikenaga, M., Shimoda, M. & Kokue, E. (2004) Pharmacokinetics of flunixin in the cat: enterohepatic circulation and active transport mechanism in the liver. *Journal of Veterinary Pharmacology and Therapeutics*, **27**, 65-69.

Konigsson, K., Torneke, K., Engeland, I. V., Odensvik, K. & Kindahl, H. (2003) Pharmacokinetics and pharmacodynamic effects of flunixin after intravenous, intramuscular and oral administration to dairy goats. *Acta Veterinaria Scandinavica*, **44**, 153-159.

McCann, M. E., Andersen, D. R., Zhang, D., Brideau, C., Black, W. C., Hanson, P. D. & Hickey, G. J. (2004) In vitro effects and in vivo efficacy of a novel cyclooxygenase-2 inhibitor in dogs with experimentally induced synovitis. *American Journal of Veterinary Research*, **65**, 503-512.

McCann, M. E., Rickes, E. L., Hora, D. F., Cunningham, P. K., Zhang, D., Brideau, C., Black, W. C. & Hickey, G. J. (2005) In vitro effects and in vivo efficacy of a novel cyclooxygenase-2 inhibitor in cats with lipopolysaccharide-induced pyrexia. *American Journal of Veterinary Research*, **66**, 1278-1284.

Navarre, C. B., Ravis, W. R., Nagilla, R., Deshmukh, D., Simpkins, A., Duran, S. H. & Pugh, D. G. (2001) Pharmacokinetics of flunixin meglumine in llamas following a single intravenous dose. *Journal of Veterinary Pharmacology and Therapeutics*, **24**, 361-364.

Odensvik, K. & Johansson, I. M. (1995) High-performance liquid chromatography method for determination of flunixin in bovine plasma and pharmacokinetics after single and repeated doses of the drug. *American Journal of Veterinary Research*, **56**, 489-495.

Ogino, T., Mizuno, Y., Ogata, T. & Takahashi, Y. (2005) Pharmacokinetic interactions of flunixin meglumine and enrofloxacin in dogs. *American Journal of Veterinary Research*, **66**, 1209-1213.

Oukessou, M. (1994) Kinetic disposition of flunixin meglumine in the camel (Camelus dromedarius). *Veterinary Research*, **25**, 71-75.

Paulson, S. K., Vaughn, M. B., Jessen, S. M., Lawal, Y., Gresk, C. J., Yan, B., Maziasz, T. J., Cook, C. S. & Karim, A. (2001) Pharmacokinetics of celecoxib after oral administration in dogs and humans: effect of food and site of absorption. *Journal of pharmacology and experimental therapeutics*, **297**, 638-645.

Pellegrini-Masini, A., Poppenga, R. H. & Sweeney, R. W. (2004) Disposition of flunixin meglumine injectable preparation administered orally to healthy horses. *Journal of Veterinary Pharmacology and Therapeutics*, **27**, 183-186.

Rantala, M., Kaartinen, L., Valimaki, E., Stryrman, M., Hiekkaranta, M., Niemi, A., Saari, L. & Pyorala, S. (2002) Efficacy and pharmacokinetics of enrofloxacin and flunixin meglumine for treatment of cows with experimentally induced Escherichia coli mastitis. *Journal of Veterinary Pharmacology and Therapeutics*, **25**, 251-258.

Riviere, J. E. (1999). *Comparative Pharmacokinetics: principles, techniques, and applications*. Blackwell Publishing, Inc., Ames, Iowa.

6. A PHYSIOLOGICALLY BASED PHARMACOKINETIC MODEL OF PROTEIN BINDING INTERACTION BETWEEN SULFAMETHAZINE AND FLUNIXIN MEGLUMINE IN SWINE

Jennifer Buur, Ronald Baynes, Geof Smith, and Jim Riviere

2007

Abstract

As the use of combination drug therapy increases, so does the chance for an adverse drug reaction due to drug-drug interactions. A physiologically based pharmacokinetic (PBPK) model was developed and validated to explore the mechanism and consequences of plasma protein binding drug interactions between sulfamethazine (SMZ) and flunixin meglumine (FLU) in swine. The model consists of four compartments for SMZ; namely quickly perfused tissues, slowly perfused tissues, liver, and blood. N4-acetyl metabolite disposition was modeled with three compartments (liver, body, and blood) and connected to the SMZ model through the liver. Protein binding was assumed to be linear and the interaction between SMZ and FLU was assumed to be competitive inhibition. The model was optimized using previously published data and validated by comparison to an interaction *in vivo* study. Values for the dissociation constant (Kd) and maximum binding capacity (Bmax) for SMZ and FLU were derived *in vitro* and were 238.8 ± 39, 802.6 ± 75, 310.5 ± 118, and 3748.5 ± 514 μMol respectively. The model accurately predicted both free and total SMZ concentrations alone and in the presence of FLU, when displacement occurred. The model had an overall correlation (R^2) of 0.85 for SMZ concentrations in plasma. This approach has use in the elucidation of the mechanistic and clinical impact of plasma protein binding interactions and ultimately in the design of dosing regimens.

Introduction

Combination drug therapy is quickly becoming the standard of practice in both human and veterinary medicine. Because of the greater number of drugs used in combination, the likelihood of an adverse drug reaction due to drug-drug interactions has vastly increased (Saltvedt et al., 2005). Safety and efficacy of chemotherapeutics is determined by the concentration of free drug in the system. Free drug concentrations are determined by, among other things, the pharmacodynamic affinity for plasma proteins defined by the dissociation constant Kd, and the maximum plasma protein binding capacity defined by Bmax (Wilkinson, 2001). Thus alterations in either Kd, Bmax, or both could cause an increase or decrease in free drug concentration. Many theoretic arguments have been presented to show that the alteration of free drug concentration within an open system, such as a patient, would be transient due to compensatory mechanisms in free drug clearance and thus plasma protein binding interactions would have no clinical effect (Benet et al., 2002; Toutain et al., 2002).

Physiologically based pharmacokinetic (PBPK) models predict drug disposition based on physiological mechanisms. These models use a series of mass balance equations to link together selected tissue and blood compartments. These models include parameters that are physiological (ie.. blood flow, tissue volume), physiochemical (ie.. tissue:blood partition coefficients) and *in vitro* (ie.. Michalis-Menten enzyme kinetics and protein binding) in nature (Grass et al., 2002; Reitz et al., 1988; Teeguarden et al., 2005). Currently, PBPK models are used in toxicology to predict internal dose metrics, in human medicine to calculate individual dose regimens for drugs of low therapeutic indices, and in veterinary medicine to estimate meat withdrawal times for drugs after extralabel use (Buur et al., 2005; Buur et al., 2006a; Craigmill, 2003; Gentry et al., 2003; Kawai et al., 1994; Tsukamoto et al., 2001). PBPK models have also been used to predict drug interactions due to enzyme inhibition and to explore mechanisms behind specific pharmacokinetic phenomenon such as time to reach equilibrium in protected spaces (Kanamitsu et al., 2000; Liu et al., 2005;

Simmons, 1996). We hypothesized that PBPK models could be used as a tool to elucidate the underlying mechanism of protein binding interactions and evaluate the interaction for clinical relevance. To our knowledge, there are no published models that predict the effect of protein binding drug interactions *in vivo* within the context of a PBPK modeling approach.

The combination of antimicrobial and non-steroidal anti-inflammatory drugs is common in both veterinary and human medicine. Sulfamethazine (SMZ) is a sulfonamide antibiotic that is labeled in swine for the treatment of bacterial pneumonia, cervical abscess, and bacterial enteritis. Flunixin meglumine (FLU) is a non-steroidal anti-inflammatory that is approved for use in swine to control pyrexia associated with swine respiratory disease (Anonymous, 2006). There is a single study in horses that reports an alteration of SMZ kinetics in horses that have been treated with FLU. The authors concluded that these differences were due to alterations in protein binding (el-Banna, 1999). While these specific drugs are not used in human medicine, they can serve as model drugs for the very common sulfonamide antimicrobial and NSAID drug classes to illustrate the impact of protein binding interactions.

The purpose of this study was to develop and validate a PBPK model that incorporates protein binding drug interactions with a second drug and to use this model to explore the clinical consequences of the possible interaction. SMZ and FLU were used as model drugs as they are not only from the most common drug classes used in human medicine, but are also a commonly used combination in swine medicine.

Materials and Methods

In Vitro Protein Binding Saturation Studies

For all protein binding studies, fresh plasma was obtained from multiple swine (ranging from 3 to 5 per experiment) using jugular venipuncture. Whole blood was spun at 1500 RPM for 10 minutes and plasma was harvested. Plasma was either stored at room temperature and

used within 3 hours of the initial blood draw or frozen immediately and stored at –4 ºC and used within 1 week of initial blood draw.

For SMZ binding saturation studies, fresh or frozen plasma was diluted 1:10 (vol/vol plasma:phosphate buffered saline pH 7.4). Plasma samples were spiked with SMZ to final concentrations of 0, 0.5, 1, 5, 10, 20, 30, 60, 100, and 150 ppm. Samples were incubated and allowed to reach equilibrium in a 37 ºC water bath for 60 minutes. One milliliter of sample was transferred to Centrifree YM-30 (Millipore, Bedford, MA) ultrafiltration cartridge (30,000 molecular weight cut off) and spun in a fixed rotor centrifuge at 2000 g for 20 minutes. Ultrafiltrate was injected directly onto the HPLC. Each concentration was repeated in triplicate. Nonspecific binding was shown to be insignificant. Mean data from multiple experiments were fit to a one site binding hyperbola, using Prism v. 4.03 for Windows (GraphPad Software, Inc, San Diego CA, USA). Statistical analysis between fresh and frozen plasma values was performed using a one site ANOVA in Prism v. 4.03 for Windows (GraphPad Software, Inc, San Diego CA, USA).

For FLU binding saturation studies, both total and non-specific binding was quantified. Fresh plasma was diluted 1:250 (vol/vol) with phosphate buffered saline (pH 7.4). Samples were spiked to FLU final concentrations of 0, 0.3, 1, 3, 30, 60, 100, 300, 600, 1000 ppm and were incubated for 60 minutes in order to reach equilibrium in a 37 ºC water bath with or without 170 ppm (dissociation constant in human plasma) phenylbutazone. One half milliliter was transferred to a Centrifree YM-30 (Millipore, Bedford, MA) ultrafiltration cartridge (30,000 molecular weight cut off) and spun in a fixed rotor centrifuge at 2000 g for 30 minutes. Ultrafiltrate was discarded and clean receptacles were placed on the ultracentrifugation devises. One milliliter of methanol was added and the devises were vortexed for 30 seconds. Samples were then respun at 2000 g for 30 minutes and the ultrafiltrate injected onto the

UPLC. Specific binding was calculated by subtracting non-specific binding from total binding. Data was fit to a one site binding hyperbola as described for the SMZ studies.

Quantification Methods

HPLC: The HPLC system consisted of a Waters Alliance 2695 Separation Module with a 996 photodiode array detector (Milford, MA). A Zorbax SB-C8 column (4.6 by 150 mm, 5 um; Agilent, Wilmington, DE) was used. All injection volumes were 10 µL and flow rates were 1 mL/min. Autosampler and column temperatures were maintained at 25 ºC and 30 ºC respectively. The optimum detector wavelength was 267 nm. Mobile-phase conditions were acetonitrile:ammonium acetate buffer (pH 4.5, 0.1M) (17:83; vol/vol). Run times were 9 minutes.

SMZ plasma samples were prepared using the technique as previously described (Buur J. et al., 2006a). Briefly, 1 mL of plasma was acidified with 20 µL O-phosphoric acid and then added to an Oasis MCX 3cc 60 mg sorbent weight (Waters, Milford, MA) cartridge that had been conditioned with 1 mL of methanol followed by 1 mL of water. Samples were washed with 1 mL of 0.1 N HCl and 1 mL of methanol and then dried under vacuum for 30 s. Elution was performed with 1 mL of ammonium hydroxide-methanol (5:95; vol/vol) and dried under vacuum for 30 s. Elution volumes were evaporated to dryness in a Turbo Vap LV evaporator (Zymark; Hopkington, MA) for 15 min. at 50 ºC and 15 mm Hg psi reagent-grade nitrogen gas. Residue was reconstituted in 0.5 mL ammonium acetate buffer (pH 4.5, 0.1M), vortexed, and then injected onto the HPLC system.

Concentrations were determined by comparison of peak areas to an external standard curve created by spiked plasma samples put through the same clean up process. Coefficients of variation for both interday and intraday were below 15% and recoveries ranged were between 90% and 105%. The standard curve was linear from 0.1 to 10 ppm. Samples were diluted

until concentrations fell within the curve limits. Quality control samples run on the day of analysis had recoveries greater than 90%. Limit of detection was 0.05 ppm and limit of quantification was 0.1 ppm.

Ultrafiltrate from SMZ protein binding studies was injected directly onto the HPLC system. Concentrations were compared to an external standard curve prepared from SMZ standards in mobile phase. The standard curve was linear from 0.05 to 10 ppm. Limit of detection and limit of quantification were 0.01 and 0.05 ppm respectively.

UPLC-MS: The Acquity UPLC-MS system (Waters, Milford, MA) consisted of a BEH C18 column (1.7 um, 2.1 by 50 mm, Waters, Milford, MA) and filter disc. The mobile phase was acetonitrile:1% acetic acid in water (50:50; vol/vol). The EMD 1000 was a single quadrupole mass spectrometer run in ESI+ mode. The ion used for quantification was 297. Column and sample temperatures were maintained at 30 ºC and 24 ºC respectively. Run times were 1.5 minutes.

FLU plasma samples were prepared using the technique as previously described (Buur et al., 2006b). Briefly, 0.5 mL of plasma was acidified using 20 µL of O-phosphoric acid. Samples were added to an Oasis MCX 6 cc 150 mg sorbent weight (Waters, Milford, MA) cartridge that had been conditioned with 3 mL of methanol followed by 3 mL of water. Samples were washed with 3 mL of 0.1N HCl and 3 mL of methanol:0.1N HCl (90:10; vol/vol) and then dried under vacuum for 30 s. Elution was achieved using 3 mL of methanol:ammonium hydroxide (5:95; vol/vol). Samples were again dried under vacuum for 30 s. Elution volumes were evaporated to dryness in a Turbo Vap LV evaporator for 20 minutes at 50 ºC and 15 mm Hg psi reagent grade nitrogen gas. Residue was reconstituted in 250 µL mobile phase and filtered through a 22 um nylon syringe filter and then injected onto the UPLC system.

Concentrations were determined by comparison of peak areas to an external standard curve created by spiked plasma samples put through the same clean up process. Coefficients of variation for both interday and intraday were below 15% and recoveries were within 15% of true concentration. The standard curve was linear from 0.01 to 10 ppm. All samples were diluted until the results fell with the curve limits. Quality control samples run on the day of analysis had recoveries greater than 90%. Limit of detection was 0.01 ppm and limit of quantification was 0.02 ppm.

In Vivo Interaction Validation Study

All procedures were approved the North Carolina State University Institutional Animal Care and Use Committee. Double lumen catheters were placed in both the left and right jugular veins of five female Yorkshire cross pigs weighing between 15.15 and 17.5 Kg. Catheterization was performed under anesthesia induced with a combination of ketamine, tiletamine, and xylazine. Catheters were placed using the Seldinger technique and placement was verified by successful blood draws. At the time of catheterization, each pig was given an IV dose of 27 mg/kg SMZ and then were started on a constant rate infusion (CRI) of SMZ at a rate of 1.5 mg/kg/hr. All CRI's were maintained by the Homepump Eclipse C-Series pump (100 mL volume, 0.5 mL/h rate, I-Flow Corp., Lake Forest, CA) attached to the backs of the pigs. All blood draws were 10 mL in volume and taken from the contralateral jugular catheter. Briefly, each study was designed to keep SMZ at steady state and look at changes due to the interactions of FLU. The first set of studies does this using a single IV bolus of FLU. The final study was designed with CRI of FLU to keep FLU also at steady state. Due to logistical complications, the CRI of FLU were unable to be maintained and so the animals were given an additional IV bolus of FLU.

Study 1 consisted of 2 pigs prepped as described above. Blood draws were performed at 0, 18, 25, 42, and 49 hours after start of the SMZ CRI to confirm steady state. At 68 hours after

the start of the SMZ CRI, a 2.0 mg/kg bolus dose of FLU was given through the second lumen of the SMZ CRI catheter. Blood draws were continued at 5, 10, 15, 30, and 45 minutes, and 1, 2, 4, 8, 12, 24, 36, 48, 60, 72, 84, and 96 hours post FLU dose. All samples were kept at 37 ºC in a hot water bath until spun at 1500 RPM for 10 minutes and the plasma was harvested. One milliliter of plasma was immediately transferred to a Centrifree YM-30 (Millipore, Bedford, MA) ultrafiltration cartridge (30,000 molecular weight cut off) and spun at 2000 g for 30 minutes. The ultrafiltrate and remaining plasma sample were frozen at –80 ºC until analyzed. Analysis occurred within 1 week of sampling.

Study 2 consisted of a single pig prepped as described above. Blood draws were performed at 22 and 28 hours post SMZ CRI to confirm steady state. At 45 hours post SMZ CRI, a 2.0 mg/kg bolus dose of FLU was given in the extra port of the SMZ CRI catheter and blood samples were drawn and processed as described in Study 1.

Study 3 consisted of 2 pigs prepped as described above. Blood draws were performed at 22 and 28 hours post SMZ CRI to confirm steady state. At 45 hours post SMZ CRI, a FLU CRI of 0.5 mg/kg/hr was started in the second lumen of the SMZ CRI catheter. Blood draws at 10, 20, 30, and 45 minutes, and 1, 2, 4, 8, 12, 24,36 and 48 hours were taken after the start of the FLU CRI. Samples analyzed at 8, 12, and 24 hours confirmed that steady state for FLU was not achieved. FLU CRI's were stopped at 36 hours and lines were flushed of all residual FLU. At 48 hours after start of the original FLU CRI, pigs were given a single 2.0 mg/kg bolus dose of FLU through the previous FLU CRI port. Blood draws occurred at 5, 10, 15, 30, and 45 minutes, and 1, 2, 4, 8, 12, 24, 36, 48, 60, and 72 hours post FLU bolus dose. All samples were processed as described in Study 1.

SMZ PBPK Model Development

A flow-limited PBPK model was developed for predicting SMZ concentrations in swine. The model consisted of tissue compartments including quickly perfused tissues, slowly perfused tissues, liver, and blood. Additional compartments for the N-acetyl metabolite were included and consisted of the liver, blood, and remaining body. In total, the final model had 7 compartments (**Figure 6.1**).

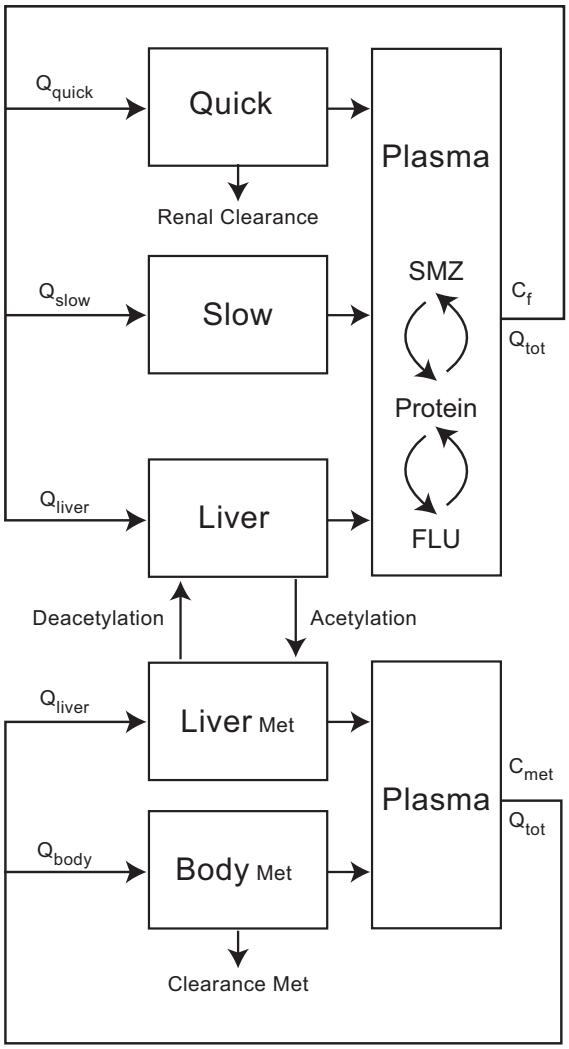

Figure 6.1 Schematic diagram of the PBPK model for Sulfamethazine in swine

Cf, free drug concentration; Cmet, concentration of metabolite; Q, tissue blood flow; Qtot, cardiac output; SMZ, sulfamethazine; FLU, flunixin meglumine; Straight arrows, blood flow; Curved arrows, protein binding equilibrium.

Physiological parameters of organ volumes and blood flow rates were taken from the literature where available (Buur et al., 2005; Lundeen et al., 1983; Pond, 2001; Tranquilli et al., 1982). Slowly perfused tissue included muscle, gastrointestinal tract, bone, and fat. Quickly perfused tissue included kidney and other tissues. Where appropriate, parameters were calculated as the difference between unity and the remaining tissues. The density of plasma was assumed to be 1 g/mL. Hepatic blood flow was modeled as the combination of hepatic arterial and portal circulations. Renal clearance is mainly due to filtration and was modeled as a first order rate constant from the quickly perfused tissue block.

Table 6.1 Final values for parameters used within the Sulfamethazine PBPK model and Sulfamethazine-Flunixin protein binding interaction model

Parameter	Units	Value	Reference
Cardiac Output	L/(h*Kg)	12	Tranquilli, Lundeen
Hematocrit	%	33	Tranquill
Blood flow	% cardiac output		
Quickly Perfused		0.51	Tranquilli, Lundeen
Slowly Perfused		0.25	Tranquilli, Lundeen
Liver		0.24	Tranquilli, Lundeen
Body (metabolite)		0.76	1-liver
Blood		1	
Organ Volume	% body weight		
Quickly Perfused		0.86	Pond
Slowly Perfused		0.07	Pond
Liver		0.02	Pond
Body (metabolite)		0.92	1-liver-plasma
Blood		0.06	Pond
Tissue:Blood Partition Coefficient			
Quickly Perfused		3.02	estimated
Slowly Perfused		1.74	estimated
Liver (parent)		0.05	estimated
Liver (metabolite)		0.079	Buur 2005
Body (metabolite)		1.297	Buur 2005
Clearance			
Hepatic	mL/(min•Kg)	0.62	Buur 2005
Renal (parent)	mL/(min•Kg)	0.34	estimated
Body (metabolite)	mL/(min•Kg)	2.56	Buur 2005
Deacetylation Rate	/h	3.66	Buur 2005
Binding Parameters			
SMZ Kd	ug/mL	65.62	*in vitro* study
SMZ Bmax	ug/mL	223.4	*in vitro* study
FLU Kd	ug/mL	152.6	*in vitro* study
FLU Bmax	ug/mL	1842.3	*in vitro* study
Protein Binding (metabolite)	%	0.57	Buur 2005

Table 6.2 Differential equations used to describe the rate of change of Sulfamethazine in each tissue compartment

Tissue Compartment	Equation
Quickly Perfused	$V_{quick} \bullet \frac{dC_{quick}}{dt} = \left(C_a - \frac{C_{quick}}{P_{quick}} \right) \bullet Q_{quick} - C_a \bullet Cl_{renal}$
Slowly Perfused	$V_{slow} \bullet \frac{dC_{slow}}{dt} = \left(C_a - \frac{C_{slow}}{P_{slow}} \right) \bullet Q_{slow}$
Liver	$V_{liver} \bullet \frac{dC_{liver}}{dt} = \left(C_a - \frac{C_{liver}}{P_{liver}} \right) \bullet Q_{liver} - C_{liver} \bullet Cl_{hepatic} + C_{livermet} \bullet Cl_{deacetylation}$
Liver (metabolite)	$V_{liver} \bullet \frac{dC_{livermet}}{dt} = \left(C_a - \frac{C_{livermet}}{P_{livermet}} \right) \bullet Q_{liver} - C_{livermet} \bullet Cl_{deacetylation} + C_{liver} \bullet Cl_{hepatic}$
Body (metabolite)	$V_{body} \bullet \frac{dC_{body}}{dt} = \left(C_a - \frac{C_{body}}{P_{body}} \right) \bullet Q_{body} - C_{body} \bullet Cl_{body}$
Plasma	$V_{blood} \bullet \frac{dC_T}{dt} = \left(\frac{C_{slow}}{P_{slow}} \bullet Q_{slow} \right) + \left(\frac{C_{fast}}{P_{fast}} \bullet Q_{fast} \right) + \left(\frac{C_{liver}}{P_{liver}} \bullet Q_{liver} \right) + IVDose - C_F \bullet Q_{tot}$
Plasma (metabolite)	$V_{blood} \bullet \frac{dC_{met}}{dt} = \left(\frac{C_{livermet}}{P_{livermet}} \bullet Q_{livermet} \right) + \left(\frac{C_{body}}{P_{body}} \bullet Q_{body} \right) - C_{met} \bullet Q_{tot}$

Subsripts: quick, slow, liver, T, F, a, livermet, body, and met are quickly perfused tissue, slowly perfused tissue, liver, plasma total drug, plasma free drug, plasma arterial concentration, liver metabolite, body metabolite, and plasma metabolite blocks respectively. C: concentration of sulfamethazine or metabolite. Q: blood flow to respective tissues with Q_{tot} being cardiac output. V: volume of respective tissues. P: tissue:blood partition coefficients for respective tissues; Cl_{renal}, $Cl_{hepatic}$, and $Cl_{deacetylation}$: Clearance for renal, hepatic, and deacetylation, respectively. IVDose: Total amount of injected sulfamethazine

Enterohepatic recycling of SMZ was considered insubstantial and not included in the model. The unique acetylation-deacetylation pathway of SMZ in swine was incorporated into the model as described previously (Buur et al., 2005). Final values can be found in **Table 6.1**.

Differential equations were used to describe the rate of change in mass in each compartment (**Table 6.2**). Model simulations were solved using ACSLxtreme, Version 2.3.0.12 (Aegis Technologies Group Inc, Huntsville, Alabama).

Protein binding was assumed to be linear in nature and free and bound drug concentrations were determined by the use of the following equations:

$$C_T = \frac{A}{V_{plasma}} \quad [1]$$

$$C_F = \frac{Kd \bullet C_T}{B_{\max} + Kd} \quad [2]$$

$$C_B = C_T - C_F \quad [3]$$

C_T, C_F, and C_B are the total, free, and bound concentration of drug in the plasma compartment respectively; A is the amount of drug; V_{plasma} is the volume of the plasma compartment; Kd is the dissociation constant for the drug; and B_{max} is the maximum binding occupancy for the drug. Mass transferred to tissue blocks was limited to free drug concentration.

Values for parameters not available in the literature were estimated using the parameter estimation module included in the simulation software. Values for Kd and B_{max} were taken from *in vitro* data. Model parameters were adjusted to fit the curve by use of a maximum-likelihood estimation algorithm. Limits were set to insure biologically plausible values. The optimization data set was created using data collected from 4 published studies (Nouws et al., 1989; Nouws et al., 1986; Sweeney et al., 1993; Yuan et al., 1997) and consisted of mean plasma concentrations calculated from 12, 6, 7, and 3 samples/data point for each of the 4 studies. Estimation and optimization was performed for the tissue:blood partition coefficients (quickly perfused, slowly perfused, liver) and renal clearance.

Validation of the SMZ model was performed by comparison of simulations to an external data set. The validation data set comprised values for total SMZ plasma concentration from 5 individual pigs reported in a previous study (Buur J. et al., 2006a). Simulated predicted values were plotted against observed values and a regression line was plotted against correlated values. Residual values were also evaluated for spread and distribution.

SMZ-FLU Protein Binding Interaction Model

Flunixin was incorporated into the SMZ model described above as a submodel within the blood compartment. Total FLU concentrations were set as constant and determined by direct analysis of blood samples. Bound and free FLU drug concentrations were modeled using **Equations 2 and 3**. Interactions between SMZ and FLU were modeled assuming competitive inhibition using the following interaction equation.

$$Kd = Kd_A \bullet \left(1 + \frac{C_{FB}}{Kd_B}\right) \qquad [4]$$

Subscripts A and B refer to SMZ and FLU respectively. The calculated Kd was then incorporated into the SMZ binding calculations within the SMZ model.

Validation of the interaction model was performed by comparing the observed data for SMZ concentration (free and total) from the *in vivo* study described above with simulated predicted values. To simulate the binding interaction, total FLU drug concentrations (directly measured from the *in vivo* study) were directly incorporated into the interaction model. The corresponding total and free SMZ concentrations were then recorded. This was repeated for each sample. The simulations were evaluated by visual comparison of predicted and observed SMZ values and by computation of residual values.

Results

In Vitro Protein Binding Characteristics for SMZ and FLU

Final binding curves for SMZ in frozen and fresh plasma, and FLU in fresh plasma are presented in **Figures 6.2 and 6.3** respectively. All curves fit a one site hyperbola. Plasma was diluted in order to eliminate the effects of ligand depletion. Final results for Kd and Bmax are shown in **Table 6.3**. There was a significant difference (p-value < 0.05) between the binding properties of SMZ in fresh vs frozen plasma. This is most likely due to conformational changes in plasma albumin during the freeze/thaw process. All later

studies were done with fresh plasma to more accurately depict *in vivo* characteristics.

In Vivo Model Validation of SMZ Model

When compared to the external data set, the SMZ PBPK model with SMZ alone had a plasma concentration correlation (R^2) of 0.85. Results of the simulation plotted against observed concentration as well as residual analysis and validation regression are presented in **Figure 6.4**. Residual analysis revealed a generalized under prediction.

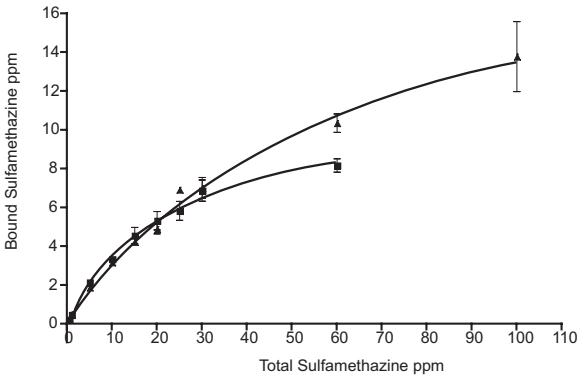

Figure 6.2 Protein binding saturation curve for Sulfamethazine in frozen (squares) and fresh (triangles) porcine plasma

Data points represent the averages from 7 experiments (frozen plasma) or 5 experiments (fresh plasma) with each experiment having 3 replicates and plasma pooled from a minimum of 3 pigs

Model Validation of SMZ-FLU Protein Binding Interaction Model

Comparisons between observed and predicted values for individual pigs are presented in **Figure 6.5** for total SMZ drug concentration. **Figure 6.6** shows a representative pig during the time of drug interaction. **Figure 6.7** presents comparisons between observed and predicted values for free SMZ drug concentration of individual pigs. Residual analysis for total and free drug SMZ

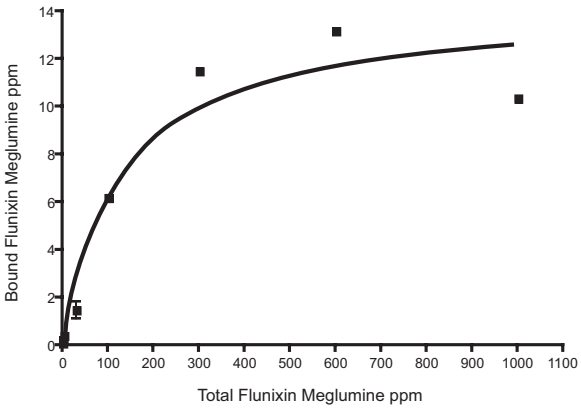

Figure 6.3 Representative protein binding saturation curve for Flunixin in fresh porcine plasma

Data points are comprised of means and standard deviations from 5 replicates and plasma was pooled from 3 pigs. Error between replicates was less than 5% and so error bars do not show on this scale

concentrations are presented in **Figures 6.8 and 6.9** respectively. Given the steady state nature of both the free and total SMZ concentrations, there was an inadequate spread of SMZ concentrations to calculate a correlation coefficient.

Table 6.3 Final protein binding kinetic parameters for Sulfamethazine in fresh and frozen porcine plasma and Flunixin in fresh porcine plasma

Drug	Kd (µMol)	Bmax (µMol)
Sulfamethazine (fresh)	235.8 ± 39*	802.6 ± 75*
Sulfamethazine (frozen)	80.9 ± 13*	409.9 ± 32*
Flunixin Meglumine	310.5 ± 118	3748.5 ± 514

* Statistically significant difference (p value < 0.05) between fresh and frozen plasma

Discussion

Due to the increase in combination drug therapy, drug-drug interactions are becoming more common within both human and veterinary medicine. We have successfully created and validated a model that accurately predicts the interactions of SMZ and FLU due to competitive protein binding interactions. Our model predicted a temporary increase in the free drug concentration due to displacement from plasma proteins. The increase in free drug concentration would allow more drug to be cleared and thus contribute to a concurrent

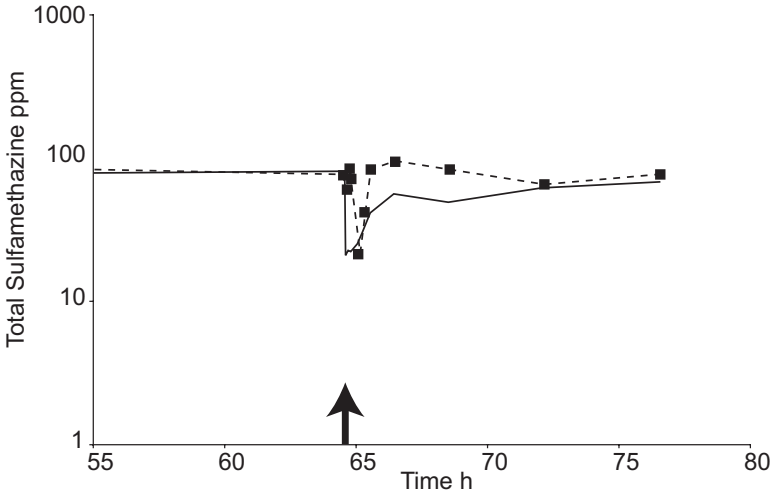

Figure 6.6 Comparison between observed (squares with dashed line) and predicted (solid line) values of total drug concentration for a representative pig at the time of interaction.

Arrow, time of FLU bolus dose.

decrease in total drug concentration. Since there was continual input of drug from the CRI, the decrease in total drug concentration would be transient in nature. These model predictions parallel the theoretical models presented by Toutain and Bousquet-Melou and by Benet and Hoener (Benet et al., 2002; Toutain et al., 2002). More importantly, these predictions were validated by comparison to the *in vivo* studies.

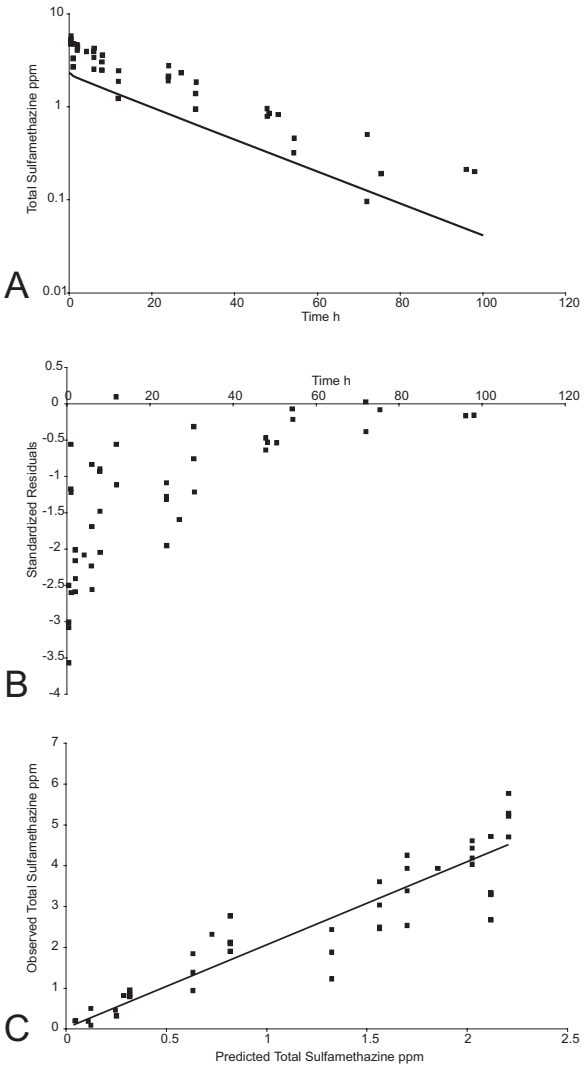

Figure 6.4 Results of validation of sulfamethazine PBPK model in swine for total drug

A) Model simulation (line) compared to external data set (squares). B) Residual plot. C) Comparison of predicted and observed data points. The solid line represents the line of best fit

The free drug concentration at steady state was accurately predicted by the model. The model slightly over predicted concentrations of free drug in 2 of the pigs. There was a wide variability of free drug concentration within each pig even at steady state. This most likely reflects interindividual variability in clearance mechanisms. Since binding properties are correlated to sample temperature (Munsey et al., 1996), variability could be due to alterations in temperature of the plasma after collection. In order to minimize the effects of temperature change, all samples were kept as close to 37 ºC as possible. Given the interindividual variability within time points, a larger number of pigs sampled could increase the overall accuracy of the model.

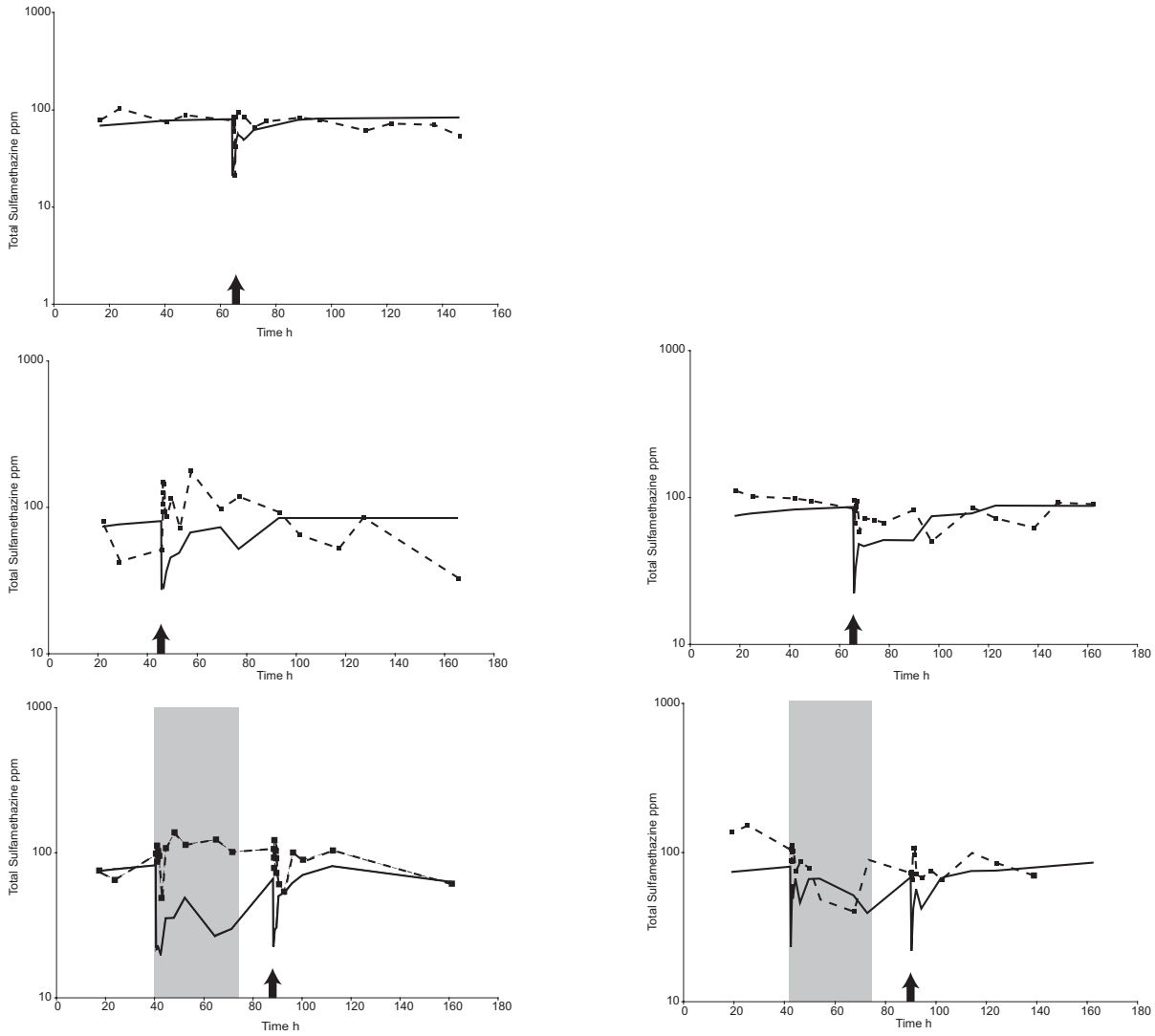

Figure 6.5 Comparison between observed (squares with dashed line) and predicted (solid line) values of total drug concentration for individual pigs using the Sulfamethazine-Flunixin protein binding interaction model

Shaded areas, time of FLU CRI; arrow, time of FLU bolus dose

Total drug concentration was accurately predicted for all but a single pig. Residual analysis for total drug concentrations showed slight under prediction at early time points and mild over prediction at later time points. In the single pig, the trend caused by the interaction between SMZ and FLU was accurately predicted even though the magnitude of the interaction was over predicted. Most likely this is due to variations in the Kd and Bmax for

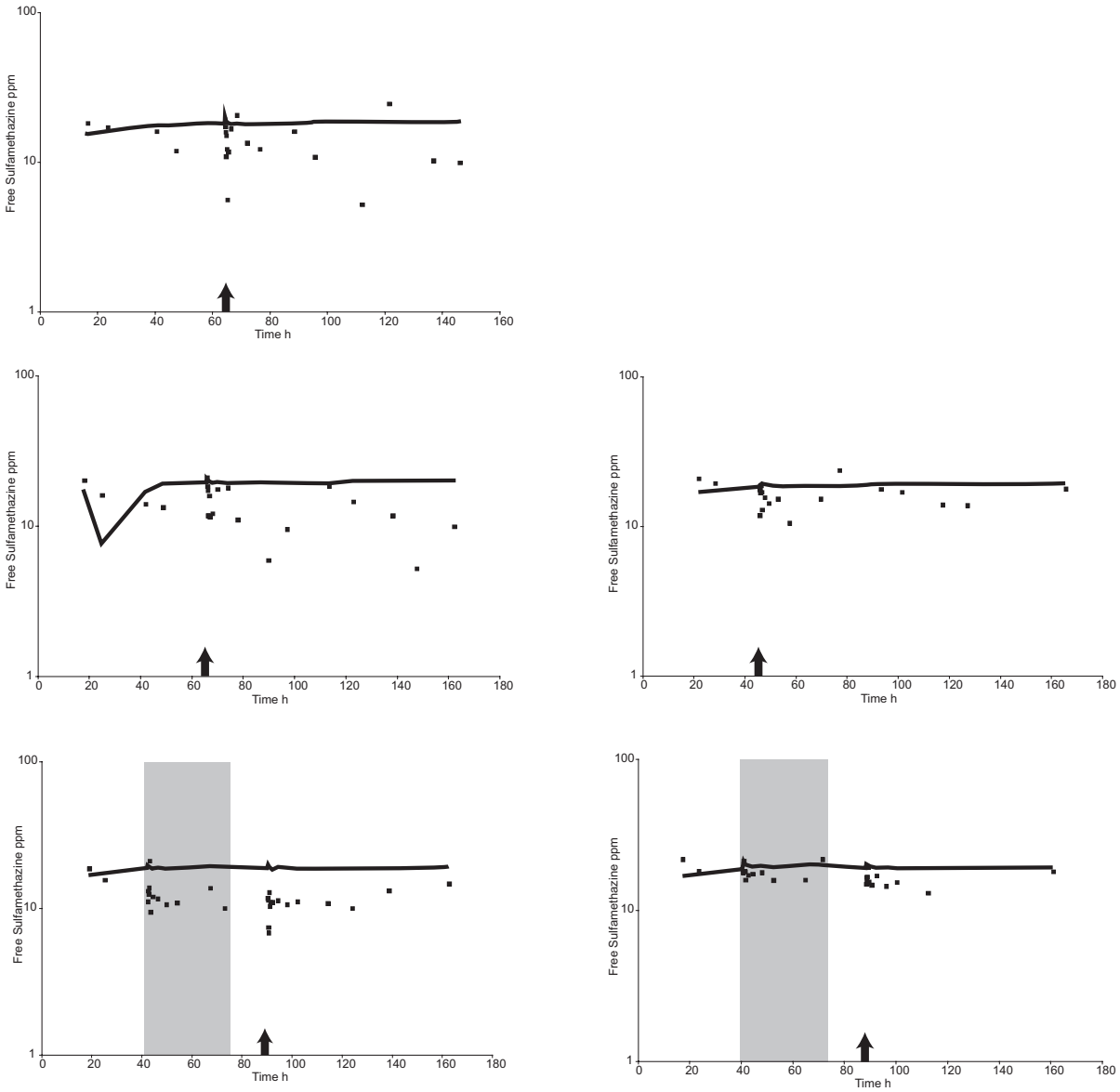

Figure 6.7 Comparison between observed (squares) and predicted (solid line) values of free drug concentration for individual pigs using the Sulfamethazine-Flunixin protein binding interaction model

Shaded areas, time of FLU CRI; arrow, time of FLU bolus dose

FLU in this pig. Values for both Kd and Bmax used in the model were derived from in the *in vitro* studies that used curve fitting of the average concentrations. The average concentrations were derived from multiple replicates and from plasma pooled from multiple pigs. Thus alterations due to interindividual variability were reduced. Individual optimization of Kd and

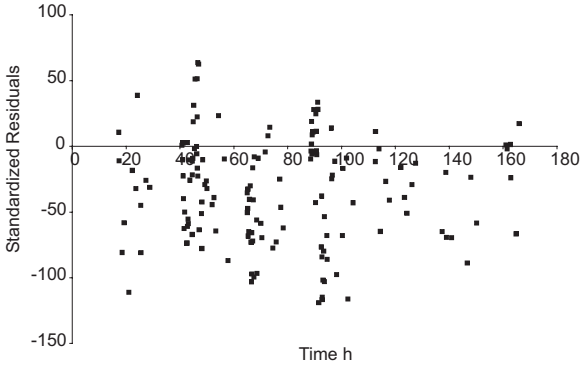

Figure 6.8 Residual plot for fit of the results of the Sulfamethazine-Flunixin protein binding model for total Sulfamethazine concentration

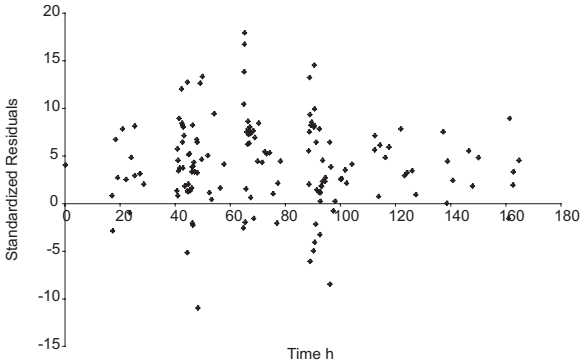

Figure 6.9 Residual plot for fit of the results of the Sulfamethazine-Flunixin protein binding model for free Sulfamethazine concentration

Bmax for individual pigs should result in greater accuracy. It is of importance to note that free drug concentrations for this pig were predicted with high accuracy.

Protein binding interactions are considered to be important for total drug concentration of drugs with low extraction ratios (ER<0.3) (Wilkinson, 2001). SMZ has an extraction ratio of 0.58 in rabbits (Reeves et al., 1988). As a moderate ER drug, you would expect a mild, but not clinically significant alteration in total drug kinetics due to changes in protein binding. Our model showed that the free drug concentration of SMZ does not alter significantly in the presence of FLU. Thus the combination drug therapy would not have clinical significance. A single study in horses showed that there was a decrease in the mean residence time (MRT) and an increase in the elimination rate (Kel) for total SMZ when administered in the presence of FLU. Authors concluded that these changes were due to displacement from plasma proteins (el-Banna, 1999). This would reflect the increase in free SMZ concentration due to displacement from plasma proteins. The increased free SMZ allows a greater fraction of total drug to be cleared at any one time, thus resulting in a decrease in total drug concentration and concurrent decrease in MRT. These conclusions are consistent with our model and with the current thinking on the clinical effects of protein binding interactions (Toutain et al., 2002).

Our model predicted a temporary decrease in total drug concentration that could alter the calculation of MRT. The horse study used single bolus doses as the dosing regimen. Since our *in vivo* studies used CRI's the binding effect of FLU was transient in nature. The PBPK model did not predict, nor was there any change in free drug concentrations in the *in vivo* experiments. Since clinical activity is based on free drug concentration, there is no evidence that this interaction would contribute to a clinical significant change in either safety or efficacy of SMZ.

The model predicted a temporary increase of free drug concentration at the time of FLU injection. This was not seen in the *in vivo* experiment. This temporary increase could have been masked by the wide variability of concentrations. Alternatively, the transient nature of the increase may have occurred prior to the first sampling time. However, the transient decrease in total drug concentration was predicted for each individual pig.

The accuracy of the model could be increased by optimizing Kd and Bmax for each individual pig. The model assumes mean values for these parameters. Flunixin binding saturation studies showed variability between experiments. This is most likely due to variability within the *in vitro* system as well as interindividual variability. The numbers of replicates and number of pigs used to pool plasma were increased in order to reduce the variability. However due to solubility issues, concentrations of FLU greater than 1000 ppm could not be achieved. Terminal portions of the protein binding saturation curve tended to have larger variation which could be explained by the precipitation of FLU within the *in vitro* system. While this affected both Kd and Bmax, the differences between the individual experiments were not statistically significant (data not shown). Also, each experiment had very good fits at early time points that correspond to concentrations found *in vivo*. It is possible that alterations in these binding parameters for each individual pig could decrease the accuracy of the model.

Individual optimization of renal and hepatic clearance would contribute to more accurate predictions. However, even without individual optimization, the model accurately predicted the trends for both free and total drug concentrations due to competitive binding interactions.

The model assumed that protein binding interaction was due to competitive inhibition. It is possible that other forms of interaction, such as allosteric/cooperative binding or noncompetitive inhibition, could contribute to the interactions seen *in vivo*. These types of interactions would contribute to different interaction curves.

We have developed and validated a PBPK model that accurately predicts changes in both total and free drug concentration due to protein binding interactions for the model drugs of SMZ and FLU. From this model, we can conclude that the interaction is not clinically significant since there was only a temporary alteration in the free drug concentration. This novel use of PBPK models represents the first time a PBPK model has been used to elucidate the underling mechanisms of plasma protein binding interactions. Beyond the use of exploring mechanisms, this type of modeling approach is also useful in elucidating the clinical implications of the drug interactions. Further research needs to be conducted on drugs that have altered binding properties and lower extraction ratios.

Acknowledgments

Funding for this project was supported in part by the Food Animal Residue Avoidance Databank (FARAD) and USDA-Cooperative State Research, Education and Extension Service grant No. 2002-45051-01362.

References

Anonymous (2006). *Compendium of Veterinary Products,* 9th Edition Eds S. Inglis. Adrian J. Bayley, Port Huron, Michigan.

Benet, L. Z. & Hoener, B. A. (2002) Changes in plasma protein binding have little clinical relevance. *Clin Pharmacol Ther*, **71**, 115-121.

Buur, J. L., Baynes, R. E., Craigmill, A. L. & Riviere, J. E. (2005) Development of a physiologic-based pharmacokinetic model for estimating sulfamethazine concentrations in swine and application to prediction of violative residues in edible tissues. *American Journal of Veterinary Research*, **66**, 1686-1693.

Buur, J., Baynes, R., Smith, G. & Riviere, J. (2006a) Use of probabilistic modeling within a physiologically based pharmacokinetic model to predict sulfamethazine residue withdrawal times in edible tissues in swine. *Antimicrob Agents Chemother*, **50**, 2344-2351.

Buur, J. L., Baynes, R. E., Smith, G. & Riviere, J. E. (2006b) Pharmacokinetics of flunixin meglumine in swine after intravenous dosing. *J Vet Pharmacol Ther*, **29**, 437-440.

Craigmill, A. L. (2003) A physiologically based pharmacokinetic model for oxytetracycline residues in sheep. *J Vet Pharmacol Ther*, **26**, 55-63.

el-Banna, H. A. (1999) Pharmacokinetic interactions between flunixin and sulphadimidine in horses. *Dtsch Tierarztl Wochenschr*, **106**, 400-403.

Gentry, P. R., Covington, T. R., Clewell, H. J., 3rd & Anderson, M. E. (2003) Application of a physiologically based pharmacokinetic model for reference dose and reference concentration estimation for acetone. *Journal of toxicology and environmental health. Part A*, **66**, 2209-2225.

Grass, G. M. & Sinko, P. J. (2002) Physiologically-based pharmacokinetic simulation modelling. *Advanced drug delivery reviews*, **54**, 433-451.

Kanamitsu, S., Ito, K., Green, C. E., Tyson, C. A., Shimada, N. & Sugiyama, Y. (2000) Prediction of in vivo interaction between triazolam and erythromycin based on in vitro studies using human liver microsomes and recombinant human CYP3A4. *Pharm Res*, **17**, 419-426.

Kawai, R., Lemaire, M., Steimer, J. L., Bruelisauer, A., Niederberger, W. & Rowland, M. (1994) Physiologically based pharmacokinetic study on a cyclosporin derivative, SDZ IMM 125. *J Pharmacokinet Biopharm*, **22**, 327-365.

Liu, X., Smith, B. J., Chen, C., Callegari, E., Becker, S. L., Chen, X., Cianfrogna, J., Doran, A. C., Doran, S. D., Gibbs, J. P., Hosea, N., Liu, J., Nelson, F. R., Szewc, M. A. & Van Deusen, J. (2005) Use of a physiologically based pharmacokinetic model to study the time to reach brain equilibrium: an experimental analysis of the role of blood-brain barrier permeability, plasma protein binding, and brain tissue binding. *J Pharmacol Exp Ther*, **313**, 1254-1262.

Lundeen, G., Manohar, M. & Parks, C. (1983) Systemic distribution of blood flow in swine while awake and during 1.0 and 1.5 MAC isoflurane anesthesia with or without 50% nitrous oxide. *Anesth Analg*, **62**, 499-512.

Munsey, T., Grigg, R. E., McCormack, A., Symonds, H. W. & Bowmer, C. J. (1996) Binding of sulphamethazine to pig plasma proteins and albumin. *J Vet Pharmacol Ther*, **19**, 135-141.

Nouws, J. F., Mevius, D., Vree, T. B. & Degen, M. (1989) Pharmacokinetics and renal clearance of sulphadimidine, sulphamerazine and sulphadiazine and their N4-acetyl and hydroxy metabolites in pigs. *Vet Q*, **11**, 78-86.

Nouws, J. F., Vree, T. B., Baakman, M., Driessens, F., Vellenga, L. & Mevius, D. J. (1986) Pharmacokinetics, renal clearance, tissue distribution, and residue aspects of sulphadimidine and its N4-acetyl metabolite in pigs. *Vet Q*, **8**, 123-135.

Pond, W. G. (2001). *Biology of the Domestic Pig.* Cornell University Press, Ithaca.

Reeves, P. T., Minchin, R. F. & Ilett, K. F. (1988) Induction of sulfamethazine acetylation by hydrocortisone in the rabbit. *Drug Metab Dispos*, **16**, 110-115.

Reitz, R. H., Mendrala, A. L., Park, C. N., Andersen, M. E. & Guengerich, F. P. (1988) Incorporation of in vitro enzyme data into the physiologically-based pharmacokinetic (PB-PK) model for methylene chloride: implications for risk assessment. *Toxicol Lett*, **43**, 97-116.

Saltvedt, I., Spigset, O., Ruths, S., Fayers, P., Kaasa, S. & Sletvold, O. (2005) Patterns of drug prescription in a geriatric evaluation and management unit as compared with the general medical wards: a randomized study. *Eur J Clin Pharmacol*, **61**, 921-928.

Simmons, J. E. (1996) Application of physiologically based pharmacokinetic modelling to combination toxicology. *Food Chem Toxicol*, **34**, 1067-1073.

Sweeney, R. W., Bardalaye, P. C., Smith, C. M., Soma, L. R. & Uboh, C. E. (1993) Pharmacokinetic model for predicting sulfamethazine disposition in pigs. *Am J Vet Res*, **54**, 750-754.

Teeguarden, J. G., Waechter, J. M., Jr., Clewell, H. J., 3rd, Covington, T. R. & Barton, H. A. (2005) Evaluation of oral and intravenous route pharmacokinetics, plasma protein binding, and uterine tissue dose metrics of bisphenol A: a physiologically based pharmacokinetic approach. *Toxicol Sci*, **85**, 823-838.

Toutain, P. L. & Bousquet-Melou, A. (2002) Free drug fraction vs free drug concentration: a matter of frequent confusion. *J Vet Pharmacol Ther*, **25**, 460-463.

Tranquilli, W. J., Parks, C. M., Thurmon, J. C., Benson, G. J., Koritz, G. D., Manohar, M. & Theodorakis, M. C. (1982) Organ blood flow and distribution of cardiac output in nonanesthetized swine. *Am J Vet Res*, **43**, 895-897.

Tsukamoto, Y., Kato, Y., Ura, M., Horii, I., Ishikawa, T., Ishitsuka, H. & Sugiyama, Y. (2001) Investigation of 5-FU disposition after oral administration of capecitabine, a triple-prodrug of 5-FU, using a physiologically based pharmacokinetic model in a human cancer xenograft model: comparison of the simulated 5-FU exposures in the tumour tissue between human and xenograft model. *Biopharm Drug Dispos*, **22**, 1-14.

Wilkinson, G. R. (2001). The Dynamics of Drug Absorption, Distribution, and Elimination. In *Goodman & Gilman's The Pharmacological Basis of Therapeutics*, 10th Edition. Eds. H. a. Limbird. McGraw-Hill, New York, 3-27.

Yuan, Z. H., Miao, X. Q. & Yin, Y. H. (1997) Pharmacokinetics of ampicillin and sulfadimidine in pigs infected experimentally with Streptococcus suum. *J Vet Pharmacol Ther*, **20**, 318-322.

7. CONCLUSIONS AND FUTURE DIRECTIONS

Conclusions

Physiologically based pharmacokinetic (PBPK) models are based on the principles of mass balance. They link together multiple tissue blocks using blood flow. The mechanistic nature of this approach makes PBPK models predictive and flexible in terms of dose, route of administration, and species. Parameter values can be described by single point estimates or by statistical distributions which then allows for exploration of the effects of population diversity on drug disposition. The inclusion of *in vitro* characteristics such as protein binding or enzyme kinetics provides the opportunity to explore more fundamental and theoretical aspects of pharmacokinetics.

The use of PBPK models is well established within toxicology where they have successfully been applied to areas of human health risk assessment. In human medicine, the PBPK approach has been used in situations of altered patient physiology or to elucidate the underlying mechanisms behind drug-drug interactions. However, PBPK models have not been applied to veterinary medicine. The studies included in this dissertation demonstrate the utility of PBPK models within veterinary medicine.

In swine, sulfamethazine (SMZ) has been consistently associated been violative tissue residues which is a threat to public health and safety (FSIS, 2001; FSIS, 2004). The validated PBPK model presented in Chapter 3 was used to explore the tissue disposition of SMZ in swine after intravenous administration. This model was able to accurately predict tissue concentrations of SMZ over time. By correlating these tissue disposition curves to the set tolerance level, appropriate meat withdrawal intervals were established to protect the food supply as is required under the provisions of the Animal Medicinal Drug Use Clarification Act (AMDUCA) ("Animal Medicinal Drug Use Clarification Act," 1994).

The PBPK model for edible tissues was further expanded in Chapter 4 to include oral route of administration. In addition, sensitive parameters were defined by log normal distributions to more accurately reflect interindividual variability within the population. The model was subsequently used to explore the effects of population diversity on meat withdrawal times. Ultimately, this model was compared to the Tolerance Limit Method currently used by the United States Food and Drug Administration (US-FDA) for the calculation of meat withdrawal times. By incorporating Monte Carlo sampling techniques, the PBPK model was able to predict the meat withdrawal time for the upper limit of the 95% confidence interval for the 99th percentile of the swine population, thus proving its utility in regulatory applications unique to veterinary medicine.

Sulfamethazine has also been associated with adverse drug reactions due to drug-drug interactions. In veterinary medicine, altered disposition of SMZ has been reported in horses when given concurrently with flunixin meglumine (FLU). The underlying mechanism was hypothesized to be due to protein binding interactions (el-Banna, 1999). With the recent approval of FLU in swine, there is an increased chance of seeing the same type of adverse drug reaction. Basic pharmacokinetic data was derived for swine (Chapter 5). This data confirmed the high protein binding profiles for swine that is also seen in other species. To explore the question of a possible interactions between SMZ and FLU in swine, we used a PBPK approach. This allowed us to study the underlying mechanism behind this drug interaction and to evaluate its clinical significance. The resulting PBPK model, presented in Chapter 6, was validated against a number of conditions including SMZ given by itself as a bolus injection, SMZ given by itself as a constant rate infusion (CRI), SMZ given as a CRI with a FLU bolus, and SMZ given as a CRI with a FLU CRI. The model predicted both total and free drug concentrations for SMZ under all of the above situations. The interaction was characterized by a decrease in total SMZ concentration with very little change in free SMZ concentration. The drug interaction mechanism was confirmed to be due to competitive

plasma protein binding inhibition. Since free drug concentration of SMZ did not change in the presence of FLU, there would be no significant clinical consequences from this drug interaction.

The successful application of the PBPK modeling approach to food safety and the study of both mechanisms and clinical consequences of drug interactions due to plasma protein binding provides evidence of the utility and need for PBPK modeling in veterinary medicine. Indeed, PBPK modeling, due to its ability to incorporate *in vitro* data into *in vivo* simulations has applications in multiple aspects of translational medicine. The models presented within this dissertation provide the basis for more accurate estimation of meat withdrawal intervals after extralabel use of SMZ in swine as well as an alternative method for the calculation of meat withdrawal times for use with approved products. In addition, the PBPK model approach can now be used to predict the clinical consequences from possible drug interactions due to plasma protein binding. Ultimately, these applications provide for safer and more efficacious drug dosing regimens for veterinary patients while increasing the safety of our food supply.

Future Directions

The work presented in this dissertation provides the basis for further applications of PBPK models within veterinary medicine. The drug interaction model can be expanded to include the accurate prediction of FLU in pigs. This would not only simplify the use of the model, but also expand its usefulness. Preliminary work using the pharmacokinetic data presented in Chapter 5 has shown that the disposition of FLU is difficult to model due to its high lipophilicity and non-specific binding to both plasma and tissue proteins. These observations would make it even more critical to model using PBPK approaches since estimation of meat withdrawal intervals using methods such as plasma half life multipliers may not be accurate. The potential for extralabel use has also increased with the recent approval of this drug for use in swine.

In addition, the exploration of drug interactions due to plasma protein binding can be expanded to include alternative model drugs. By looking at drugs with high affinity binding, or that have more extreme extraction ratios, the consequences of alterations in plasma protein binding can be further elucidated. High affinity drugs such as warfarin or phenylbutazone, high extraction ratio drugs such as propranolol, or low extraction drugs such as diazepam would all be candidates. The systematic modeling of more extreme cases would further clarify when drug interactions of this nature would be clinically significant.

Finally, the use of PBPK models in veterinary medicine can be directly applied to the design of rational drug dosing regimens for drugs with low therapeutic indices. Specifically, the PBPK approach could be used to simultaneously model sites of action and toxicity to help optimize dosing regimens. This would be most useful in the area of cancer chemotherapeutics. There is significant evidence that standard methods of dosing (ie. by body weight or by surface area) do not reliably achieve maximum efficacy while decreasing toxicity. Additionally, many of these patients have altered states of physiology due to concurrent disease. The mechanistic aspect and flexibility of PBPK models would make it uniquely qualified to explore this area of need.

References

Animal Medicinal Drug Use Clarification Act (1994). United States Food and Drug Administration. Title 21 Code of Federal Regulations, part 530.

el-Banna, H. A. (1999) Pharmacokinetic interactions between flunixin and sulphadimidine in horses. *Dtsch Tierarztl Wochenschr*, **106**, 400-403.

FSIS (2001). *2000 FSIS National Residue Program Data.* Eds Food Safety Inspection Service. United States Department of Agriculture, Washington, DC.

FSIS (2004). *2003 FSIS National Residue Program Data.* Eds Food Safety Inspection Service. United States Department of Agriculture, Washington, DC.

APPENDICES

PBPK Sulfamethazine Meat Withdrawal Time Model Code

```
!-----------------------------------------------------------------------
!
! Global Terms Block
!
!-------------------------------------------------

global body weight          ! kg
global qtot                       !total cardiac output L/h
global ivdose                     !mg/kg total
global pcv                        !PCV %
global vmuscle              !volume of muscle (L) assumes density of 1g/L
global vfat                       !volume of fat - L
global vliver                     !volume of liver - L
global vkidney              !volume of kidney - L
global vblood                     !volume of blood - L
global vot                        !volume of other tissues - L
global qmuscle              !blood flow through muscle L/h
global qfat                       !blood flow through fat L/h
global qliver                     !blood flow through liver L/h
global qkidney              !blood flow through kidney L/h
global qot                        !blood flow through other tissues L/h
global Pmuscle              !tissue-plasma partition coefficient for muscle
global Pfat                       !tissue-plasma partition coefficient in fat
global Pliver                     !tissue-plasma partition coefficient in liver
global Pkidney              !tissue-plasma partition coefficient in kidney
global Pot                        !tissue-plasma partition coefficient in other tissues
global pbinding             !percent of protein binding SMZ
global POdose               !oral dose mg/kg
global podays                     !days of administration
global vbcmuscle                  !volume blood within muscle L
global vbcfat                     !volume blood within fat L
global vbcliver             !volume blood within liver L
global vbckidney            !volume blood within kidney L
global vbcot                      !volume blood within other tissues L
global Plivermet            !tissue-plasma partition coefficient for metabolite in liver
global Pbindingmet                !percent of protein binding metabolite
global Pbody                      !tissue-plasma partition coefficient for metabolite in body
global ivdosemet            !dose for metabolite mg/kg
global pomaintdose                !oral maintenance does mg/kg

initial
constant body weight = 100        kg
constant Qcar = 12                !blood flow L/h/kg
constant ivdose = 0               !mg/kg
constant podose = 0               !mg/kg
constant podays = 0               !days
constant qcmuscle = 0.25  !fx of blood flow to muscle %
constant qcfat = 0.08             !fx of blood flow to fat %
constant qckidney = 0.1188        !fx of blood flow to kidney %
constant qcliver = 0.38     !fx of blood flow to liver including portal flow %
```

```
constant vmusclefx = 0.4   !% of bw that is muscle
constant vfatfx = 0.34     !% of bw that is fat
constant vkidneyfx = 0.004          !% of bw that is both kidneys
constant vliverfx = 0.02   !% of bw that is liver
constant vbloodfx = 0.06   !% of bw that is blood
constant pcv = 0.35                 !% PCV
constant Pmuscle = 0.08
constant Pfat = 0.336
constant Pkidney = 1.68
constant Pliver = 0.378
constant Pot = 0.1
constant pbinding = .57
constant vbcmuscle = 0.026
constant vbcfat = 0.04
constant vbcliver = 0.115
constant vbckidney = 0.105
constant vbcot = 0.09115
constant Plivermet = 0.079
constant Pbindingmet = 0.57
constant Pbody = 1.297     !arbitrary partition coefficient for body
constant ivdosemet = 0.0
constant pomaintdose = 0

vmuscle = vmusclefx * body weight                   !L assumes density of 1 g/L
vfat = vfatfx * body weight
vkidney = vkidneyfx * body weight
vliver = vliverfx * body weight
vblood = vbloodfx * body weight
vot = body weight - (vmuscle + vfat + vkidney + vliver + vblood)
qtot = (qcar * body weight) * (1 - pcv)         !L/h
qcot = 1 - (qcmuscle + qcfat + qckidney + qcliver)
qmuscle = qcmuscle * qtot                           !L/h
qfat = qcfat * qtot
qkidney = qckidney * qtot
qliver = qcliver * qtot
qot = qcot * qtot
end

!---------------------------------------------------------------------
!
! Chronic Oral Dose Simulator
!
!---------------------------------------------------------------------

global body weight
global podose
global podays
global pomaintdose
```

```
dose = podose*bodyweight*1000                    !converts to ug
enddose = podays*24                                      !converts to h
startdose = pomaintday * 24                              !convert to h
constant kst=0.25
constant a0 = 0
constant pomaintday = .1

maintdose = pomaintdose*bodyweight*1000          !convert to ug

rate = -kst*a
a    = integ(rate, a0)
o    = - rate

discrete nextdose
 interval period = 24.0
 if (t .lt. startdose) a = a + dose
 if (t .ge. startdose) a = a + maintdose
 if (t .ge. enddose) a = 0
end

!-------------------------------------------------------------------------
!
! Absorption from GI to Portal Vein
!
!-------------------------------------------------------------------------

! mass rate absorbed by the body
constant ka=3.997                    !absorption rate constant from GI tract to blood(1/time)
ro   = ka*amnt
! amount of change at the site of absorption
rate = inp – ro

! amount at the site of absorption
constant a0 = 0.0                    !initial amount at the site of absorption
amnt = integ(rate, a0)

!-------------------------------------------------------------------------
!
!Tissue Block - Kidney
!
!-------------------------------------------------------------------------

initial
timekidneycross = 0.0
end

global body weight
global vkidney
global qkidney
global Pkidney
global vbckidney
```

```
Q1 = qkidney

! -----elimination parameters
constant Clrenal = 0.03                    !renal clearance mL/min/kg
constant a0=0.0                            !initial amount of chemical in the tissue

! -----concentration of chemical in the compartment
C = a/Vkidney                              !ug/L

! -----concentration of chemical in tissue blood
Ctb = C/pkidney                            !ug/L
Ch = (vbckidney*Ctb) + (1-vbckidney)*C     !concentration of homogenate sample

! -----elimination
Kel = Clrenal/1000 * 60 * body weight      !converts CL to L/h
rex = Kel * C                                    !based on GFR,dependent on Ca not Ctb

! -----rate of change of amount of chemical in the compartment
r = Q1*(Ca - Ctb) – rex

! -----amount of chemical in the compartment
a = intvc(r, a0)

schedule chkidneycross .xn. (ch-100)

discrete chkidneycross
timekidneycross=t
end

!-------------------------------------------------------------------------
!
!Tissue Block – Other Tissues
!
!-------------------------------------------------------------------------

global vot
global qot
global pot
global vbcot

q = qot
constant a0=0.0                    !initial amount of chemical in the tissue
constant rex = 0

! -----concentration of chemical in the compartment
C = a/vot                                  !ug/L

! -----concentration of chemical in tissue blood
Ctb = C/pot                        !mass/volume
Ch = (vbcot*Ctb) + (1-vbcot)*C     !concentration of homogenate sample
```

```
! -----rate of change of amount of chemical in the compartment
r = Q*(Ca - Ctb) – rex

! -----amount of chemical in the compartment
a = intvc(r, a0)

!-------------------------------------------------------------------------
!
! Tissue Block - Muscle
!
!-------------------------------------------------------------------------

Initial
timemusclecross=0.0
end

global vmuscle
global qmuscle
global Pmuscle
global vbcmuscle

q = qmuscle
constant a0=0.0                          !initial amount of chemical in the tissue
constant rex = 0                         !no elimination from muscle

! -----concentration of chemical in the compartment
C = a/Vmuscle                            !ug/L

! -----concentration of chemical in tissue blood
Ctb = C/pmuscle                          !ug/L
Ch = (vbcmuscle*Ctb) + (1-vbcmuscle)*C   !concentration of homogenate sample

! -----rate of change of amount of chemical in the compartment
r = Q*(Ca - Ctb) – rex

! -----amount of chemical in the compartment
a = intvc(r, a0)

SCHEDULE Chmusclecross .xn. (ch-100)

discrete Chmusclecross
timemusclecross=t
end
```

```
!-----------------------------------------------------------------------
!
! Tissue Block - Fat
!
!-----------------------------------------------------------------------

initial
timefatcross = 0.0
end

global vfat
global qfat
global pfat
global vbcfat

q = qfat
constant a0 = 0                          !initial mass in fat
constant rex = 0                         !no elimination in fat

! -----concentration of chemical in the compartment
C = a/Vfat                                       !ug/L

! -----concentration of chemical in tissue blood
Ctb = C/pfat                                     !ug/L
Ch = (vbcfat*Ctb) + (1-vbcfat)*C         !concentration of homogenate sample

! -----rate of change of amount of chemical in the compartment
r = Q*(Ca - Ctb) – rex

! -----amount of chemical in the compartment
a = intvc(r, a0)

schedule chfatcross .xn. (ch-100)
discrete chfatcross
timefatcross = t
end

!-----------------------------------------------------------------------
!
! Tissue Block - Liver
!
!-----------------------------------------------------------------------

initial
timelivercross = 0.0
end
```

```
global body weight
global qliver
global vliver
global Pliver
global vbcliver

q = qliver

! -----elimination parameters
constant a0=0.0                          !initial amount of chemical in the tissue
constant Clhepatic = .62                 !hepatic clearance in mL/min/kg

! -----concentration of chemical in the compartment
C = a/Vliver                                    !ug/L

! -----concentration of chemical in tissue blood
Ctb = C/pliver                           !ug/L
Ch = (vbcliver*Ctb) + (1-vbcliver)*C     !concentration of homogenate sample

! -----elimination
kel = clhepatic/1000 * 60 * body weight  !converts to L/h
rex = kel * Ctb

! -----rate of change of amount of chemical in the compartment
r = inp2 + rdac + Q*(Ca - Ctb) – rex

! -----amount of chemical in the compartment
a = intvc(r, a0)

schedule chlivercross .xn. (ch-100)
discrete chlivercross
timelivercross = t
end

!-------------------------------------------------------------------------
!
! Tissue Block – Liver Metabolite
!
!-------------------------------------------------------------------------

global qliver
global vliver
global Plivermet

initial
constant a0=0
Q = qliver
constant Kdac = 3.66                     !rate of deacytlation 1/time
end

C = a/Vliver
```

```
! -----concentration of chemical in tissue blood
Ctb = C/Plivermet
rdac = Kdac*Ctb*Vliver

! -----rate of change of amount of chemical in the compartment
r = Q*(Ca - Ctb) - rdac + ract

! -----amount of chemical in the compartment
a = intvc(r, a0)

!-----------------------------------------------------------------------
!
! Tissue Block – Body Metabolite
!
!-----------------------------------------------------------------------

global body weight
global qtot
global vliver
global qliver
global Pbody

initial
constant a0=0
Vbody = body weight – vliver                !tissue volume
Q = qtot – qliver                           !blood flow rate through the tissue
constant Clmet = 2.558                      !Body clearance mL/min/kg
end

! -----elimination parameters
C = a/Vbody

! -----concentration of chemical in tissue blood
Ctb = C/Pbody
kel = Clmet*bodyweight*60/1000
rex = kel*Ca

! -----rate of change of amount of chemical in the compartment
r = Q*(Ca - Ctb) - rex

! -----amount of chemical in the compartment
a = intvc(r, a0)
```

```
!----------------------------------------------------------------------
!
! Plasma Blood Block – Sulfamethazine
!
!----------------------------------------------------------------------

global qtot
global vblood
global pbinding
global ivdose
global body weight

initial
constant a0 = 0
constant TimeIV = 0.00278                                   !Time it takes to bolus dose h
timeplasmacross = 0.0
end

RIV = (Ivdose*bodyweight*1000)/TimeIV              !rate of IV injection ug/h
IVZONE = RSW(t.GE.timeiv,0.0,1.0)
IV = RIV*IVzone                                             !IV infusion rate ug/h

! -----set the maximum and minimum of blood flow rate check criteria
constant Qmin=0.99
constant Qmax=1.01

! -----check if the sum of blood flow rates=QTOT?
QCHECK = (Q1 + Q2 + Q3 + Q4 + Q5)/QTOT
termt(QCHECK.lt.Qmin,'sum of blood flow is less than QTOT')
termt(QCHECK.gt.Qmax,'sum of blood flow is larger than QTOT')

! -----concentration of plasma
Cv = a/Vblood * (1-pbinding)

! -----rate of change of amount of chemical in venous compartment
r = (Q1*Ctb1 + Q2*Ctb2 + Q3*Ctb3 + q4*Ctb4 + q5*Ctb5) + IV - QTOT*Cv
!
! -----amount of chemical in the compartment
a = intvc(r, a0)

schedule cvplasmacross .xn. (cv-100)
discrete cvplasmacross
timeplasmacross = t
end
```

```
!-----------------------------------------------------------------------
!
! Plasma Blood Block - Metabolite
!
!-----------------------------------------------------------------------

global qtot
global pbindingmet
global Vblood
global ivdosemet
global body weight

initial
amet = ivdosemet*bodyweight*1000                    !converts to ug
a0=amet
end

! -----set the maximum and minimum of blood flow rate check criteria
constant Qmin=0.99
constant Qmax=1.01

! -----check if the sum of blood flow rates=QTOT?
QCHECK=(Q1 + Q2)/QTOT
termt(QCHECK.lt.Qmin,'sum of blood flow is less than QTOT')
termt(QCHECK.gt.Qmax,'sum of blood flow is larger than QTOT')
! -----concentration of chemical in venous compartment
Cv = a/Vblood*(1-pbindingmet)

! -----rate of change of amount of chemical in venous compartment
r = Q1*Ctb1 + Q2*Ctb2 - QTOT*Cv

! -----amount of chemical in the compartment
a = intvc(r, a0)
```

PBPK Sulfamethazine Protein Binding Interaction Model Code

```
!-------------------------------------------------------------------------
!
! Global Terms Block
!
!-----------------------------------------------

global body weight                  ! kg
global qtot                         !total cardiac output L/h
global smzivdose                    !mg/kg total IV dose SMZ
global pcv                          !PCV %
global vliver                       !volume of liver - L
global vblood                       !volume of blood - L
global votslow                      !volume of slowly perfused tissues - L
global votfast                      !volume of quickly perfused tissue - L
global qliver                       !blood flow through liver L/h
global qotslow                      !blood flow through slowly perfused tissues L/h
global qotfast                      !blood flow through quickly perfused tissues L/h
global Pliver                       !tissue-plasma partition coefficient in liver
global Potslowsmz                   !tissue-plasma partition coefficient in slow
global Plivermet            !tissue-plasma partition coefficient in liver metabolite
global Pbindingmet                  !% protein binding for metabolite
global Pbody                        !tissue-plasma partition coefficient body metabolite
global smzcridose                   !SMZ CRI dose mg/kg/h
global smzKd                        !SMZ dissociation constant ppm
global smzbmax              !SMZ maximum binding capacity ppm
global fluKd                        !FLU dissociation constant ppm
global flubmax              !FLU maximum binding capacity ppm

initial
constant body weight = 100          !kg
constant Qcar = 12                  !blood flow L/h/kg
constant smzivdose = 0      !mg/kg
constant qcliver = 0.24     !fx of blood flow to liver including portal flow %
constant qcotslow = 0.51    !fx of blood flow to slow tissues
constant qcotfast = 0.25    !fx of blood flow to highly perfused tissues
constant vliverfx = 0.02    !% of bw that is liver
constant vbloodfx = 0.06    !% of bw that is blood
constant votslowfx = 0.86   !% of bw that is going to slowly perfused tissues
constant votfastfx = 0.06   !% of bw that is going to highly perfused tissues
constant pcv = 0.35                 !% PCV
constant Pliver = 0.05
constant Potslowsmz = 1.74
constant Potfastsmz = 3.02
constant Plivermet = 0.079
constant Pbindingmet = 0.57
constant Pbody = 1.297      !arbitrary partition coefficient for body
constant smzcridose = 0     !mg/kg/minute
constant smzKd = 65.62      !ug/mL
constant smzbmax = 223.4    !ug/mL
constant fluKd = 152.6      !ug/mL
constant flubmax = 1842.25          !ug/mL
```

```
vliver = vliverfx * body weight
vblood = vbloodfx * body weight
votslow = votslowfx * body weight
votfast = votfastfx * body weight
qtot = (qcar * body weight) * (1 - pcv)
qcotslow = 1 - (qcliver + qcotfast)
qotfast = qcotfast * qtot
qliver = qcliver * qtot
qotslow = qcotslow *qtot
end

!-------------------------------------------------------------------------
!
! Intravenous Dosing Simulation Block
!
!-------------------------------------------------------------------------

global smzivdose
global body weight
global smzcridose

initial
constant TimeIV = 0.00278
constant tzsmz   = 0.0                                  !start time for SMZ
constant deltsmz = 0.0                                  !duration of infusion for SMZ
end

!bolus dosing SMZ
RIVsmz = (smzivdose*bodyweight*1000)/TimeIV             !rate of IV injection ug/h
IVZONEsmz = RSW(t.GE.timeiv, 0.0,1.0)
IVsmz = RIVsmz*IVzonesmz                                !IV infusion rate ug/h

!CRI dosing SMZ
initial
schedule infusionsmz/startsmz .at. tzsmz
schedule infusionsmz/stopsmz  .at. tzsmz + deltsmz
outsmz = 0.0
end

discrete infusionsmz
if(startsmz) outsmz = smzcridose*bodyweight*1000
if(stopsmz)  outsmz = 0.0
end
```

```
!----------------------------------------------------------------------
!
! Plasma Blood Block - Sulfamethazine
!
!----------------------------------------------------------------------

global qtot
global vblood
global smzivdose
global body weight
global smzKd
global smzbmax
global fluKd
global flubmax

initial
constant a0 = 0
end

! -----set the maximum and minimum of blood flow rate check criteria
constant Qmin=0.99
constant Qmax=1.01

! -----check if the sum of blood flow rates=QTOT? for smz
QCHECKsmz = (Q1 + Q2 + Q5)/QTOT
termt(QCHECKsmz.lt.Qmin,'sum of blood flow is less than QTOT smz')
termt(QCHECKsmz.gt.Qmax,'sum of blood flow is larger than QTOT smz')

!Protein Binding SMZ
smzCt = a/Vblood                                !concentration of total drug ug/l
smzk = smzKd*(1 + (fluCf/flukd))                !adjusted Kd with competitive interaction
smzCf = (smzk*smzCt)/(smzbmax + smzk)  !concentration of free drug, linear binding
smzCb = smzCt - smzCf                           !concentration of bound drug

!Protein Binding FLU
fluCt = 0                                       !concentration of total FLU
fluCf = (fluk*fluCt)/(flubmax + fluKd)          !concentration of free FLU
fluCb = fluCt – fluCf                           !concentration of bound FLU

! -----rate of change of amount of SMZ in venous compartment
r = Q1*Ctb1 + Q2*Ctb2 + Q5*Ctb5 + IVsmz + CRIsmz - Qtot*smzCf

! -----amount of chemical in the compartment SMZ
a = intvc(r, a0)
```

```
!-----------------------------------------------------------------------
!
!Plasma Blood Block - Metabolite
!
!-----------------------------------------------------------------------

global qtot
global pbindingmet
global Vblood
global body weight

initial
a0=amet
end

! -----set the maximum and minimum of blood flow rate check criteria
constant Qmin=0.99
constant Qmax=1.01

! -----check if the sum of blood flow rates=QTOT?
QCHECK=(Q1 + Q2)/QTOT
termt(QCHECK.lt.Qmin,'sum of blood flow is less than QTOT')
termt(QCHECK.gt.Qmax,'sum of blood flow is larger than QTOT')

! -----concentration of chemical in venous compartment
Cv = a/Vblood*(1-pbindingmet)

! -----rate of change of amount of chemical in venous compartment
r = Q1*Ctb1 + Q2*Ctb2 - QTOT*Cv

! -----amount of chemical in the compartment
a = intvc(r, a0)
!-----------------------------------------------------------------------
!
! Tissue Block – Slowly Perfused Tissue
!
!-----------------------------------------------------------------------

global votslow
global qotslow
global potslowsmz

q = qotslow
constant a0=0.0              !initial amount of chemical in the tissue
constant rex = 0             !no elimination from slow

! -----concentration of chemical in the compartment
C = a/votslow                          !ug/L

! -----concentration of chemical in tissue blood
Ctb = C/potslowsmz
```

```
! -----rate of change of amount of chemical in the compartment
r = Q*(Ca - Ctb) – rex

! -----amount of chemical in the compartment
a = intvc(r, a0)

!-----------------------------------------------------------------------
!
! Tissue Block – Quickly Perfused Tissue
!
!-----------------------------------------------------------------------

global votfast
global qotfast
global potfastsmz
global body weight

q = qotfast
constant a0=0.0                         !initial amount of chemical in the tissue
constant Clrenal = 0.34                 !renal clearance mL/min/kg

! -----concentration of chemical in the compartment
C = a/votfast                                   !ug/L

! -----concentration of chemical in tissue blood
Ctb = C/potfastsmz

!elimination
Kel = Clrenal/1000 * 60 * body weight   !converts CL to L/h
rex = Kel * C                                   !based on GFR, dependent on Ca not Ctb

! -----rate of change of amount of chemical in the compartment
r = Q*(Ca - Ctb) - rex

! -----amount of chemical in the compartment
a = intvc(r, a0)

!-----------------------------------------------------------------------
!
! Tissue Block - Liver
!
!-----------------------------------------------------------------------

global body weight
global qliver
global vliver
global Pliver

q = qliver
```

```
! -----elimination parameters
constant a0=0.0                          !initial amount of chemical in the tissue
constant Clhepatic = .62                 !hepatic clearance in mL/min/kg

! -----concentration of chemical in the compartment
C = a/Vliver                                        !ug/L

! -----concentration of chemical in tissue blood
Ctb = C/pliver                           !ug/L

! -----elimination
kel = clhepatic/1000 * 60 * body weight  !converts to L/h
rex = kel * Ctb

! -----rate of change of amount of chemical in the compartment
r = rdac + Q*(Ca - Ctb) – rex

! -----amount of chemical in the compartment
a = intvc(r, a0)

!-----------------------------------------------------------------------
!
! Tissue Block – Liver Metabolite
!
!-----------------------------------------------------------------------

global qliver
global vliver
global Plivermet

initial
constant a0=0
Q = qliver
constant Kdac = 3.66                     !rate of deaceytlation 1/h
end

C = a/Vliver

! -----concentration of chemical in tissue blood
Ctb = C/Plivermet

rdac = Kdac*Ctb*Vliver

! -----rate of change of amount of chemical in the compartment
r = Q*(Ca - Ctb) - rdac + ract

! -----amount of chemical in the compartment
a = intvc(r, a0)
```

```
!-------------------------------------------------------------------------
!
! Tissue Block – Body Metabolite
!
!-------------------------------------------------------------------------

global body weight
global qtot
global vliver
global qliver
global Pbody

initial
constant a0=0
Vbody = body weight – vliver                    !tissue volume
Q = qtot - qliver                               !blood flow rate through the tissue
constant Clmet = 2.558                          !Clearance Body mL/min/kg
end

! -----elimination parameters
C = a/Vbody

! -----concentration of chemical in tissue blood
Ctb = C/Pbody
kel = Clmet*bodyweight*60/1000
rex = kel*Ca

! -----rate of change of amount of chemical in the compartment
r = Q*(Ca - Ctb) - rex

! -----amount of chemical in the compartment
a = intvc(r, a0)
```